LIÈGE université
Gembloux
Agro-Bio Tech

Study on bioactivities of quinoa-derived peptides in alleviating intestinal diseases and their physicochemical properties

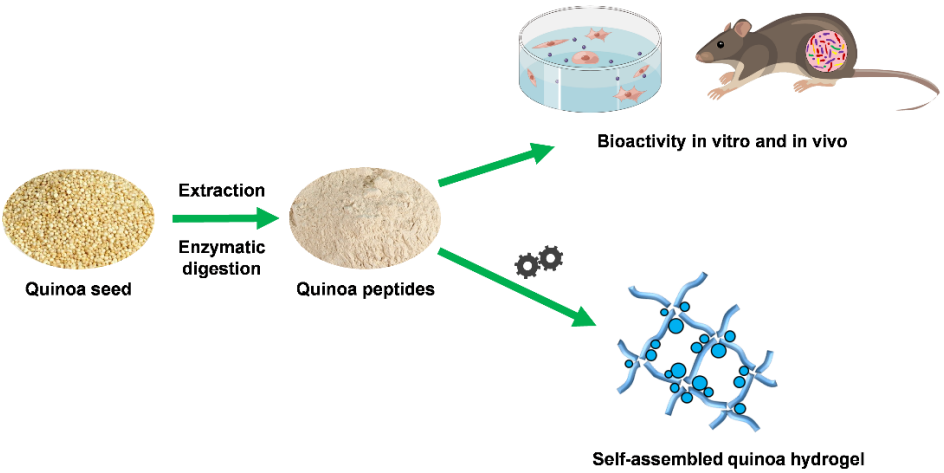

Author: Xin Fan

Supervisor: Prof. Christophe Blecker

Co-supervisor: Prof. Guixing Ren

Year: 2023

COMMUNAUTÉ FRANÇAISE DE BELGIQUE

UNIVERSITÉ DE LIÈGE – GEMBLOUX AGRO-BIO TECH

Study on bioactivities of quinoa-derived peptides in alleviating intestinal diseases and their physicochemical properties

Xin Fan

Etude des peptides bioactifs dérivés du quinoa : soulagement des maladies intestinales et propriétés physicochimiques

Promoteurs: Prof. Christophe Blecker
Prof. Guixing Ren

Année civile: 2023

Abstract

Xin Fan (2023). "Study on bioactivities of quinoa-derived peptides in alleviating intestinal diseases and their physicochemical properties" (PhD Dissertation in English).

Gembloux, Belgium, Gembloux Agro-Bio Tech, University of Liege.

141 pages, 23 figures, 9 tables.

Summary:

Quinoa (Chenopodium quinoa Willd.) is a pseudocereal initially consumed by Andean cultures as a staple food. Due to its higher nutritional properties and sustainable agronomical properties, quinoa has been mentioned as a "perfect and strategic food". Compared to traditional cereals, quinoa seed is high in protein with larger amount of essential amino acids, especially lysine and cysteine. Recently, quinoa protein has been considered an alternative to animal-based proteins because of its gluten-free nature and high digestibility. However, although the physicochemical properties of quinoa protein have been investigated in previous studies, little attention has been paid to its chemopreventive effect on gastrointestinal health. Moreover, more research is required on the physicochemical characteristics and biological activities of quinoa-derived peptides.

In this study, novel peptides were first obtained from quinoa proteins through simulated gastrointestinal digestion. They were identified by liquid chromatography–tandem mass spectrometry (LC–MS/MS). The anticancer activity of these peptides was evaluated using an antiproliferative assay in colon cancer Caco-2 cells. Combined with the result of the histone deacetylase 1 (HDAC1) inhibitory activity assay, the highly anticancer-active peptides were screened. Molecular docking was used to analyze the binding site between peptides and HDAC1, and results showed that three peptides were bound in the active pocket of HDAC1. Moreover, RT-qPCR and Western blot showed that the expression of HDAC1, NFκB, IL-6, IL-8, and Bcl-2 was significantly decreased, whereas caspase3 expression showed a remarkable evaluation. Therefore, quinoa peptides may protect against cancer development by inhibiting HDAC1 activity and regulating the expression of cancer-related genes.

Then, the effect of quinoa proteins and their hydrolysate on an azoxymethane/dextran sulfate sodium (AOM/DSS)-induced mouse model of colorectal cancer (CRC) was investigated, and their underlying mechanism was explored using gut microbiota analysis and short chain fatty acid (SCFA) production analysis. The results showed that quinoa proteins or their hydrolysate mitigated the clinical symptoms of CRC and increased SCFA contents in colon tissues. Moreover, administration of quinoa proteins or their hydrolysate partially alleviated gut microbiota dysbiosis in CRC mice by decreasing the abundance of pathogenic bacteria and increasing the abundance of probiotics. These findings indicated that the modulation of gut microbiota by quinoa protein diet intervention may ameliorate AOM/DSS-induced CRC.

In addition, this study provided a mild and efficient enzymatic method for producing

plant-based peptides with decent gel-forming ability from quinoa proteins. After alkaline protease treatment, hydrogels made with quinoa protein hydrolysis exhibited potent self-assembly capacity, enhanced gel hardness, and improved rheological properties, which were primarily attributed to the hydrogen bonding force and hydrophobic aggregation caused by hydrophobic group exposure. Moreover, amino acid and proteomics analyses suggested that the amino acid composition and sequence of quinoa peptides significantly influenced the formation of self-assembled hydrogels.

Overall, the in vitro and in vivo anti-colon cancer bioactivity of quinoa protein and its derived peptides was further explored, and a cost-effective approach to improving the gelling ability of quinoa protein was established. These findings could potentially replace the use of chemically synthesized peptides in various applications, laying the theoretical basis for the development of novel natural plant-based functional foods.

Keywords: quinoa proteins, enzymatic hydrolysis, colon cancer, molecular docking, gastrointestinal digestion, gut microbiota, gelation, physicochemical properties

Résumé

Xin Fan (2023). "Etude des peptides bioactifs dérivés du quinoa : soulagement des maladies intestinales et propriétés physicochimiques" (thèse de doctorat en anglais).

Gembloux, Belgique, Gembloux Agro-Bio Tech, Université de Liège.

141 pages, 23 figures, 9 tableaux.

Résumé:

Le quinoa (*Chenopodium quinoa* Willd.) est une pseudo-céréale consommée initialement dans la culture andine comme aliment de base. En raison de ses propriétés nutritionnelles supérieures et de sa production agronomique durable, le quinoa a été qualifié comme un "aliment idéal et stratégique". Par rapport aux céréales traditionnelles, les graines de quinoa sont riches en protéines avec une plus grande quantité d'acides aminés essentiels, en particulier la lysine et la cystéine. Récemment, les protéines de quinoa ont été considérées comme une alternative de choix aux protéines d'origine animale en raison de l'absence de gluten et de leur haute digestibilité. Cependant, bien que les propriétés physicochimiques des protéines de quinoa aient été étudiées dans des études antérieures, peu d'attention a été accordée à leur effet chimiopréventif sur la santé gastro-intestinale. De plus, des recherches supplémentaires sont nécessaires sur les caractéristiques physicochimiques et les activités biologiques des peptides dérivés du quinoa.

Dans cette étude, de nouveaux peptides de quinoa ont été tout d'abord obtenus à partir de protéines de quinoa par digestion gastro-intestinale simulée. Ils ont été identifiés par chromatographie liquide – spectrométrie de masse en tandem (LC – MS/MS). L'activité anticancéreuse de ces peptides a été évaluée à l'aide d'un test antiprolifératif dans des cellules Caco-2 du cancer du côlon. En combinaison avec le résultat du test d'activité inhibitrice de l'histone désacétylase 1 (HDAC1), les peptides hautement anticancéreux ont été criblés. L'amarrage moléculaire a été utilisé pour analyser le site de liaison entre les peptides et l'HDAC1. Les résultats ont montré que trois peptides étaient liés dans la poche active de HDAC1. De plus, la RT-qPCR et le Western blot ont montré que l'expression des HDAC1, NFκB, IL-6, IL-8 et Bcl-2 était significativement diminuée, alors que l'expression de la caspase3 présentait une évaluation remarquable. Par conséquent, les peptides de quinoa peuvent protéger contre le développement du cancer en inhibant l'activité HDAC1 et en régulant l'expression de gènes liés au cancer.

Ensuite, l'effet des protéines de quinoa et de leur hydrolysat sur un modèle murin de cancer colorectal (CCR) induit par l'azoxyméthane/dextrane sulfate de sodium (AOM/DSS) a été étudié, et son mécanisme sous-jacent a été exploré à l'aide de l'analyse du microbiote intestinal et de la production des acides gras à chaîne courte. (SCFA). Les résultats ont montré que les protéines de quinoa et leur hydrolysat atténuait les symptômes cliniques du CCR et augmentait la teneur en AGCC dans les tissus du côlon. De plus, l'administration de protéines de quinoa ou de leur hydrolysat a partiellement atténué la dysbiose du microbiote intestinal chez les souris CRC en diminuant l'abondance de bactéries pathogènes et en augmentant l'abondance de

probiotiques. Ces résultats ont indiqué que la modulation du microbiote intestinal par une intervention diététique à base de protéines de quinoa pourrait améliorer le CCR induit par l'AOM/DSS.

Par ailleurs, cette étude a fourni une méthode enzymatique douce et efficace pour produire des peptides d'origine végétale dotés d'une capacité gélifiante. Après traitement par protéase alcaline, les hydrogels fabriqués à partir des hydrolysats de protéines de quinoa présentaient une forte capacité d'auto-assemblage, une dureté de gel améliorée et des propriétés rhéologiques supérieures, principalement attribuées à la force de liaison hydrogène et à l'agrégation hydrophobe provoquée par l'exposition du groupe hydrophobe. De plus, l'analyse des acides aminés et l'approche protéomique suggèrent que la composition en acides aminés et la séquence des peptides de quinoa influencent de manière significative la formation d'hydrogels auto-assemblés.

Dans l'ensemble, la bioactivité anti-cancer du côlon in vitro et in vivo des protéines de quinoa et des peptides qui en dérivent a été explorée plus en détail, et une approche économiquement rentable pour améliorer la capacité de gélification des protéines de quinoa a été établie. Ces découvertes pourraient potentiellement conduire au remplacement de peptides synthétisés chimiquement dans diverses applications, jetant ainsi les bases théoriques du développement de nouveaux aliments fonctionnels naturels à base de plantes.

Mots-clés: protéines de quinoa, hydrolyse enzymatique, cancer du côlon, docking moléculaire, digestion gastro-intestinale, microbiote intestinal, gélification, propriétés physico-chimiques

Acknowledgments

I would like to express my sincere thanks to all of the members who has helped and supported me during my Ph. D period.

First of all, I would like to extend my sincere gratitude to my thesis jury members, Prof. Marie-Laure Fauconnier, Prof. Christophe Blecker, Prof. Guixing Ren, Prof. Lizhen Zhang, Prof. Nicolas Jacquet, Prof. Paul Malumba Kamba, for their helpful comments and encouragement. Especially thanks to my supervisors, Prof. Christophe Blecker and Prof. Guixing Ren who give me such a precious opportunity to pursue my Ph. D in Beijing and Gembloux. Under your guidance, I can complete my doctoral research and graduation thesis. Prof. Christophe Blecker gave me innovative and constructive suggestions based on my research foundation, and provided professional comments in terms of the thesis framework and content. Prof. Guixing Ren gave me the greatest support and help in my research direction and experiments.Besides, I also want to thank other professors and teachers for constructive opinions and guidance on my research.

Life is not easy, and PhD life is often a bit boring. Fortunately, my family and friends have always been with me and supported me unconditionally during this period, which gave me the energy and confidence to complete my Ph. D work.

Thanks to all members of Food Science and Formulation Laboratory of TERRA namely Lynn Doran, Marjorie Servais, Sandrino Filocco, Andreea Kerezsi, Kouassi Kouakou Alfred, Mariem Boukraa, Arpita Chakraborty, Laurent Seutin, Ines Othmeni, Xia Li, Yatao Huang, Shuyi Qian, Siyang Deng, Fangzhou Wang, Xiaoxian Liu. All of you are so kind to me, welcome me to the lab and taught me a lot of experimental knowledge related to my research. Moreover, we also spent so many happy times together in and out of the lab.

I also want to thanks all the members of my chinese lab, Key Laboratory of Quality Evaluation and Nutrition Health of Agro-Products, CAAS, for your help and guidance in my study and life. They are Peiyou Qin, Yang Yao, Xiushi Yang, Huimin Guo, Yuqiong Hao, Cong Teng, Zhenxing Shi, YingYing Zhu, Bao Xing, Weiyi Zhang, Yinhuan Chen, Menghan Sun, Kaili Zhu, Zhuo Zhang, Yuqing Guo, Siyu Wang, Zuchen Wei, Biao Zhang, Manli Zhu, Yajie Li.

In addition, sincere thanks to the China Scholarship Council (CSC)'s financial support and the support of the joint training program between Chinese Academy of Agricultural Sciences (CAAS) and Gembloux Agro-Bio Tech of University of Liège.

Last but not least, I want to express my sincere gratitude to my family and friends for their support and encouragement, especially my mother for her selfless dedication and love throughout my life.

Xin Fan

November, 2023 in Gembloux, Belgium

Table of Contents

List of Figures

List of Tables

List of Abbreviations

QP: quinoa protein
QPH: quinoa protein hydrolysate
LC–MS/MS: liquid chromatography–tandem mass spectrometry
GC–MS: Gas chromatography-mass spectrometry
HDAC1: histone deacetylase 1
RT-qPCR: real-time quantitative polymerase chain reaction
AOM/DSS: azoxymethane/dextran sulfate sodium
CRC: colorectal cancer
SCFAs: short chain fatty acids
FTIR: Fourier transform infrared spectroscopy
SEM: scanning electron microscopic
HFD: high-fat diet
QPI: quinoa protein isolate
DPP-IV: dipeptidyl peptidase-IV
GI: gastrointestinal
IBD: inflammatory bowel disease
ZO-1: zonula occludens-1
IFN-γ: pro-inflammatory cytokine interferon-γ
IL-6: interleukin-6
LPS: lipopolysaccharide
TNF-α: tumor necrosis factor-α
IELs: intraepithelial lymphocytes
LPLs: lamina propria lymphocytes
OB: oat bran
NF-κB: nuclear factor-κB
BLIDF: bioactivity of insoluble dietary fiber from barley leaf
PPARγ: peroxisome-proliferators-activated receptor γ
HCl: hydrochloric acid
NaOH: sodium hydroxide
MWCO: molecular weight cut-off
ATCC: American Type Cell Collection
SAHA: suberoylanilide hydroxamic acid
EMT: epithelial–mesenchymal transition

PBMCs: peripheral blood mononuclear cells
ROS: reactive oxygen species
DAI: disease activity index
PBS: phosphate-buffered saline
H&E: hematoxylin and eosin
EI: Electron bombardment ion
LEfSe: Linear discriminate analysis effect size
NMDS: Nonmetric multi-dimensional scaling
SIM: selected ion monitoring
DH: degree of hydrolysis
SDS-PAGE: sodium dodecyl sulfate-polyacrylamide gel electrophoresis
GPC: gel permeation chromatography
RI: refractive indices
SH: sulfhydryl
DTNB: 5,5'-dithio-bis-(2-nitrobenzoic acid)
EDTA: ethylenediaminetetraacetic acid
ATR: diamond attenuated total reflectance
PITC: phenylisothiocyanate pre-column
AGC: automatic gain control
HCD: high-energy dissociation
FDR: false discovery rate
FSD: Fourier self-deconvolution

1

Chapter I General introduction

1. Context and objectives

1.1. Context

Quinoa (*Chenopodium quinoa* Willd.), a pseudocereal that originated in the Andean region of South America, has higher nutritional properties and sustainable agronomical properties (Montserrat-de la Paz et al., 2021). There are many bioactive compounds found in quinoa, such as polysaccharides, saponins, flavonoids and proteins. These are considered to have health benefits (Pereira, Cadavez, Barros, Encina-Zelada, & Ferreira, 2020). Protein is thought to be the main nutritional advantage of quinoa grains, with protein content ranging from 9.15% to 21.02% (Gonzalez et al. 2012). Compared to traditional cereals, quinoa seed is high in protein with larger amount of essential amino acids especially lysine and cysteine. In addition, more scientists are trying to offer it as an alternative for animal-based proteins because of its gluten-free nature and high digestibility (Ruales et al., 1992; Navruz-Varli et al., 2016). However, although the physicochemical properties and some in vitro bioactivities of quinoa protein (QP) have been studied in past research, little attention has been paid to its chemopreventive effect on gastrointestinal health (Moura et al., 2015).

Recent studies have shown that quinoa proteins or its derived peptides have a variety of positive bioactivities, including antioxidant activity, antihypertensive effect and anti-colon cancer activity in vitro (Swieca, Seczyk, Gawlik-Dziki, & Dziki, 2014; Vilcacundo, Miralles, Carrillo, & Hernandez-Ledesma, 2018; Guo et al., 2020; Srdic, Ovcina, Fotschki, Haros, & Llopis, 2020). Although quinoa protein has shown antiproliferative activity in human colorectal cancer (CRC) cell lines after simulating gastrointestinal digestion, it is unclear which protein fragments or peptides are more effective and what mechanism of action is in their inhibiting cancer ability.

In fact, compared with the experimental results in vitro, the process of metabolism and function of these bioactive substances in vivo is more complicated. There have been several studies on the effect of quinoa components in chronic diseases. For example, Llopis et al. (2020) showed that administration of quinoa appears to promote positive effects of intestinal innate immune modulation and ameliorate hepatocarcinoma within the gut-liver axis. Cao et al. (2020) demonstrated that quinoa polysaccharide supplementation could ameliorate the hyperlipemia induced by HFD in association with modulating gut microbiota in a positive way. In addition, quinoa also established a prebiotic effect and its prebiotic potential could be added as a premise for improving or maintaining gastrointestinal health through the equilibrium of intestinal microbiota (Gullon et al., 2016). In recent years, the functional role of quinoa protein and peptides in relieving chronic diseases has gradually received attention. Following previous work, Guo et al. (2020) measured the antihypertensive property of quinoa protein under simulated gastrointestinal digestion and they found that quinoa protein hydrolysate (QPH) effectively controlling blood pressure in spontaneously hypertensive model rats from 2 h to10 h after oral administration. Besides, Vilcacundo and co-workers demonstrated that quinoa-derived peptides might

be responsible for the antioxidant effects and some of them showed anti-cancer effects in colon cancer cells (Vilcacundo et al., 2018). Although some beneficial functions exerted by quinoa protein have been examined, there are limited in vivo experiments about the bioactivity and mechanism of quinoa protein in alleviating colitis and colon cancer.

Furthermore, the physicochemical properties and metabolic process of quinoa protein during gastrointestinal digestion also need to be investigated, which would be helpful to explore the its underlying mechanism on colorectal cancer, and develop a targeted delivery system for quinoa protein hydrolysate.

1.2. Objectives

The aim of this study is to investigate the effects of quinoa protein and its derived peptides in alleviating colorectal cancer in vitro and in vivo, and to develop a colorectal cancer-relief hydrogel from quinoa protein with minimal adverse side effects and biocompatible properties. The objectives include the following three aspects :

(1) To investigate the anti-colon cancer activity and mechanism of quinoa protein and peptides in Caco-2 Cells.

(2) To compare the effects of quinoa protein and quinoa protein hydrolysate on alleviating CRC development, and to analyze the correlation between phenotypic indicators, gut microbiota, and SCFAs in colon tissues.

(3) To formulate self-assembly peptides with gel-forming ability from quinoa proteins via a mild enzymatic method.

2. Research roadmap and outline

2.1. Research roadmap

The research roadmap is presented in Figure 1-1.

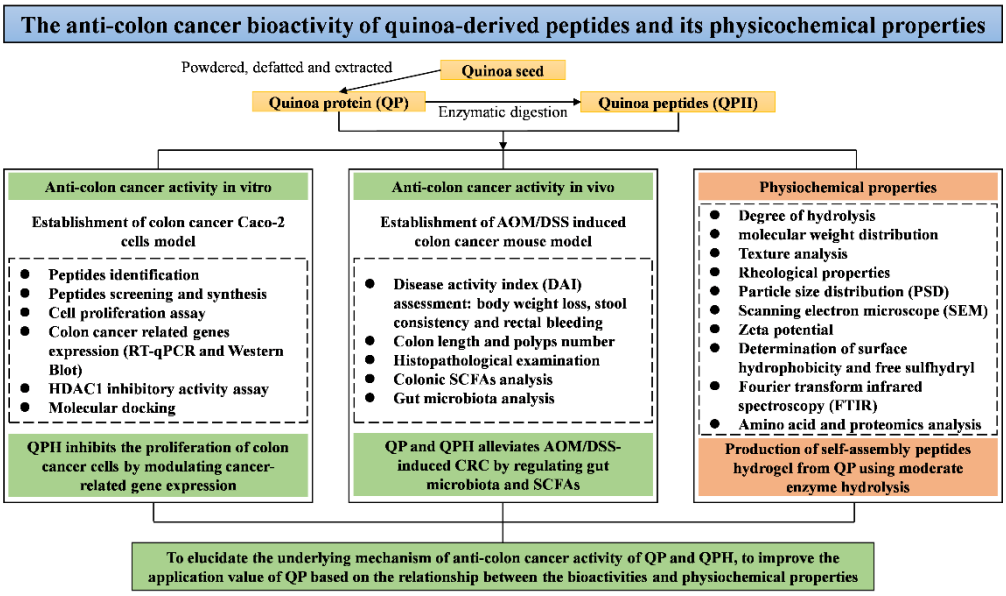

Figure 1-1. The research roadmap of this thesis.

2.2. Outline

In Chapter II, the literature review summarizes different bioactivities of quinoa proteins and peptides in vitro, the effects of quinoa proteins and peptides on gastrointestinal diseases in vivo, and the research progress on the gelation properties of quinoa proteins and peptides.

In Chapter III, we assessed the capability of quinoa peptides released during the simulated gastrointestinal digestion to affect the viability of human colon cancer Caco-2 cells, and screened peptides with HDAC1 inhibitory activity. The structure-activity relationship of these peptides was explored by molecular docking. Furthermore, RT-qPCR and Western blot were assayed to investigate the possible mechanism of quinoa peptides in alleviating colon cancer.

In Chapter IV, a CRC mouse model was induced by an azoxymethane/dextran sulfate sodium (AOM/DSS) and different doses of quinoa proteins and peptides were used to intervene in CRC mouse. The pathological data, SCFAs content and gut microbiota were analyzed to investigate the effects of quinoa protein and quinoa protein hydrolysate on CRC development

In Chapter V, the physicochemical properties of the quinoa peptides hydrogels were determined. Molecular weight, degree of hydrolysis, gel hardness, rheological properties were determined to compare the gelation ability. Particle size distribution and scanning electron microscopic (SEM) observation were conducted to analyze the microstructure. Then, surface hydrophobicity. zeta potential, free sulfhydryls, Fourier transform infrared spectroscopy (FTIR), and amino acid and proteomics analysis were

measured to deduce the potential gelation mechanism of the quinoa hydrogels.

2

Chapter II Literature review on bioactivities and gelation properties of quinoa protein and its derived peptides

Introduction to Chapter 2

In this chapter, the various in vitro bioactivities of quinoa proteins and peptides, their effects on gastrointestinal disorders in vivo, and the advancement of research on their gelation properties are all summarized in this review.

This work is an original contribution, adapted from: Ren, G., Fan, X. (*co-first author*), Teng, C., Li, Y., Everaert, N., Blecker, C. (2021). The beneficial effect of coarse cereals on chronic diseases through regulating gut microbiota. Foods, 10 (11), 2891. DOI: 10.3390/foods10112891.

1. Introduction

The drastic changes that are occurring in the world's ecology are having a significant impact on human life, particularly by limiting food supply by affecting crop yield and quality. Therefore, in addition to staple food crops, finding nutrient-dense alternative crops that can adapt to climate change is critical. From a nutritional standpoint, the usefulness or functionality of any grain as a food is primarily determined by the quantity and quality of protein it contains. Moreover, natural plant protein has received a lot of attention due to its safety, high biocompatibility, nutritional value, and low cost, which is very important for the food and pharmaceutical industries (Amanda, Moreno, & Carciofi, 2020). Recently, coarse cereals have attracted wider attention because of their functional component content and balanced amino acid profile. Among these cereal crops, quinoa appears to be a good choice in this case because it can meet almost all nutritional needs while also providing compounds with health-promoting properties (Ruiz et al., 2014).

Quinoa is a pseudo cereal native to the Andes of South America. Quinoa has been grown as a new alternative crop in many places because of its high nutritional properties and environmental adaptability (Castro et al., 2019). Salt stress induces better absolute and relative growth rates, and quinoa can adapt to drought-affected environments through its high-water use efficiency. At present, quinoa is grown in South America, North America, Asia, Europe and other places. Peru is the largest producer and exporter of quinoa, and Peru and Bolivia together account for 90 % of the world’s production, with global increases in the past few years approaching a total of 160,000 metric tons (Fathi & Kardoni, 2020). Quinoa is rich in functional ingredients, which are of great significance for improving human health by serving as antioxidant (Daliri, Ahmadi, Pezeshki, Hamishehkar, & Ghorbani, 2021), hypolipidemic (Cao et al., 2020), antidiabetic (Mudgil, Kilari, Kamal, Olalere, & Maqsood, 2020; Tan, Chang, Liu, Li, & Zhao, 2020), anti-inflammatory (Yao et al., 2015), and anticancer (Mohamed, Fouda, & Mohamed, 2019; Stiki, Milini, Kosti, Jovanovi, & Pei, 2020). These functional ingredients mainly include polyphenols, flavonoids, carbohydrates, peptides and saponins. The bioactive compounds in quinoa and the methodologies for their identification are shown in Figure 2-1 and Table 2-1, respectively. In addition, quinoa can be regarded as an important raw material for development as a functional ingredient and food to improve human health. However, these bioactivities of quinoa are the results of in vitro chemical or cell experiments, and the mechanism are not clear, which hinders the breeding of high-quality quinoa varieties and the development of high value products.

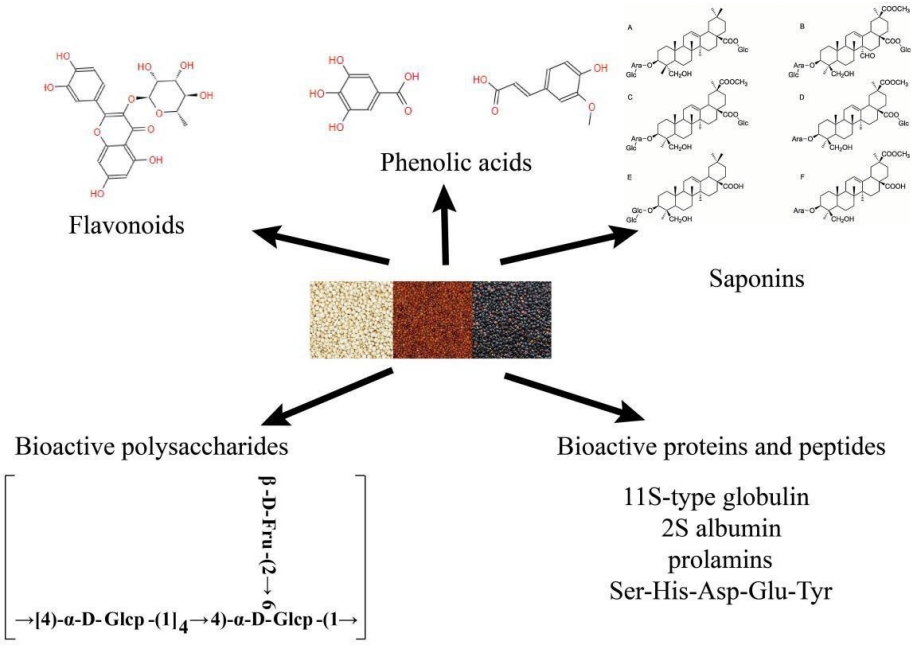

Figure 2-1. The basic structures of some representative bioactive compounds isolated from quinoa.

In recent years, growing demand for plant-based proteins as alternatives to dairy protein owing to high nutritional value, high protein digestibility and favorable functional properties. Therefore, more in-depth research has been carried out on the nutritional value of quinoa and the development of quinoa products, especially quinoa protein. However, as mentioned above, research on the bioactive compounds of quinoa is still very limited, and the research on quinoa protein is in its early stages.

Table 2-1. Bioactive compounds in quinoa and their methods of identification.

Family	Compounds	Identification methodology	References
Polyphenols	Rutin, vanillic acid, ferulic acid, kaempferol, quercetin derivatives, p-coumaric, daidzein, caffeine, caffeic acid, pinocembrin, apigenin, pinocembrin	HPLC-DAD-MS, LC-ESI-QTOF-MS, HPLC-DAD, UHPLC/ESI-Orbitrap MS	(Tang et al., 2015; Antognoni et al., 2021)
Flavone	Quercetin, kaempferol, myricetin, isorhamnetin, Quercetin glucuronide, Kaempferol glucuronide, Kaempferol 3-O-glucoside, Kaempferol pentosyl rhamnoside, Kaempferol, Quercetin-3-O-(2″-apiosyl)-rutinoside	HPLC-ESI-MS3 HPLC	(Tang et al., 2015; Balakrishnan et al., 2020; Ritva et al., 2010)
Saponins	Phytolaccagenic acid, Oleanolic acid, Serjanic acid, Hederagenin	HPLC, HPLC/MS, 1D and 2D-NMR	(Yousif et al., 2020; Xue et al., 2020)
Bioactive polysaccharides	SQAP-1, SQAP-2, SQWP-1, SQWP-2, QWP-1, QWP-2, QAP-1, QAP-2	1D and 2D-NMR, GC-MS	(Hu et al., 2017; Teng et al., 2020; Teng et al., 2021)
Bioactive proteins and peptides	QPH, BAPs, globulins, albumins, prolamins, QPN	HPLC, FTIR, IFS	(Vilcacundo et al., 2018; Guo et al., 2021; Mudgil et al., 2020; Daliri et al., 2021; Zhang et al., 2021)
Phytoecdysteroid	20-hydroxyecdysone	LC–UV–MS	(Graf et al., 2014)

1.1. Quinoa proteins and their bioactivities in vitro

Quinoa is considered to be a nutritional grain mainly because of its high protein content and balanced proportion of amino acids, especially lysine and arginine. In a recent study, the protein content of six quinoa varieties was measured and found to range from 15.6 % to 18.7 % (Gómez, Prieto, Sobrado, & Magro, 2021). In another study, the composition and secondary structure of six different quinoa varieties from China were investigated (Wang, Zhao, & Yuan, 2020). The molecular weight of the quinoa protein isolate (QPI) ranged from 10.0 kDa to 50.0 kDa with β-sheets forming the main secondary structure and comprising 30.86 % to 36.88 % of the protein. Spectrum deconvolution techniques are often used to identify secondary protein structures. Using these methods, strong peak differences were identified in the protein secondary structure of different quinoa cultivars (García-Parra, Roa-Acosta, García-Londoño, Moreno-Medina, & Bravo-Gomez, 2021). Titicaca seed proteins had a larger ratio of β-sheet-1 and β-sheet-2 and contained β-turns-1, while Narino mainly contained β-turns-2, β-turns-3 and α-helices. The secondary structure spectrum can also be used as a fingerprint for each variety. An improved spectral method could be used to identify genetic variation and control the quality of adulterated flour. According to Drzewiecki et al. (2018), the absorption bands of quinoa associated with –NH groups at 1657 cm^{-1} and 1549 cm^{-1} represent the amide I and amide II bands, respectively, and can be attributed to the aromatic C–H bend protein structure. This structural feature is also related to antioxidant activity of quinoa proteins. The protein in quinoa seeds is mainly composed of 11S globulin (37 %) and 2S albumin (35 %), both of which are stabilized by disulfide bonds (Drzewiecki et al., 2018). In addition, quinoa seeds contain low concentrations of gliadin (0.5–7 %), which is suitable for people with celiac disease (Dakhili, Abdolalizadeh, Hosseini, Shojaee-Aliabadi, & Mirmoghtadaie, 2019). Lunasin is a new anticancer peptide that exists widely in soybean and maize, and it has been detected in quinoa by UPLC-ESI-MS, with the planting location affecting the quantity in the grain (ranging from 1.01 × 10–3 mg/g to 4.89 × 10–3 mg/g) (Ren, Zhu, & Shi, 2017). Lysine is described as the first limiting amino acid (Sheng, Xin, Wang, Peng, & Li, 2019) and it can promote human development and enhance immune function, making it an essential nutrient for children. Researchers have shown that quinoa is rich in lysine and it can promote the absorption and transport of calcium in the body (Stikic et al., 2012).

Many studies have confirmed that bioactive peptides in quinoa have hypoglycemic, hypotensive and hypolipidemic activities. Indeed, quinoa protein hydrolysates treated with different food grade enzymes inhibited dipeptidyl peptidase-IV (DPP-IV) and α-glucosidase angiotensin converting enzyme (Mudgil et al., 2020). Further, effective bioactive peptides have been obtained by synergistic treatment of quinoa protein with pepsin and pancreatin; peptides with molecular weight < 5 kDa showed antioxidant activity, and peptides with molecular weight > 5 kDa showed the strongest anticancer activity (Vilcacundo, Miralles, Carrillo, & Hernandez-Ledesma, 2018). The main protein precursors of quinoa peptides are 13S globulin seed storage protein 2-like, legumin A-like, and 11S globulin seed storage protein 2-like, accounting for 32.15 %, 21.01 % and 20.25 % of the total peptides, respectively (Guo, Hao, Fan, Richel, &

Ren, 2021).

1.2. The effect of Quinoa proteins and their hydrolysate on gastrointestinal diseases in vivo

The gastrointestinal (GI) tract is the main interface for the interaction of dietary compounds and the organism. This complex system has developed multiple protective mechanisms against pathogens and toxic agents from the external environment, and it maintains a specialized balance of GI homeostasis, which is crucial for the digestive system to absorb nutrients and water (Fernandez-Tome, Hernandez-Ledesma, Chaparro, Indiano-Romacho, Bernardo, & Gisbert, 2019). However, poor lifestyle habits and imbalanced diet are the main reasons for the increasing incidence of gastrointestinal diseases such as inflammatory bowel disease (IBD), colorectal cancer (CRC), intestinal barrier dysfunction, etc.

Dietary interventions are not thought of as replacing agents in conventional medical therapies, but may be effective as complementary strategies for GI disorders (Gassull, 2006). Moreover, dietary molecules can influence the mechanisms of nutrient sensing and bioavailability, as well as the composition and metabolism of the gut microbiota, which ultimately might also affect GI homeostasis (Donaldson, Lee, & Mazmanian, 2016).

Quinoa protein and its hydrolysate have been proved to have various health benefits in vitro. However, it needs to be clear that in vitro methods cannot capture all of the in vivo complexity of in vivo experiments. Protein or other active ingredients must pass through the digestive system in order to perform their bioactive functions in vivo. Since there are currently very few studies on quinoa in alleviating intestinal diseases in vivo, we also make reference to studies on intestinal diseases of other coarse cereals in this section.

1.2.1. Inflammatory Bowel Disease

Recently, growing evidence points to the potential role of dietary bioactive compounds and microbiota modulation in IBD (Lee et al., 2015; Larussa, Imeneo, & Luzza, 2017). The effect of whole-grain components on regulating the gut microbiota is summarized in Table 2-2. For instance, intake of oat β-glucan significantly ameliorated the clinical features of ulcerative colitis in mice, attenuating the severe colonic inflammatory status and improving colonic mucosal barrier function concurrently with regulating gut-derived SCFAs and intestinal microbial metabolic profiles (Bai et al., 2021). According to the authors, the reversed expression levels of zonula occludens-1 (ZO-1), occludin, claudin-1, and claudin-4 indicated that oat β-glucan promoted tight junction protein formation and restored intestinal epithelial barrier function. Moreover, they proved that pro-inflammatory cytokine interferon-γ (IFN-γ) and interleukin-6 (IL-6) were inhibited, while the production of SCFAs (especially acetate and propionate) increased, playing an important role in regulating intestinal epithelial tight junctions in UC mice. In a similar experiment, the low-molecular-weight form of β-glucan had a positive effect on the colon tissue of rats with lipopolysaccharide (LPS)-induced enteritis, resulting in changes in the levels of

IL-10, IL-12, and tumor necrosis factor-α (TNF-α), as well as the number of intraepithelial lymphocytes (IELs) and lamina propria lymphocytes (LPLs) (Wilczak et al., 2015). Moreover, a statistically significant reduction in the formation of hydroxybutyric acid and enhanced concentrations of lactic acid and propionic acid were observed, which was consistent with the number of lactic acid bacteria. This suggests an improvement in the alimentary tract contents.

Oat bran is one of the major byproducts in the processing of husked oat, and it contains relatively high levels of protein, minerals, vitamins, and soluble β-glucan (Menon, Gonzalez, Ferruzzi, Jackson, Winderl, & Watson, 2016). He et al. investigated the effects of oat bran on nutrient digestibility, intestinal microbiota, and inflammatory responses in the hindgut of growing pigs. After supplementing with 10% oat bran (OB), the dietary nutrient digestibility showed no differences between the OB group and the control group on day 28. However, the mRNA expression of IL-8, nuclear factor-κB (NF-κB), and TNF-α was decreased in the OB group. Moreover, the abundances of *Prevotella*, *Butyricicoccus*, and *Catenibacterium* were increased in the colonic digesta, which may contribute to ameliorating inflammatory responses in the hindgut via enhancing the fermentation of fiber to produce SCFAs. Similarly, insoluble fiber in oat hulls could alleviate necrotic enteritis, and broilers fed with oat hulls had heavier gizzards compared with those without oat hulls. The gut microbiota composition was also improved by increasing the abundance of *Clostridium perfringens* and reducing the abundance of *Lactobacillus* and *Salmonellae* (Kheravii, Swick, Choct, & Wu, 2018). However, despite the fact that dietary fiber has been proved to be an effective strategy to prevent and relieve IBD through gut microbiota modulation, the function of soluble dietary fiber was found to be more favorable than that of insoluble dietary fiber. Tian et al. evaluated the bioactivity of insoluble dietary fiber from barley leaf (BLIDF) in inhibiting gut inflammation through regulating the intestinal microbiota in dextran sulfate sodium (DSS)-induced colitis mice. After intake of a BLIDF-supplemented diet for 28 days, they found that BLIDF markedly attenuated the severity of inflammation in DSS-induced acute colitis mice and increased the abundance of *Parasutterella*, *Erysipelatoclostridium*, and *Alistipes*, while the abundance of *Akkermansia* was significantly decreased. Moreover, BLIDF feeding can reverse the DSS-induced decline of short-chain fatty acids and secondary bile acids in mice feces (Tian, Li, Ma, Feng, Hu, & Chen, 2021). Likewise, Li et al. explored the potential modulating roles of gut microbial metabolites of BL (barley leaf) in protecting against colitis and elucidated the underlying molecular mechanisms. They reported that supplementing with BL ameliorated DSS-induced gut microbiota dysbiosis and resulted in the enrichment of the microbiota-derived purine metabolite inosine, which could simulate peroxisome-proliferators-activated receptor γ (PPARγ) signaling to improve intestinal mucosal barrier functions in human colon epithelial cells (Li, Feng, Tian, Ji, Hu, & Chen, 2021).

It is also noteworthy that consumption of many purified dietary fibers has not been shown to increase the diversity of gut microbiota. The beneficial effects of whole grains on health are likely to be a combined result of many components within the grain rather than one specific component (Fardet, 2010; Rose, 2014). It was demonstrated that consumption of quinoa alleviated clinical symptoms according to

the reduced disease activity index and the degree of histological damage. Compared to the control group, the species richness and diversity were increased in the quinoa consumption group, while abnormal expansion of the phylum Proteobacteria was decreased. Moreover, the overgrowth of the genera *Escherichia*/*Shigella* and *Peptoclostridium* was inhibited, whereas the abundances of *Firmicutes* and *Bacteroidetes* did not change significantly in the quinoa treatment group (Liu, Zhang, Qiu, Fan, Ding, & Liu, 2018). Another experiment investigated the effect of a buckwheat diet in a high-fat diet-induced gastritis mice model. The results showed that gastritis was lessened after intake of buckwheat, and the microbial dysbiosis induced by a high-salt diet could be recovered (Li, et al., 2020). In the case of millet whole grain, its consumption by DSS-induced colitis murines alleviated the symptoms of enteritis to varying degrees, and completely alleviated DSS-induced dysbiosis. Moreover, the decreased levels of IL-6 and claudin2 expression in the colon indicated that systemic inflammation and gut barrier function was improved after the consumption of millet whole grain (Zhang, Liu, Zhang, Yang, Wang, & Li, 2021).

1.2.2. Colorectal Cancer

Epidemiological studies have suggested that IBD patients exhibit a higher risk of CRC and that the incidence of cancer is positively correlated with the duration of IBD (Nadeem, Kumar, Al-Abbasi, Kamal, & Anwar, 2020). A recent study suggested that coarse cereal diets are beneficial for relieving CRC. Zhang et al. reported that intake of foxtail millet ameliorated AOM/DSS-induced colitis-associated CRC in mice via the activation of AHR and GPCRs and the inhibition of STAT3 phosphorylation by the microbial metabolites of the foxtail millet. In line with a previous study, the abundances of *Bifidobacterium* and *Bacteroidales_S24-7* were increased after millet consumption, compared to the control group (Zhang et al., 2020). Similarly, Yang et al. studied the effect of sorghum in an HFD-induced CRC mice model. The results showed that sorghum exhibited tremendous anti-CRC effects by suppressing the growth and metastasis of cancerous colon epithelial cells, as well as protecting against gut microbiota alterations linked to colitis (Yang et al., 2019).

Collectively, IBD, CRC, and intestinal barrier dysfunction could be alleviated by intake of a diet supplemented with coarse cereals or their bioactive components, due to the changes in relative gene expression, reduction of inflammatory cytokines (IL-6, IL-8, IL-10, etc.) and increased production of SCFAs demonstrated to be affected by the composition of gut microbiota.

Table 2-2. Effect of whole-grain components on gut microbiota of gastrointestinal diseases host.

Cereal	Component	Pathological Type	Study Characteristics	Pathological Parameters	Changes in Gut Microbiota	Reference
barley	leaf	colitis	female C57Bl/6J mice	IL-4 ↑, IL-10 ↑, TNF-α ↓, stool frequency ↑, gut transit time ↓, inosine ↑, guanosine ↑, glucose ↓, lactic acid ↑, body Weight ↑	*Proteobacteria* ↓, *Enterobacteriaceae* ↑, *Firmicutes* ↑, *Bacteroidetes* ↓, *Lactobacillus* ↑	(Li et al., 2021)
	insoluble fiber	colitis	female C57BL/6J mice	IL-6 ↓, TNF-α ↓, IL-1β ↓, IL-4 ↓, IL-10 ↓, SCFAs ↑, secondary bile acids ↑, body Weight ↑	*Akkermansia* ↓, *Parasutterella* ↑, *Erysipelatoclostridium* ↑, *Alistipes* ↑, *Verrucomicrobia* ↓	(Tian et al., 2021)
buckwheat	whole grain	gastritis	SPF male C57BL/6 mice	IL-6 ↓, IL-1β ↓, IL-18 ↓, TH17 ↓, TGF-β ↓, IL-17A ↓, ILA ↑	*Unclassified_Lachnospiraceae* ↓, *Un-classified_Clostridiales* ↓, *Unclassified_Rikenellaceae* ↓, *Oscil-lospira* ↓, *Unclassified_S24-7* ↑, *Lactobacillus* ↑	(Y. Li, Li, et al., 2020)
millet	polyphenol	colorectal cancer	male C57BL/6J mice	COX-2 ↓and EMR1 ↓, PCNA cells ↓, caspase 3 ↑	*Firmicutes* ↑, *Bacteroidetes* ↓, *Prevotella* ↓, *Corprobacillus* ↑, *Parabacteroides* ↑, *AF12* ↑, *Coprococcus* ↑, *Oscillospira* ↑, *Ruminococcus* ↑, *Prevotella* ↓,	(Yang, Shan, Zhang, Shi, Li, & Li,

					Desulfovibrio ↓	2020)
	tryptophan and fiber	colorectal cancer	SPF male BALB/c mice	IL-6 ↓, IL-17 ↓, MPO ↓, MCP-1 ↓, serum C-P ↓, IFN-γ ↓, LSP ↓, COX-2 ↓, iNOS ↓, FOXP3 ↑, IL-22 ↑, ZO-1 ↑, IL-10 ↑, occludin ↑, Bcl-2 ↑, PCNA ↑, VEGF ↑, AHR ↑, SCFAs ↑	*Allobaculum* ↑, *Bifidobacterium* ↑, *Bacteroidales_S24-7* ↑, *Alistipes* ↓,	(Zhang et al., 2020)
	whole grain	acute ulcerative colitis	male C57BL/6 mice	IL-6 ↓, claudin2 ↓, ZO-1 ↑, occludin ↑, claudin 2↓	*Muribaculaceae* ↑	(Zhang et al., 2021)
	bran	inflammatory	pig	IL-8 ↓, colonic IL-8 ↓, NF-κB ↓, TNF-α ↓	*Catenibacterium* ↑, *Peptococcus* ↓, *Prevotella* ↑, *Butyricicoccus* ↑, *Catenibacterium* ↑, *Coprococcus* ↓, *Desulfovibrio* ↓	(He et al., 2018)
oat						
	β-glucan	enteritis	male SD rats	IL-12 ↓, IL-1α ↓, β, IL-6 ↓, IL-10 ↑, TNF-alpha ↑, lactic acid ↑, propionic acid ↑, hydroxybutyric acid ↓	-	(Wilczak et al., 2015)
	fiber	necrotic enteritis	broiler chickens	succinic acid ↑, acetic acid ↓, propionic acid ↓, valeric acid ↓	*Perfringens* ↑, *Lactobacillus* ↓, *Salmonellae* ↓,	(Kheravi et al.,

						2018)
quinoa	whole grain	colonic colitis	male C57BL/6 mice	IL-6 ↓, IL-1β ↓, IFN-γ ↑	*Proteobacteria* ↓, *Escherichia/Shigella* ↓, *Peptoclostridium*↓, *Bacteroidetes* ↑, *Verrucomicrobia* ↑	(Liu et al., 2018)
sorghum	whole grain	colorectal cancer	human female C57BL/6 mice	-	*Bacteroides* ↑, *Fusobacterium* ↑, *Dorea,Porphyromonas* ↑, *Pseudomonas* ↓, *Prevotella* ↓, *Acinetobacter* ↓, *Catenibacterium* ↓	(Yang et al., 2019)

1.3. Gelation properties

Quinoa protein have been proved not only to have nutritional and health benefits, but also to possess some physicochemical and functional properties that contribute food processing and development. Some recent studies have focused on the gelling and emulsifying properties of quinoa proteins (Lingiardi, Galante, de Sanctis, & Spelzini, 2022). In general, protein gel-forming ability affects food texture and sensory perception, and plays an important role in drug delivery systems. Moreover, it is worth noting that several plant-based proteins have shown better gelation properties than themselves after specific treatments (De Leon Rodriguez & Hemar, 2020). The gel-forming process could be triggered by heating treatment, pH changes, addition of divalent ions, ultrasonic treatments and some mild enzymatic hydrolysis (Mäkinen, Zannini, & Arendt, 2015; Ruiz et al., 2016; Kaspchak et al., 2017).

To date, most of QP gels were obtained through varying degrees of heat treatment. Moreover, several studies also have explored the effects of other factors on QP heat-set gelation. Salt addition and pH adjustment at an appropriate protein concentration could facilitate the gel formation, thereby lowering the gelation temperature and enhancing the gel strength (Kaspchak et al., 2017).

In a previous study, Mäkinen, Zannini, and Arendt (2015) explored the microstructure of QP cold-set gels prepared by heating 5% QP at 100 ℃ for 15 min at pH 8.5 and 10.5. The G′ values of QP gels increased with the rising pH (pH 8.5-10.5). The structure of QP gels at different pH was visualized under a confocal microscope. At pH 8.5, the images showed that the QP gels created by acidifying the heated solution was coarse and had irregular particle clusters. However, the structure of QP gels obtained from 5% QP solution at pH 10.5 was regular, and solubility of QP gels at pH 10.5 was higher than that of QP gels at pH 8.5. Moreover, non-heat-treated and pH 8.5 heated samples shared a similar particle size distribution at pH of high protein solubility (pH 3.0 and 8.0), whereas heating QP samples at pH 10.5 caused a dissociation into small particles (0.2–0.8 μm) and larger aggregates (30–200 μm) bounded by hydrophobic interactions.

In another study of Ruiz et al. (2016), the effects of pH on the heat-set QP gel formation and its microstructure were investigated. QP was extracted by adjusting pH from 11.0 to 8.0, followed by acid precipitation at pH 4.5. It was found that QP yield and denaturation decreased as the extraction pH declined. However, there was no gel formation observed after heating 10% QP at pH 11.0 or 10.0. Much aggregation was observed in 10% QP heated at pH 8.0 and 9.0 and eventually formed the denser structured semi-solid gels. For pH 8.0 and pH 9.0, the gelation temperature was around 70 °C, however for pH 10.0 and 11.0, the G′ values continued to rise after cooling. Kaspchak et al. (2017) also studied the influence of pH on the QP heat-set gelation. The pH 3.5 QP gel was denser and more viscoelastic than the pH 7.0 QP gel, which was coarser and showed syneresis. Notably, an elevated protein concentration (15%) resulted in a higher G′ value at pH 7.0, whereas the G′ value did not alter with increasing protein content at pH 3.5. Moreover, the highest G′ value was about 30000 Pa, detected in the 10% QP gel at pH 3.5.

Based on the study of pH-induced gelling process, the effect of divalent ions on the formation of QP heat-set gels was further studied (Kaspchak et al., 2017). At pH 3.5, G′ values of QP gels were decreased after adding $CaCl_2$ and $MgCl_2$, whether the protein concentration was 10% or 15%. For the 10% QP gels, the G′ values of gels with CaCl2 and MgCl2 were approximately 10000 Pa and 3000 Pa, respectively. Then, as the concentration increased to 15%, $CaCl_2$-added gel showed a lower G′ value at 6000 Pa, while the G′ value of $MgCl_2$-added gel reached 20000 Pa. There were similar trends in G′ values of QP gels in the absence of divalent ions at each concentration. Moreover, the 10% QP gel without salt exhibited the highest G′ value at about 30000 Pa. At pH 7.0, G′ values of QP gels without divalent ions were lower than those at pH 3.5 at each concentration. Furthermore, inappropriately adding $CaCl_2$ and $MgCl_2$ led to weaker gels than those without ions. The G′ value of 15% QP gel with $CaCl_2$ was lower than 900 Pa and the G′ value less than 500 Pa for 15% QP gel with $MgCl_2$ addition.

Recently, the influence of various thermal methods on the gel formation was studied (Wang, Dong, Zhu, Shen, Wu, & Zhang, 2021). The researchers discovered that when treated to either no thermal treatment or microwave heating, at least 12% concentration of QP isolates were required to produce firm gels. The concentration of the isolates required to reach 16% or 20%, respectively, to be able to gel when exposed to boiling or baking. Besides, even at a 20% concentration, steaming had a negative effect on the gelation capabilities, and no gel was formed. Likewise, Shen, Tang, and Li (2021) focused on the dying methods of heat-set QP gels. The results demonstrated that spray and vacuum treatments produced weaker gels with lower G′ and G″ values than freeze-drying, which might be due to declined protein solubility.

In addition to the effects of these factors above, enzymatic treatment, as an efficient and mild method, can change and modify the structure of gel. Peptide hydrogels produced from natural proteins via enzymatic hydrolysis have good gel-form properties, and the structural changes of these hydrogels may further affect their own bioactivities. In a recent work, quinoa protein hydrolysate obtained from an *Aspergillus niger* serin peptidase hydrolysis could be employed in the development of semi-solid systems (Galante, De Flaviis, Boeris, & Spelzini, 2020). Additionally, the antioxidant activity of these QP gels was modified during the gelling process.

2. Conclusion and future trends

Quinoa protein is an excellent source of protein due its nutritional value, health benefits and favorable physiochemical properties. Quinoa peptides, as derivatives of quinoa protein, further improve these advantages, thereby making quinoa protein an alternative for other grains to relieve food supply pressure and has the potential to replace dairy protein to promote health. However, most of the bioactivities of quinoa proteins and peptides are based on in vitro experimental results, and the mechanism is unclear. Moreover, in vivo experiments need to be carried out to verify their actual bioactivities and efficacy. In terms of gel properties of quinoa protein and its peptides, the applications of gels or hydrogels obtained from them are still in early stages and urgently require development. At the same time, the relationship between gel

capacities and bioactivities of quinoa protein and peptides also needs to be investigated, which could facilitate the exploitation of drug and cell delivery systems.

3

Chapter III Anti-Colon Cancer Activity of Novel Peptides Isolated from In Vitro Digestion of Quinoa Protein in Caco-2 Cells

Introduction to Chapter 3

According to the literature review in chapter 2, quinoa contains many bioactive substances that are beneficial to health, among which protein considered to be its main nutritional advantage. Recent studies have proved that quinoa proteins or their derived peptides possess different positive bioactivities. However, there are few studies on the anticancer activity of quinoa peptides, and the action mechanism has not been clarified. Additionally, as the main site of nutrition absorption, the incidence of colon cancer increases due to unhealthy diet and habits. Therefore, in this chapter, we investigated the anti-colon cancer activity and mechanism of quinoa protein and peptides in Caco-2 Cells.

This work is an original contribution, adapted from: Fan, X., Guo, H., Teng, C., Zhang, B., Blecker, C., Ren, G. (2022). Anti-Colon Cancer Activity of Novel Peptides Isolated from In Vitro Digestion of Quinoa Protein in Caco-2 Cells. Foods, 11 (2), 194. DOI: 10.3390/foods11020194.

Abstract

Quinoa peptides are the bioactive components obtained from quinoa protein digestion, which have been proved to possess various biological activities. However, there are few studies on the anticancer activity of quinoa peptides, and the mechanism has not been clarified. In this study, the novel quinoa peptides were obtained from quinoa protein hydrolysate and identified by liquid chromatography–tandem mass spectrometry (LC–MS/MS). The anticancer activity of these peptides was predicted by PeptideRanker and evaluated using an antiproliferative assay in colon cancer Caco-2 cells. Combined with the result of histone deacetylase 1 (HDAC1) inhibitory activity assay, the highly anticancer activity peptides FHPFPR, NWFPLPR, and HYNPYFPG were screened and further investigated. Molecular docking was used to analyze the binding site between peptides and HDAC1, and results showed that three peptides were bound in the active pocket of HDAC1. Moreover, real-time quantitative polymerase chain reaction (RT-qPCR), and Western blot showed that the expression of HDAC1, NFκB, IL-6, IL-8, Bcl-2 was significantly decreased, whereas caspase3 expression showed a remarkable evaluation. In conclusion, quinoa peptides may have the potential to protect against cancer development by inhibiting HDAC1 activity and regulating the expression of the cancer-related genes, which indicates that these peptides could be explored as functional foods to alleviate colon cancer.

Keywords: hydrolysate; antiproliferative activity; HDAC1; inhibitory activity; molecular docking

1. Introduction

The gastrointestinal tract is the main place for food digestion and nutrition absorption, and it is the organ that forms the protective barriers, including the mucosal gel layer, pH modulation, and the gut-associated lymphoid tissue, to the external environment (Muenchau et al., 2019; Yan, Sun, Yuan, & Yang, 2017). In recent years, unhealthy eating habits and diet structure have led to an increasing trend of CRC incidence rate, showing a younger trend (Wang et al., 2019). Thus, the interaction between foods and the digestive tract plays an important role in gastrointestinal health. Recent studies have proved the protective role of milk and whole grain on colorectal cancer, and plant-derived compounds possess the ability to inhibit malignant cell proliferation (Neri-Numa et al., 2013; Vieira et al., 2017). Because of their health-promoting benefits and no side effects, many plant-derived peptides are extensively applied in functional foods and nutraceuticals (Chakrabarti, Jahandideh, & Wu, 2014).

Quinoa (*Chenopodium quinoa* wild.) is a pseudocereal with higher nutritional properties due to dietary fiber, vitamins, minerals, and especially its larger amount of essential amino acids (Ruales & Nair, 1992). Recently, quinoa proteins and peptides have been demonstrated to possess a variety of beneficial effects, including antioxidant activity, immunometabolic effect, and antihypertensive effect (Guo et al., 2020; Srdic, Ovcina, Fotschki, Haros, & Llopis, 2020; Swieca, Seczyk, Gawlik-Dziki, & Dziki, 2014; Vilcacundo, Miralles, Carrillo, & Hernandez-Ledesma, 2018). Although quinoa protein has exhibited antiproliferative activity in human colorectal cancer cell lines after simulated gastrointestinal digestion (Vilcacundo, Miralles, Carrillo, & Hernandez-Ledesma, 2018), it is not clear which protein fragments or peptides are more effective and what their mechanism of action is in cancer inhibition.

Histone acetylation and deacetylation are important for the regulation of gene expression (L. B. Zhang et al., 2018). The family of HDACs includes 18 members, and class I HDACs (HDAC 1, 2, 3, and 8) is considered to be the most important ones (Weichert, 2009). Recent studies suggest that HDAC1 has been identified as a therapeutic target for cancer treatment (L. B. Zhang et al., 2018). For example, HDAC1 expression was increased in colorectal cancer and gastric cancer (Eshelman, Shah, Raup-Konsavage, Rennoll, & Yochum, 2017; Q. Zhang et al., 2015). In contrast, HDAC1 knockdown causes cell cycle arrest, reduces cancer cell viability, and induces cancer cell apoptosis (Selokar, St John, Revay, King, Singla, & Madan, 2013). Moreover, pharmacological inhibitors of class I HDAC activity (HDACi) are potent inducers of growth arrest, differentiation, and apoptosis of colon cancer cells in vitro and in vivo (Mariadason, 2008). Except for drug inhibitors, plant-derived peptides have also been shown to be effective inhibitors for the regulation of acetylation and deacetylation. Among them, soybean peptide lunasin has been widely studied as a chemopreventive agent with potential anti-cancer effects (Hsieh, Martinez-Villaluenga, de Lumen, & Hernandez-Ledesma, 2018). In colon cancer cells, lunasin can exert the anti-cancer activity through the regulation of histone acetylation and deacetylation, and the 50% inhibition of lunasin was found to be 61.7 μM (Dia & de Mejia, 2010; Galvez, Chen, Macasieb, & de Lumen, 2001). In addition, the underlying molecular mechanisms of HDAC were also investigated. In breast cancer cells,

HDAC1 can induce proliferation through the upregulation of Snail/IL-8 signals, and IL-8 can suppress the apoptosis of breast cancer MCF-7 cells by down-regulating caspase-3 and up-regulating Bcl-2 (Tang et al., 2017). Meanwhile, IL-6 was also important as IL-8 for the progression of breast cancer cells, and the expression and release of IL-6 and IL-8 were regulated via MAPK and NF-κB mediated (Hartman et al., 2013; Phuagkhaopong et al., 2017). Moreover, HDAC1 has been demonstrated to promote cancer progression by activating HIF1α/VEGFA, ROS/TNF-α, and c-Myc/miR-34a signaling pathways (Chen et al., 2020; Liu et al., 2018; Zhu, Shan, Schiller, Mai, & Peng, 2010). However, there was no research about the quinoa derived peptides as HDAC1 inhibitors in colon cancer.

The purpose of this study was to assess the capability of quinoa peptides released during the simulated gastrointestinal digestion to affect the viability of human colon cancer Caco-2 cells, and screen peptides with HDAC1 inhibitory activity. The structure-activity relationship of these peptides was explored by molecular docking. Furthermore, RT-qPCR and Western blot were assayed to investigate the possible mechanism of quinoa peptides in alleviating colon cancer.

2. Materials and methods

2.1. Materials and Reagents

Quinoa seed (*Mengli-I*) was purchased from the Inner Mongolia Yiji Biotechnology Company (Ulanqab, China). Pepsin from porcine gastric mucosa and pancreatin from porcine pancreas were from Sigma-Aldrich (St. Louis, MO, USA). Hydrochloric acid (HCL), sodium hydroxide (NaOH) and *n*-hexane were acquired from Sinopharm Chemical Reagent Co. Ltd. (Shanghai, China). The VivaFlow 200 tangential flow ultrafiltration system with a molecular weight cut-off (MWCO) of 5 kDa (Sartorius Stedim Biotech, Goettingen, Germany) was used in the ultrafiltration. The primers were synthesized by Sangon Biotech Corporation (Shanghai, China) and the primers used in this work are shown in Table 3-1. Specific primary antibodies against GAPDH, HDAC1, NFκB, IL-6, IL-8, Bcl-2, caspase3 were purchased from Bioss Inc. (Beijing, China).

Table 3-1. Primers used in this study.

Primer name	Gene	Sequence (5' - 3')
GAPDH - F	GAPDH	GTATCGTGGAAGGACTCATGAC
GAPDH - R	GAPDH	ACCACCTTCTTGATGTCATCAT
HDAC1 - F	HDAC1	ATCCGCATGACTCATAATTTGC
HDAC1 - R	HDAC1	GGATGGAGCGCAAGAATTTAAT
EP300 - QF	EP300	GTTCCTTCCTCAGACTCAGTTC
EP300 - QR	EP300	CATTATAGGAGAGTTCACCGGG
NFκB - F	NFκB	GGCGAGAGGAGCACAGATAC

NFκB - R	NFκB	CGGCAGTCCTTTCCTACAAG
TNF-α- F	TNF-α	TAGCCCATGTTGTAGCAAACCC
TNF-α- R	TNF-α	GGACCTGGGAGTAGATGAGGT
Snail - F	Snail	TTTACCTTCCAGCAGCCCTA
Snail - R	Snail	GGACAGAGTCCCAGATGAGC
MAPK - F	MAPK	TGCACATGCCTACTTTGCTC
MAPK - R	MAPK	AGGTCAGGCTTTTCCACTCA
VEGFA - F	VEGFA	GCAGAATCATCACGAAGTGGT
VEGFA - R	VEGFA	CCAGGGTCTCGATTGGATGG
c-Myc - F	c-Myc	AGCGACTCTGAGGAGGAACA
c-Myc - R	c-Myc	CTCTGACCTTTTGCCAGGAG
IL-8 - F	IL-8	GTGCAGTTTTGCCAAGGAGT
IL-8 - R	IL-8	AAATTTGGGGTGGAAAGGTT
IL-6 - F	IL-6	AGACAGCCACTCACCTCTTCA
IL-6 - R	IL-6	TTCTGCCAGTGCCTCTTTGCT
Bcl-2 - F	Bcl-2	TGGGATTCCTGCGGATTGAC
Bcl-2 - R	Bcl-2	GTCTACTTCCTCTGTGATGTTGT
Caspase3 - F	Caspase3	GGTTCATCCAGTCGCTTTGT
Caspase3 - R	Caspase3	CGGTTAACCCGGGTAAGAAT

2.2. Preparation of Quinoa Protein Concentrate, Quinoa Protein Hydrolysate and Quinoa Peptides

The quinoa protein was prepared following the protocol of Guo et al. with slight modifications (Guo et al., 2020). Quinoa seeds were washed five times with distilled water to remove saponins, and dried in a 50 °C drying oven. The dried seeds were ground to flour by using FOSS CT293 Cyclotec (Foss Tecatur AB, Hillerød, Denmark), sifted through a 60-mesh sieve, and defatted with n-hexane. The defatted quinoa flour was suspended in water (1:10, *w/v*), and its pH was adjusted to 8.0 with 2 M NaOH. The suspension was stirred for 1 h and centrifuged at 6000× *g* for 30 min at room temperature. Adjusting the pH of the supernatant to 4.0 with 2 M HCl. The supernatant stabilized for 1 h at 4 °C and was then centrifuged for 30 min at 6000× *g*. The precipitate was freeze-dried and stored at 4 °C for the next experiment.

The quinoa protein hydrolysate was prepared following the previous study (Vilcacundo, Miralles, Carrillo, & Hernandez-Ledesma, 2018). Briefly, QP was dissolved in deionized water (1:100, g/mL) and adjusted the pH of QPH solution to pH 2.0 with addition of 1M HCl. Then the solution was hydrolyzed by pancreatin (5%, *w/w*) for 1 h in a 37 °C water bath shaker, stopping the reaction by adjusting the pH at 7.0 with 1 M NaOH. Simulated intestinal fluid containing pancreatin (5%, *w/w*) was mixed with hydrolysate in the gastric phase for 1 h at 37 °C in a water bath. The reaction was stopped in a boiling water bath for 5 min. QPH digest was cooled to

room temperature and collected after centrifugation. The suspension was frozen and stored at −20 °C. The control sample without enzyme was used in the same condition.

QPH digest was filtered through a 5 kDa ultrafiltration membrane. Fractions MW < 5 kDa and MW > 5 kDa were obtained and frozen dried and kept at −20 °C until further analysis. The fraction with high antiproliferative activity was further identified using electrospray ionization quadrupole time-of-flight mass spectrometry as described in our previous study [11].

2.3. Peptide Screening and Synthesis

The potential peptide candidates were searched against the BIOPEP database (http://www.uwm.edu.pl/biochemia, accessed on 5 May 2021). The potential biological activity of these identified peptides was predicted using the scores calculated in PeptideRanker (http://distilldeep.ucd.ie/PeptideRanker/, accessed on 5 May 2021) and the theoretical bioactivity was scored from 0 to 1 so that the higher value means a higher probability of being bioactive. The toxicity of all these peptides was scored in ToxinPred (http://crdd.osdd.net/raghava/toxinpred/, accessed on 5 May 2021).

The predicted potential bioactivity peptides were synthesized through the conventional Fmoc solid-phase synthesis method at Sangon Biotech Co., Ltd. (Shanghai, China). The purity of the peptide was verified by high performance liquid chromatography (HPLC). Molecular masses were confirmed using liquid chromatography–tandem mass spectrometry (LC–MS/MS).

2.4. Cell Proliferation Assay

The human CRC cell line Caco-2 was obtained from American Type Cell Collection (ATCC, Manassas, VA, USA) and cultured in MEM medium supplemented with 20% FBS, 1% penicillin, and 1% streptomycin. Cells were maintained at 37 °C in a humidified incubator containing 5% CO_2 and 95% air. The medium was changed every 24 h. All cells were assayed within 5–15 passages. Utilizing the CCK-8 kit (Biorigin, Beijing, China), the toxicity test was first performed. Caco-2 cells (100 uL) were incubated in the 96-well plate (1×10^5 cells/well) for 24 h, then the original medium was replaced with fresh medium containing different concentrations of QP (1-8 g/L), QPH (1-8 g/L), fraction MW < 5 kDa(1-8 g/L), fraction MW > 5 kDa(1-8 g/L), and selected peptides ranging from 0 to 2 g/L. After 24 h co-cultivation, the medium was discarded and washed with PBS 2 times, and a fresh medium with 10% CCK-8 reagent was added to each cell. Another 1 h later, the absorbance (OD value) was determined by an enzyme-labeling instrument at a wavelength of 450 nm. Experiments were performed in triplicate with at least three replicates per concentration, and results were expressed as percentage of negative control (non-treated Caco-2 cells).

For the proliferation experiments, Caco-2 cells were seeded into 96-well plates at a density of 2.5×10^4 per well for 24 h, the incubation was continued for 72 h. After that, the subsequent washing and CCK-8 reaction process were the same as performed in the toxicity test. Finally, the absorbance was also detected at 450 nm. Analyses were

performed in triplicate with at least three replicates per concentration, and results were also shown as the percentage of non-treated Caco-2 cells.

2.5. HDAC1 Inhibitory Activity Assay

HDAC1 activity was determined using the HDAC1 inhibitor screening assay kit (Abnova, Taipei, Taiwan). The assay was performed according to the manufacture instruction manual. Briefly, the sample wells were added 140 μL assay buffer, 10 μL diluted HDAC1, and 10 μL peptide samples (0.05–2 g/L). The trichostatin A was set as the positive control, and the sample buffer was set as the negative control. We initiated the reactions by adding 10 μL of HDAC substrate to all the wells being used. Cover the plate with the plate cover and incubate on a shaker for 30 min at 37 °C. Remove the plate cover and add 40 μL of developer. Cover the plate with the plate cover and incubate for 15 min at room temperature. Remove the plate cover and read the fluorescence using an excitation wavelength of 340–360 nm and an emission wavelength of 440–465 nm. IC_{50} values were calculated using GraphPad Prism 8 software. Analyses were performed in triplicate with at least three replicates per concentration.

2.6. Molecular Docking

The crystal structure of HDAC1 was obtained from the Protein Data Bank (PDB ID: 4BKX). Water, sulfate and acetate molecules were removed from the system. Meanwhile, structural zinc ion was left because of its importance in the catalytic activity and conserved position of the crystal structure of HDAC1. The structure of studied peptides was constructed using UCSF Chimera 1.13.1. Molecular docking simulations were performed using MGL Tools 1.5.6 and AutoDock Tools 4.2 (Trott & Olson, 2010), and the grid box was centered on Zn^{2+}. The best docking models of peptides in the active pocket of HDAC1 were displayed according to the binding energy value. Finally, the binding sites were analyzed by using PyMOL 1.5.0.3.

2.7. Quantitive Real Time-Polymerase Chain Reaction (RT-qPCR)

After co-cultivation with different concentrations of selected peptides, total RNA of Caco-2 cells was extracted using TRIzol Reagent (Life Technologies, Carlsbad, CA, USA) according to the manufacturer's protocol. Total RNA was treated with DNase I and reverse-transcribed into cDNA using the cDNA Synthesis SuperMix kit (TransGen Biotech, Beijing, China). The mRNA expressions were then quantified by RT-qPCR using the TransStart Top Green qPCR Supermix kit (TransGen Biotech, Beijing, China) and the Applied Biosystems 7500 real-time PCR systems (Applied Biosystems, USA). Analyses were performed in triplicate with at least three replicates per sample, and gene expression was normalized to the geometric mean of reference genes (GAPDH) using the $2^{-\Delta\Delta Ct}$ method.

2.8. Western Blot Analysis

Total proteins were extracted using mammalian protein extraction kit (CWBIO, Beijing, China). After being treated with different concentrations of selected peptides,

Caco-2 cells were washed three times with PBS and incubated with lysis buffer on ice for 20 min. Subsequently, the cell lysate was centrifuged at 12,000× *g* at 4 °C for 20 min to collect the supernatant. The protein samples for each treatment were loaded and separated in 12% sodium dodecyl sulfate-polyacrylamide gel. Then, all samples were transferred to an Immun-Blot PVDF membrane (0.22 um) using Bio-Rad trans-blot apparatus (Bio-Rad, Cambridge, MA, USA). When the transfer was achieved, the membrane was blocked in blocking buffer at room temperature. After 1 h of blocking, the membrane was incubated with primary antibody at 4 °C for overnight, followed by incubation with a secondary antibody (goat anti-rabbit IgG-HRP) for 1 h at room temperature. After hybridization, the membrane was incubated in immobilon ECL ultra Western HRP substrate (Millipore Corporation, MA, USA) for 20 min. The specific band for the target protein was detected by Tanon 5200 (Tanon Corporation, Shanghai, China). The bands were quantified using ImageJ, and the intensities of the bands were normalized to loading control (GAPDH). Experiments were repeated at least four times per sample.

2.9. Statistical Analysis

All data are expressed as the means ± standard deviation (SD). Differences among groups were determined by one-way ANOVA analysis and Duncan's multiple range tests with SPSS software (IBM, New York, NY, USA). Significant differences were expressed at $p < 0.05$ and $p < 0.01$.

3. Results

3.1. Antiproliferative Activity of QPH against Caco-2 Cells

The quinoa protein yield and purity were detected according to the previous method, the results were 6.85% and 86.02%, respectively. The hydrolysis degree of QPH was examined by Adler–Nissen's method and the result was 20.46%.

In this study, the toxicity test was performed in Caco-2 cells. The number of viable cells was calculated by a CCK-8 assay after being incubated with different concentrations of samples for 24 h. As shown in Figure 3-1A, no toxicity was observed over four groups at concentrations ranging from 1 to 8 g/L. When the concentrations of samples were up to 16 g/L, four groups all showed slight toxicity. The antiproliferative activity was assessed using a CCK-8 assay. The result was shown in Figure 3-1B, the proliferation of Caco-2 cells was gradually inhibited with the increasing sample concentration (1–8 g/L) after 72 h incubation with samples. Meanwhile, the QPH and fraction < 5 kDa have higher inhibitory activities than QP and fraction > 5 kDa, and the inhibition rate under QPH and fraction < 5 kDa treatment can reach 51.45 and 53.93%, respectively, at a concentration of 8 g/L.

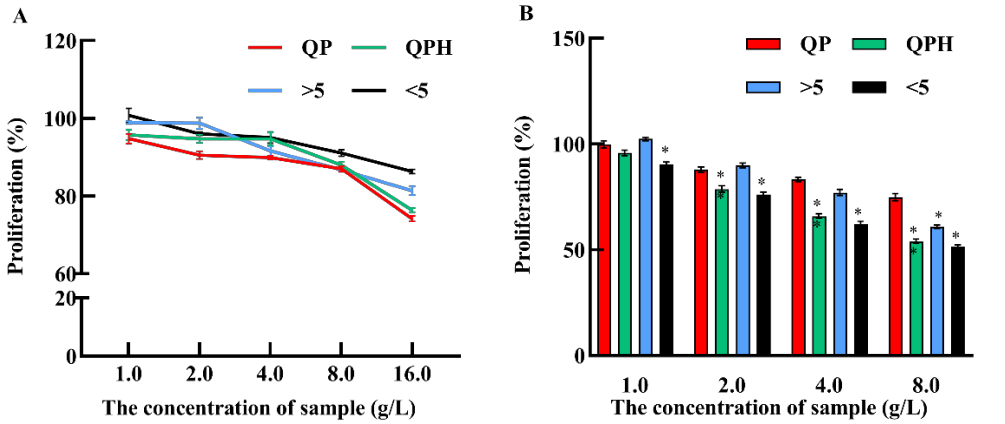

Figure 3-1. Cytotoxic effect and anti-proliferative activity of different fractions from quinoa protein on Caco-2 cells. (A) Dose dependent effect of different quinoa protein fractions on Caco-2 cells after 24 h treatment; (B) the cell proliferation rate of Caco-2 cells under gradient concentration of quinoa protein fractions after 72 h treatment. QP: quinoa protein concentrate, QPH: quinoa protein hydrolysate, >5 kDa: fractions MW > 5 kDa, <5 kDa: fractions MW < 5 kDa. * $p < 0.05$ and ** $p < 0.01$ indicate significant and highly significant differences between the QP and other treatments, respectively.

3.2. In Silico Analysis and Antiproliferative Activity of Quinoa Peptides

Based on the results of the previous step, fraction < 5 kDa possessed stronger antiproliferative activity. Using ESI-Q-TOF–MS/MS to detect the quinoa peptides of fractions < 5 kDa, the identification and *in silico* analysis results are listed in Table 3-2, and the MS spectrum are shown in Figure S1. The bioactivity of identified peptides was predicted using the PeptideRanker program, and thirteen quinoa peptides were predicted to have high bioactivity with predicted scores over 0.7. The prediction results of ToxicPred showed that none of them were considered to be toxic. Among these peptides, some of them share similar amino acid sequences. For example, FHPFPR was measured as a part of PNFHPFPR, SLPNFHPFPR and NSLSLPNFHPFPR. Similarly, SVENWFPLPR and INNIFRPF contained sequence NWFPLPR and NIFRPF, respectively. Nevertheless, according to the PeptideRanker score results, the shorter peptides, including FHPFPR, NWFPLPR and NIFRPF, have higher activity.

Table 3-2. Identification of quinoa peptides (fraction < 5 kDa) and their PeptideRanker score and toxicity.

No.	Peptide	Ion (m/z)	Calculated Mass	Peptides Score	Toxicity
1	FHPFPR	799.90	799.92	0.9745	Non
2	NWFPLPR	929.00	929.08	0.9722	Non
3	PNFHPFPR	1011.15	1011.14	0.9631	Non

4	NIFRPF	793.00	792.92	0.9402	Non
5	SLPNFHPFPR	1211.40	1211.38	0.9388	Non
6	INNIFRPF	1020.20	1020.19	0.8666	Non
7	SVENWFPLPR	1244.50	1244.40	0.8594	Non
8	NSLSLPNFHPFPR	1525.80	1525.72	0.8383	Non
9	NSWGPNWGDHG	1226.10	1226.22	0.8118	Non
10	HYNPYFPGGA	1122.20	1122.19	0.8021	Non
11	FGGGTLGHPW	1028.10	1028.12	0.7855	Non
12	GLESPNYPWPH	1296.40	1296.39	0.7791	Non
13	HGSLGFLPR	983.10	983.13	0.7758	Non

Subsequently, a CCK-8 assay was conducted to characterize which peptides are mostly responsible for inhibiting cancer cell proliferation. The results were listed in Table 3-3. In a certain range, the inhibition rate increased with increased peptides concentrations. However, there was no significant change was observed while the concentration of peptides was up to 2 g/L. Among these peptides, the peptides FHPFPR, PNFHPFPR, NWFPLPR and HYNPYFPGGA had more than 30% inhibition at a concentration of 1 g/L.

Table 3-3. Dose-dependent effects of quinoa peptides released from gastrointestinal digestion on cell viability.

Peptide	Viable Cells (%) at Different Concentrations (g/L)				
	0	1×10^{-1}	5×10^{-1}	1	2
FHPFPR	99.96 ± 1.53	90.04 ± 1.26 ^{e}	75.46 ± 0.86 ^{f}	51.41 ± 0.80 ^{k}	50.82 ± 0.76 ^{j}
NWFPLPR	101.01 ± 1.12	92.86 ± 1.10 ^{d}	79.99 ± 0.86 ^{e}	64.02 ± 1.39 ^{j}	63.18 ± 0.83 ^{i}
PNFHPFPR	100.97 ± 2.29	90.46 ± 1.43 ^{e}	77.26 ± 1.65 ^{f}	65.32 ± 1.45 ^{j}	61.67 ± 1.64 ^{i}
NIFRPF	100.75 ± 1.69	100.10 ± 1.03 ^{a}	85.11 ± 0.66 ^{d}	70.29 ± 0.56 ^{h}	70.55 ± 2.01 ^{g}
SLPNFHPFPR	99.55 ± 0.95	97.79 ± 1.14 ^{bc}	87.21 ± 0.32 ^{d}	78.51 ± 0.26 ^{g}	78.00 ± 0.80 ^{f}
INNIFRPF	100.40 ± 0.39	100.40 ± 1.29 ^{a}	92.05 ± 1.07 ^{c}	80.44 ± 0.68 ^{f}	80.61 ± 0.41 ^{e}
SVENWFPLPR	100.42 ± 0.75	99.43 ± 1.39 ^{ab}	95.50 ± 3.60 ^{b}	92.14 ± 0.69 ^{c}	91.04 ± 1.53 ^{c}
NSLSLPNFHPFPR	99.21 ± 1.60	100.79 ± 0.52 ^{a}	92.78 ± 2.20 ^{c}	86.55 ± 0.58 ^{e}	83.56 ± 0.71 ^{d}
NSWGPNWGDHG	101.06 ± 1.21	98.87 ± 0.60 ^{abc}	98.60 ± 2.28 ^{a}	99.58 ± 1.08 ^{a}	97.92 ± 1.41 ^{a}
HYNPYFPGGA	101.54 ± 0.74	93.69 ± 0.68 ^{d}	82.34 ± 1.36 ^{e}	67.44 ± 1.26 ^{i}	67.10 ± 1.87 ^{h}
FGGGTLGHPW	98.81 ± 1.76	97.09 ± 0.74 ^{c}	91.65 ± 0.43 ^{c}	90.41 ± 0.69 ^{d}	89.72 ± 0.60 ^{c}
GLESPNYPWPH	100.33 ± 1.34	99.75 ± 1.06 ^{a}	99.32 ± 1.05 ^{a}	97.40 ± 0.73 ^{b}	97.70 ± 0.33 ^{ab}
HGSLGFLPR	100.26 ± 1.66	97.35 ± 1.03 ^{c}	96.91 ± 0.77 ^{ab}	96.81 ± 0.88 ^{b}	95.80 ± 0.62 ^{b}

Results are shown as mean ± standard deviation (SD). Values not sharing the same small letter in a column indicate significant changes between samples, by Fisher's test ($p < 0.05$).

3.3. HDAC1 Inhibitory Activity of Quinoa Peptides

To measure the effect of the identified quinoa peptides on HDAC1 activity, an HDAC1 inhibitory activity assay was conducted. For these peptides, half of them can reach to IC50 value, including FHPFPR, PNFHPFPR, NWFPLPR, HYNPYFPGGA, NIFRPF, SLPNFHPFPR and INNIFRPF (Figure 3-2). The rest of the peptides failed

to attain the IC50 value. Moreover, the shorter peptides have higher HDAC1 inhibitory activity, as predicted in Section 3.2. Taken together with the result of cell proliferation, quinoa peptides FHPFPR, NWFPLPR and HYNPYFPG were used for the next experiments, and their HDAC1 inhibitory activity were performed with IC50 values of 0.87, 1.27, and 1.85 g/L, respectively.

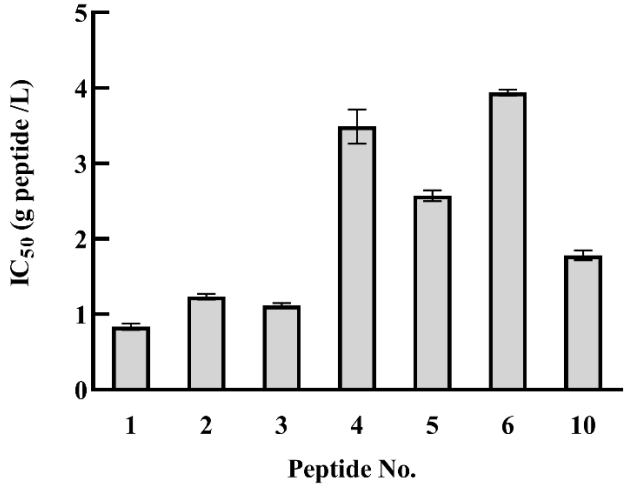

Figure 3-2. HDAC1 inhibitory activities of quinoa peptides obtained from QPH fraction < 5 kDa. 1: FHPFPR, 2: NWFPLPR, 3: PNFHPFPR, 4: NIFRPF, 5: SLPNFHPFPR, 6: INNIFRPF, 10: HYNPYFPGGA. HDAC1: histone deacetylase 1, QPH: quinoa protein hydrolysate.

Molecular docking simulations of HDAC1-peptide were conducted using the AutoDock Vina program of AutoDock Tools 4.2. The best binding poses of FHPFPR, NWFPLPR, HYNPYFPGGA to inhibit HDAC1 activity were shown in Figure 3-3, and the binding energy of these peptides were -6.56, -6.48, -6.41 kcal/mol.

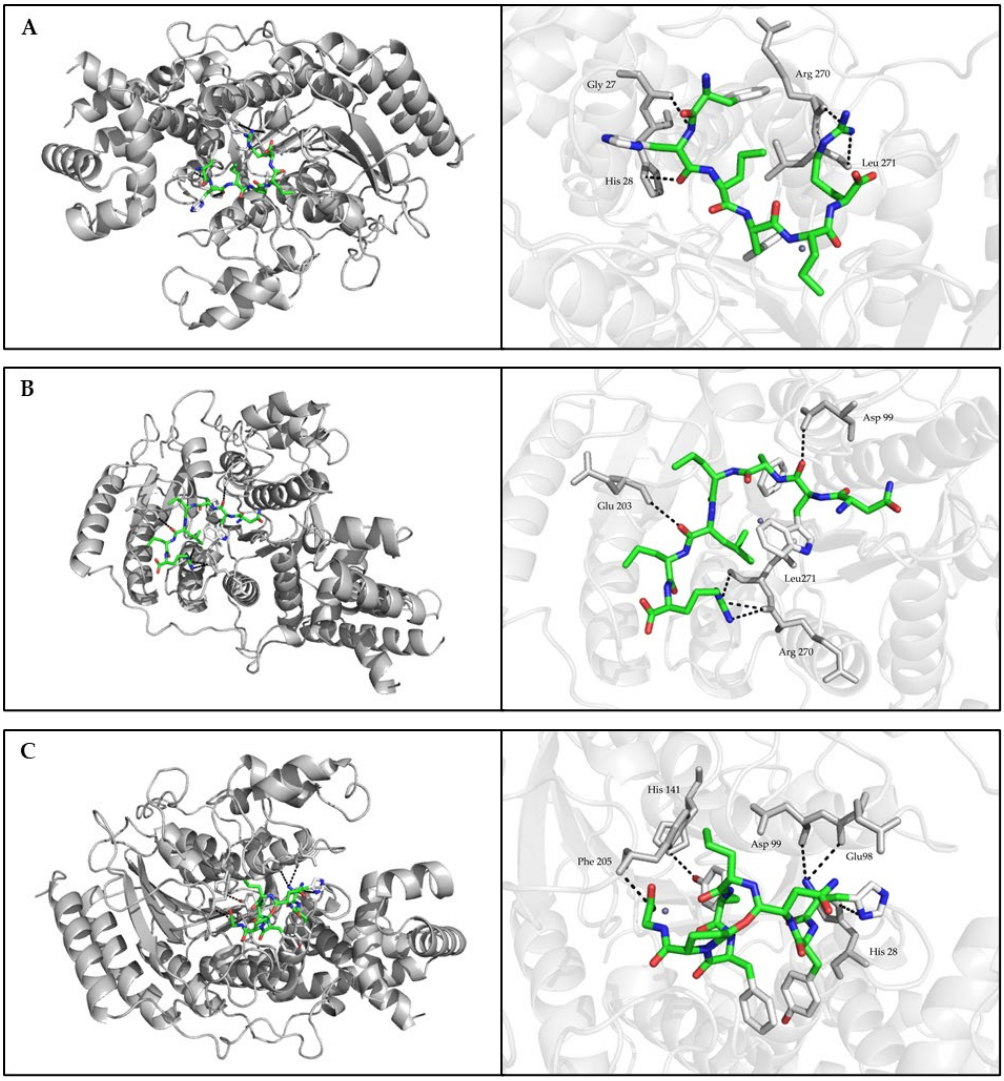

Figure 3-3. Best binding mode between HDAC1 and studied peptides retrieved from focused molecular docking. (A) FHPFPR, (B) NWFPLPR, (C) HYNPYFPGGA. The general overview was shown in the left panel. The interaction (block dotted lines) between the residues of HDAC1 (grey sticks) and peptides (green sticks) was zoomed in the right panel.

3.4. The Effect of Quinoa Peptides on HDAC1-Induced Cancer Progression

Although quinoa peptides have been demonstrated to possess various bioactivities, the mechanisms by which these anti-cancer peptides exert their inhibitory effect in human colon cancer cells are not fully understood. Until recently, the inhibitory effect

of HDAC1 has been proved in different types of cancer cells, including breast cancer, gastric cancer, pancreatic cancer, non-small cell lung cancer, and colon cancer. Targeted inhibition of HDAC is an effective anticancer therapy (Galvez, Chen, Macasieb, & de Lumen, 2001).

To study which regulation HDAC1 may participate in to inhibit the proliferation of colon cancer Caco-2 cells, qPCR and Western blot were carried out to detect related target genes. The results of mRNA expression were shown in Figure 3-4.

After treatment with peptides 1, 2, 10 in Caco-2 cells, the HDAC1 expression was significantly suppressed, whereas the expression of EP300 was not significantly changed. Previous studies reported that two small soluble members of CXC chemokine family, IL-6 and IL-8, are critical to the development of cancer cells (Hartman et al., 2013; Singh, Simoes, Howell, Farnie, & Clarke, 2013). We detected the expression of these genes, and the results showed that there was a significant decrease in IL-6 and IL-8 expression after treatment. Compared to the control, the expression of IL-6 and IL-8 was downregulated to 0.18–0.38 and 0.54–0.69 fold, respectively. Further research suggested IL-8 can inhibit the apoptosis of human breast cancer cells via up-regulating Bcl-2 and down-regulating caspase-3 (Tang et al., 2017). In this study, Bcl-2 expression was inhibited with the down-regulation of IL-8 while caspase3 expression was significantly decreased. In addition, NF-κB and MAPK were important signals responsible for the transcriptions of IL-8 and IL-6 (Phuagkhaopong et al., 2017). Moreover, the expression results showed that NF-κB was significantly repressed after treatment while not MAPK, and there was a slight downregulation in the Snail expression. In previous studies, tumor-related genes TNF-α, VEGFA, and c-Myc were considered to serve important roles in tumorigenesis and tumor development and regulated by HDAC1 (Chen et al., 2020; Liu et al., 2018; Zhu et al., 2010). We tested the effects of quinoa peptides on the expression of TNF-α, VEGFA, and c-Myc. The data showed that TNF-α expression fold change was downregulated to 0.60–0.82, However, there was a minor decrease in the expression of VEGFA and c-Myc.

Subsequently, a Western blot assay was conducted to confirm the expression in protein levels of related genes with significant changes mentioned above (Figure 3-5). The results showed that the expression levels of HDAC1, IL-6, IL-8, NFκB, Bcl-2 were significantly increased. In contrast, there was a significant increase in caspase3 expression. The expression levels of all the above proteins were consistent with the results on the transcription level.

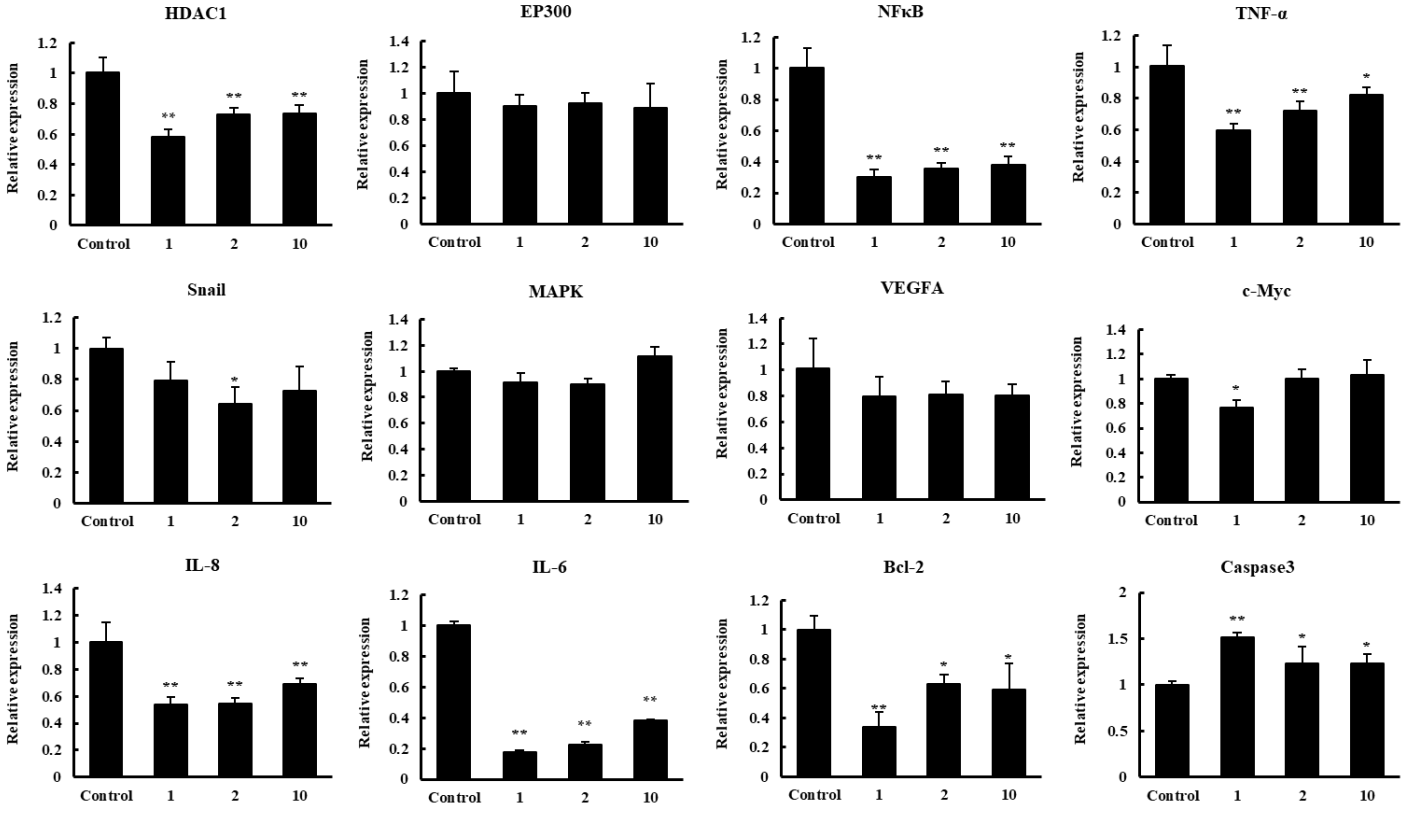

Figure 3-4. The effect of quinoa peptides 1, 2, 10 on the mRNA transcript levels of HDAC1, EP300, NFκB, TNF-α, Snail, MAPK, VEGFA, c-Myc, IL-8, IL-6, Bcl-2, and caspase3. The mRNA expres-sion results are displayed as the fold increase of mRNA expression normalized to GAPDH and shown in mean ± SD. * $p < 0.05$ and ** $p < 0.01$ versus control group.

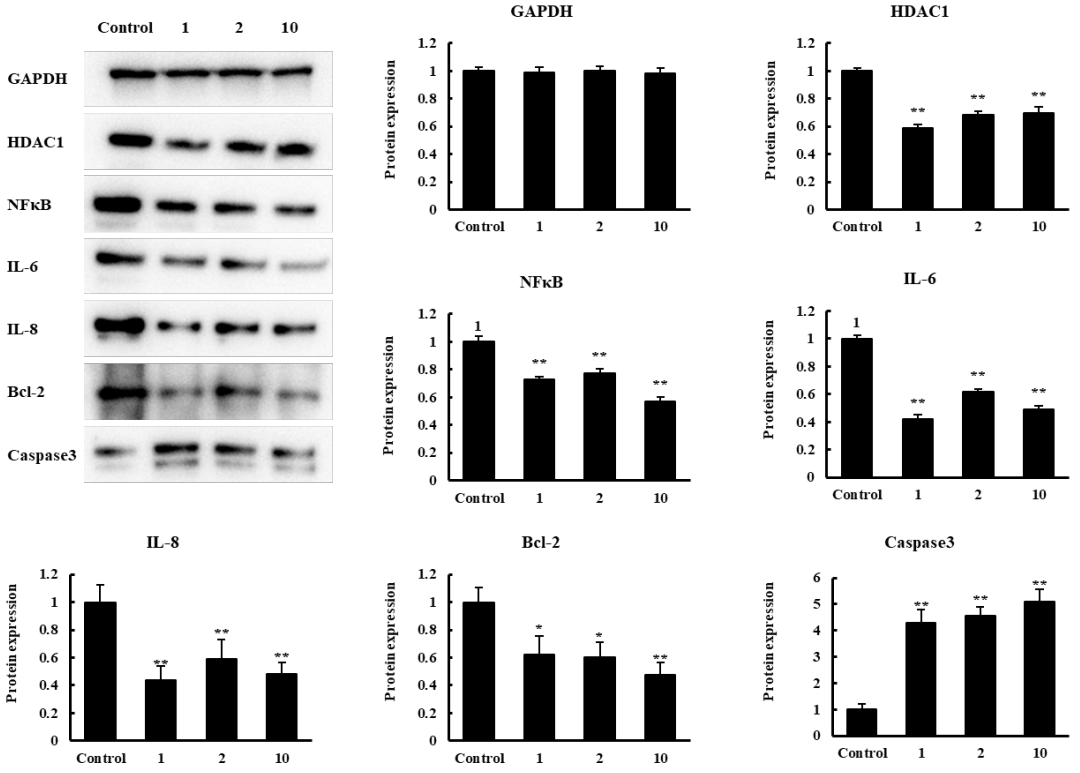

Figure 3-5. Western blot analysis. The effect of quinoa peptides 1, 2, 10 in protein levels of GAPDH, HDAC1, NFκB, IL-6, IL-8, Bcl-2, caspase3. GAPDH was set as the loading control. Expression was normalized to GAPDH expression and shown in mean ± SD. * $p < 0.05$ and ** $p < 0.01$ versus control group.

4

Chapter IV Supplementation of quinoa peptides alleviates colorectal cancer and restores gut microbiota in AOM/DSS-treated mice

Introduction to Chapter 4

According to the chapter 2 and chapter 3, quinoa derived peptides showed anti-cancer effects in cultured colon cancer cells. However, most of these experiments were chemical and cell experiments carried out in vitro. No study has focused on their effects in vivo, particularly on intestinal diseases. On the one hand, the incidence of intestinal diseases, especially colitis and colon cancer, is rising rapidly and tends to be younger. On the other hand, as the site of digestion and absorption of various nutritional active substances, intestinal health is required for the bioactive substances to function. Therefore, in this chapter, we investigated the effect of quinoa protein and its hydrolysate on an azoxymethane/dextran sulfate sodium (AOM/DSS)-induced mouse model of colorectal cancer (CRC) and examined its underlying mechanism using gut microbiota analysis and short chain fatty acids (SCFAs) production analysis.

This work is an original contribution, adapted from: Fan, X., Guo, H., Teng, C., Yang, X., Qin, P., Richel, A., Zhang, L., Blecker, C., Ren, G. (2023). Supplementation of quinoa peptides alleviates colorectal cancer and restores gut microbiota in AOM/DSS-treated mice. Food Chemistry, 408, 135196. DOI: 10.1016/j.foodchem.2022.135196.

Abstract

Quinoa protein hydrolysate has been previously reported to exert anti-cancer effects in cultured colon cancer cells. Here, we investigated the effect of quinoa protein and its hydrolysate on an azoxymethane/dextran sulfate sodium (AOM/DSS)-induced mouse model of colorectal cancer (CRC) and examined its underlying mechanism using gut microbiota analysis and short chain fatty acids (SCFAs) production analysis. Our results showed that quinoa protein or its hydrolysate mitigated the clinical symptoms of CRC and increased SCFAs contents in colon tissues. Moreover, administration of quinoa protein or its hydrolysate partially alleviated gut microbiota dysbiosis in CRC mice by decreasing the abundance of pathogenic bacteria and increasing the abundance of probiotics. Additionally, PICRUSt analysis revealed that the functional profile of gut microbiota in the quinoa protein treated groups was more similar to that of the control group. These findings indicated that the modulation of gut microbiota by quinoa protein diet intervention may ameliorate AOM/DSS-induced CRC.

Keywords: quinoa protein hydrolysate; gastrointestinal digestion; short chain fatty acids; microbial dysbiosis; colon cancer

1. Introduction

Colorectal cancer (CRC) is the third most common cancer and the second leading cause of cancer deaths worldwide, and its incidence has been increasing globally, especially in high income regions (Akimoto et al., 2021). It is estimated than in 2019, there were 145,600 new CRC cases and approximately 51,020 CRC deaths (Siegel, Miller, & Jemal, 2019). Moreover, CRC incidence and mortality have been rising among young people aged 18 to 35, which has been attributed to modifiable risk factors like alcohol consumption, obesity, physical inactivity, consumption of red and processed meat, and low consumption of dietary fiber and whole grains (Islami et al., 2018; Keum & Giovannucci, 2019). Currently, CRC is mainly treated using radiotherapy, chemotherapy, surgery, immunotherapy, or targeted therapy. However, these treatments are primarily used for advance-stage colon cancer. Recently, dietary intervention is recognized as an effective strategy without side effects and has drawn increasing attention (Piawah & Venook, 2019; Yoo et al., 2018).

Bioactive peptides are small in size, flexible in structure, easily absorbed, and nontoxic. Many studies have shown that bioactive peptides can improve the intestinal microenvironment, enhance the intestinal barrier, and suppress CRC development (Sah, Vasiljevic, McKechnie, & Donkor, 2015; Zhao, Hu, Zuo, & Wang, 2018). Peptides isolated from the common beans Azufrado Higuera and Bayo Madero exhibited strong antiproliferative effects against RKO, HCT-116, and KM12L4 colon cancer cells (Vital, de Mejia, Dia, & Loarca-Pina, 2014). Lunasin, a bioactive peptide identified in soybean, was reported to inhibit the growth of KM12L4 colon cancer cells by triggering cell cycle arrest at the G2/M phase and activating the mitochondrial pathway of apoptosis (Dia & Gonzalez de Mejia, 2011; Dia & Mejia, 2010). Similarly, lunasin also exerted potent anti-colon cancer effects by promoting apoptosis in HCT-116 colon cancer cells (Montales, Simmen, Ferreira, Neves, & Simmen, 2015).

The gut microbiota is an important part of the gut microenvironment and has a significant role in host physiology in health and disease. Recent studies have highlighted the relationship between the gut microbiota and gastrointestinal tract disorders, including colorectal cancer (Saus, Iraola-Guzman, Willis, Brunet-Vega, & Gabaldon, 2019). It was reported that the gut microbiota composition differs between healthy individuals and those with CRC, and that gut microbiota changes may affect metabolism and immune function (Wang et al., 2018). Moreover, dietary interventions influence intestinal disorders by directly or indirectly modifying the gut microbiota, and consequently have a beneficial impact on host health (Aleksandrova, Romero-Mosquera, & Hernandez, 2017).

Quinoa (Chenopodium quinoa Willd.), a pseudocereal that originated in the Andean region of South America, is a nonconventional source of protein with excellent nutritional value (Montserrat-de la Paz et al., 2021). Additionally, recent studies indicated that quinoa protein hydrolysate has health benefits, including the capacity to scavenge 2,2-diphenyl-1-picrylhydrazyl and peroxyl radicals, as well as antihypertensive and anti-colon cancer effects (Aluko & Monu, 2003; Guo et al., 2021; Nongonierma, Le Maux, Dubrulle, Barre, & FitzGerald, 2015; Vilcacundo, Miralles, Carrillo, & Hernandez-Ledesma, 2018). However, because most of these findings are

based on in vitro studies, they may not reflect the in vivo situation. In this study, we used a mouse model of azoxymethane/dextran sulfate sodium (AOM/DSS)-induced CRC to study the effects of quinoa protein and quinoa protein hydrolysate on CRC development. The aims of this study were to (1) compare the effects of quinoa protein and quinoa protein hydrolysate on alleviating CRC, (2) determine the content of short chain fatty acids (SCFAs) in colon tissues, (3) analyze changes in gut microbiota composition, and (4) determine the correlation between phenotypic indicators, gut microbiota, and SCFAs in colon tissues.

2. Materials and methods

2.1. Materials and Reagents

Quinoa seeds (*Mengli-I*) were obtained from the Inner Mongolia Yiji Biotechnology Company (Ulanqab, China). Hydrochloric acid (HCl), sodium hydroxide (NaOH), and n-hexane were purchased from Sinopharm Chemical Reagent Co. Ltd. (Shanghai, China). Porcine gastric mucosa pepsin and porcine pancreatin were purchased from Sigma-Aldrich (St. Louis, MO, USA). Hematoxylin and eosin were purchased from Biorigin (Beijing, China). AOM and DSS were purchased from MP Biomedicals Inc. (Irvine, CA, USA).

2.2. Sample preparation

The quinoa protein was prepared as described in our previous study with slight modifications (Fan et al., 2022). Briefly, quinoa flour was defatted with acetone and ethanol. The defatted quinoa flour was suspended in distilled water (1:10, *w/v*), and the pH was adjusted to 8.0 using 2 M NaOH. The suspension was then mixed on a magnetic stirrer for 1 h and then centrifuged at 7500 g for 30 min at room temperature. The supernatant was then collected, its pH adjusted to 4.0, and then left to stand for 1 h at 4°C. It was then centrifuged and the precipitate was neutralized and freeze-dried. The quinoa protein hydrolysate was obtained as previously described. Briefly, 1 g quinoa protein was dissolved in 100 mL of deionized water and adjusted the pH of the mixture to around 2.0. Gastric digestion was done by adding pancreatin (5%, *w/w*) to the quinoa protein solution followed by incubation on a water bath shaker for 1 h at 37°C. Digestion was then stopped by adjusting the pH to 7.0 using 1 M NaOH. The gastric digest was then mixed with an intestinal fluid mimic containing pancreatin (5%, *w/w*) and incubated for 1 h at 37°C. The reaction was then stopped by heating for 5 min at 100°C on a water bath. The Quinoa protein hydrolysate digest was then cooled to room temperature and collected after centrifugation. The suspension was freeze-dried and stored at 4°C.

2.3. Animals and experimental design

Mouse experimental protocols adhered to National Institutes of Health guidelines for the care and use of laboratory animals. Ethical approval for mouse experiments was granted by the experimental animal ethics committee of Pony testing international group (approval number: PONY-2020-FL-85). Six-week-old male C57BL/6 mice

were purchased from Beijing Vital River Laboratory Animal Technology Co., Ltd. (Beijing, China) and housed in cages with stainless steel grids at 18–25°C, 60±5% humidity, with standard 12:12 h light-dark cycles. The mice were first acclimatized for 7 days with free access to a standard chow (AIN-93M Diet, Beijing Huafukang Bioscience Co., Ltd., Beijing, China) and sterile water. The mice were randomly divided into the control (CTL) group, the AOM/DSS-induced (CRC) group, the AOM/DSS + low quinoa protein (QPL) group, the AOM/DSS + high quinoa protein (QPH) group, the AOM/DSS + low quinoa protein hydrolysate (QPHL) group, and the AOM/DSS + high quinoa protein hydrolysate (QPHH) group. Each group consisted of 8 mice (4 mice in each cage).

The mouse model of CRC was induced by AOM/DSS as described previously (X. Wu et al., 2018). To this end, the mouse groups were intraperitoneally injected with AOM (12 mg/kg body weight), except for the control group which received an equal volume of saline solution. After 7 days, they received four DSS cycles (molecular weight: 36,000–50,000; MP biomedicals, LLC, Canada) (Figure 4-1A). In each DSS cycle, the mice received 1.5% (*w/v*) DSS in drinking water for 5 days followed by 7 days of tap water to allow recovery. After AOM injection, mice in the QPL, QPH, QPHL, and QPHH groups were intragastrically administered 100 mg/kg/day of quinoa protein, 400 mg/kg/day of quinoa protein, 100 mg/kg/day of quinoa protein hydrolysate, and 400 mg/kg/day of quinoa protein hydrolysate, respectively (Figure 1A). Mice in the control and CRC groups were treated with sterile saline solution. The dietary dose of quinoa protein and its hydrolysate used in this study is equivalent to approximately a daily dose of 0.77 g or 3.08 g quinoa protein or its hydrolysate for human diet in a 70 kg adult according to the equivalent surface area dosage conversion factors. These doses of quinoa protein or its hydrolysate were reasonably acceptable for human intake.

2.4. Disease activity index assessment and sample collection

Disease activity index (DAI) was measured once every three days and included body weight loss, stool consistency and rectal bleeding. The DAI score was calculated as described previously (Zeng et al., 2021). For body weight loss scoring, 0 indicated no weight loss while 1, 2, 3, and 4 indicated weight losses of 1%–5%, 5%–10%, 10%–15%, and >20%, respectively. For stool consistency scoring, 0 indicated normal consistency while 1, 2, and 3 indicated soft but formed stool, very soft stool, and diarrhea, respectively. Rectal bleeding was scored as follows: stool with occult blood; 0, does turn blue after 2 min; 1, appears light blue; 2, appears blue; 3, appears dark blue; 4, visible blood traces in the stool.

After four cycles of oral DSS administration, the mice were sacrificed through cervical dislocation. Fecal samples were collected from the colon and stored at -80°C for further study. Colon tissues were obtained, washed with phosphate-buffered saline (PBS), and colon length and number of polyps determined. Colons were then cut longitudinally into two segments, and one part was frozen at -80°C while the other part was fixed in 4% phosphate-buffered formaldehyde solution.

2.5. Histopathological examination

Colon tissues were fixed in 4% phosphate-buffered formaldehyde for 24 h at 4°C. They were then washed with PBS (10 mM, pH 7.4), dehydrated in an ethanol gradient (50%, 70%, 95%, and 100% ethanol), and embedded in paraffin (n = 8 per group). The paraffin blocks were then sectioned at 5 μm, stained with hematoxylin and eosin (H&E) and histological alterations of colon tissues analyzed.

2.6. Colonic SCFAs analysis using gas chromatography-mass spectrometry (GC-MS)

The SCFAs content in colon tissue was determined using gas GC-MS (Thermo TRACE 1310-ISQ, Thermo, American) and quantified relative to acetic acid, propionic acid, isobutyric acid, butyric acid, isovaleric acid, valeric acid, and caproic acid (Sigma-Aldrich). Briefly, an appropriate amount of colon tissue (100 mg) was transferred into a 2 mL centrifuge tube. Next, 50 μL of 15% phosphoric acid, 100 μL of internal standard (125 μg/mL isohexanoic acid) solution and 400 μL of ether, were added and the tissue homogenized for 1 min. After centrifugation at 12000 rpm for 10 min at 4°C, the supernatants were transferred into gas chromatography (GC) sample vials. The samples were then subjected to GC-MS analysis using an Agilent capillary column HP-INNOWAX (30 m × 0.25 mm × 0.25 μm), an injection volume of 1 μL at a split injection ratio of 10:1, and injection port, ion source, and transfer line temperatures of 250°C, 300°C, and 250°C, respectively. The temperature program was as follows: 90°C for 2 min, rise to 120°C at a rate of 10°C/min, rise to 150°C at a rate of 5°C/min, rise to 250°C at a rate of 25°C/min, and hold at 250°C for 2 min. Helium was used as carrier gas at a flow rate of 1 mL/min. mass spectrometry (MS) conditions: electron bombardment ion (EI) source, electron energy: 70 eV, and selected ion monitoring (SIM) mode.

2.7. Gut microbiota analysis

Total genomic DNA was extracted from fecal samples using an E.Z.N.A.® soil DNA Kit (Omega Bio-Tek, Norcross, GA, USA) according to manufacturer instructions. DNA concentration and purity were determined on a NanoDrop 2000 spectrophotometer (Thermo Fisher Scientific, Wilmington, NC, USA). The universal primers 338F (5'-ACTCCTACGGGAGGCAGCAG-3') and 806R (5'-GGACTACHVGGGTWTCTAAT-3') were used to amplify the V3–V4 region of 16S rRNA genes on a GeneAmp 9700 thermocycler (ABI, Vernon, CA, USA). The PCR products were then separated on a 2% agarose gel and recovered from the excised agarose gel using an AxyPrep DNA gel extraction kit (Axygen Biosciences, Union City, CA, USA). Amplicon quality was determined using a QuantiFluor™-ST system (Promega, Madison, WI, USA). The purified amplified fragment was constructed into a PE 2×300 library following the standard Illumina MiSeq platform protocol (Illumina, San Diego, CA, USA), followed by paired-end reading. Raw sequence reads were analyzed using QIIME2. Alpha diversity indices, including observed OTUs, Chao1 richness estimator, Shannon diversity index, and Faith's phylogenetic diversity index, were used to estimate microbial diversity within individual samples. To determine the structural variation of microbial communities, beta diversity was estimated by calculating unweighted UniFrac distances across the samples and visualized using

nonmetric multi-dimensional scaling (NMDS). Linear discriminate analysis effect size (LEfSe) was used to mine for differences in microbial diversity across the samples using a threshold of 2.0. The Kyoto Encyclopedia of Genes and Genomes ortholog functional profile of the gut microbiota was predicted using Phylogenetic Investigation of Communities by Reconstruction of Unobserved States (PICRUSt) and functional annotation performed using MetaCyc and ENZYME database.

2.8. Statistical analysis

Data are presented as mean±SEM for the indicated number of independently performed experiments. One-way ANOVA with Brown–Forsythe and Welch ANOVA tests was used to compare normally distributed data. Kruskal–Wallis test with Dunn's multiple comparison test was used to compare abnormally distributed data. Spearman's rank correlation coefficient was used for correlation analysis and the data visualized using the R package, pheatmap.

3. Results

3.1. Tumorigenesis was suppressed after dietary intervention in CRC mice

Using liquid chromatography-tandem mass spectrometry (LC-MS/MS), we recently identified several novel peptides from quinoa protein hydrolysate (Table 4-1) with anticancer activity (Fan et al., 2022). Here, we investigated the anti-colon cancer effects of quinoa protein hydrolysate using a mouse model of AOM/DSS-induced CRC, which is a commonly used model of colitis-associated colon cancer (Li et al., 2020). Seven-week-old male C57BL/6 mice in groups QPL, QPH, QPHL, and QPHH were intragastrically treated with quinoa protein or its hydrolysate for 8 weeks, while mice in the CTL and CRC groups received an equal volume of saline solution. From the second week, the body weight of the AOM/DSS-treated mice decreased continuously but was slightly recovered upon DSS withdrawal. Compared with the CRC group, the final body weights of the QPH and QPHH groups were significantly increased ($p<0.01$ and $p<0.001$, respectively), while the body weight of mice in the QPL and QPHL groups was unchanged (Figure 4-1B).

Table 4-1. Identification of novel quinoa peptides with anticancer activity from quinoa protein hydrolysate.

Peptide	Ion (m/z)	Calculated Mass
FHPFPR	799.4175	799.4129
NWFPLPR	928.4823	928.4919
PNFHPFPR	1010.5108	1010.5086
NIFRPF	792.4279	792.4283
SLPNFHPFPR	1210.6265	1210.6247
INNIFRPF	1019.5569	1019.5552
SVENWFPLPR	1243.6362	1243.6349
NSLSLPNFHPFPR	1524.7869	1524.7837

NSWGPNWGDHG	1225.4908	1225.4901
HYNPYFPGGA	1121.4963	1121.4930
FGGGTLGHPW	1027.4891	1027.4876
GLESPNYPWPH	1295.5946	1295.5935
HGSLGFLPR	982.5378	982.5349
WTAPTIPNPEYKGPW	1755.8777	1755.8620
IMGPNYIPGEK	1217.6107	1217.6114
PIIADPK	752.4444	752.4432
LSLGVAGSRPGFEG	1345.6989	1345.6990
SFGDAYGNQVYVPR	1571.7369	1571.7369
TPVNWKPGEK	1154.6079	1154.6084
LSGGDHIHSGTVVG	1334.6588	1334.6579
GHVIGLPAGVS	1005.5578	1005.5607
YTQSGGVRPF	1110.5469	1110.5458
SQYPGQQQQPR	1315.6301	1315.6269
PVASGGIHV	835.4576	835.4552
TRGDIIAIPPGAV	1278.7920	1278.7296
LSVNIDNPER	1155.5919	1155.5884
KQNIDRPSLA	1140.6244	1140.6251
KTNDNAMISPL	1202.5970	1202.5965
VPEAVAKPEL	1051.5949	1051.5913
ALHIVGPDK	948.5409	948.5393
KAEIHYGTGAI	1158.6028	1158.6033
YLAGNPQGGQER	1288.6229	1288.6160
THGWIGTDIT	1099.5349	1099.5298
ISGITNGAMTGSDPK	1447.6993	1447.6977
YQISPSEAH	1030.4712	1030.4720
RDNIQGITKPA	1211.6639	1211.6622
HLDMSVEK	957.4742	957.4590

DAI is a comprehensive measure of disease severity, including weight loss, stool consistency, and rectal bleeding (Jairath et al., 2019). When compared to mice in the CTL group which were disease-free, the DAI values of AOM/DSS-treated mice were elevated before partially recovering. Administration of different doses of quinoa protein or its hydrolysate improved the DAI index to various extents. When compared with the CRC group, the DAI score was markedly decreased in the QPHH group ($p<0.05$) as well as in the QPH and QPHL groups, although the difference was not significant. In addition, QPL supplementation had little effect on the DAI index (Figure 4-1C).

Colon shortening is a common feature of colitis-associated colon cancer in the AOM/DSS-induced CRC model (X. L. Wu et al., 2020). When compared with the CTL group, we found that colon length was markedly decreased in the CRC group and that QPH, QPHL, and QPHH significantly prevented colon shortening upon AOM/DSS administration (CTL: 7.64±0.70 cm; CRC: 5.15±0.56 cm; QPL: 5.53±0.30 cm; QPH: 6.49±0.34 cm; QPHL: 6.06±0.24 cm; QPHH: 6.96±0.50 cm; Figure 4-1D–E). Moreover, when compared with the CTL group, polyp number was significantly

reduced in the QPH ($p<0.01$) and QPHH ($p<0.01$) groups, and slightly decreased in the QPL and QPHL groups (Figure 4-1F). H&E-analysis of the colorectal sections revealed that when compared with the CTL group, which exhibited no colon injury, intact colon mucosa, and orderly arranged glandular cells, treatment with AOM/DSS disrupted the colonic crypts, goblet cells, and intestinal epithelia. Different degrees of recovery were observed upon treatment of the AOM/DSS-treated mice with quinoa protein or its hydrolysate. Moreover, the QPHH treated group exhibited remarkable restoration of the intestinal epithelium and colonic crypts (Figure 4-1G).

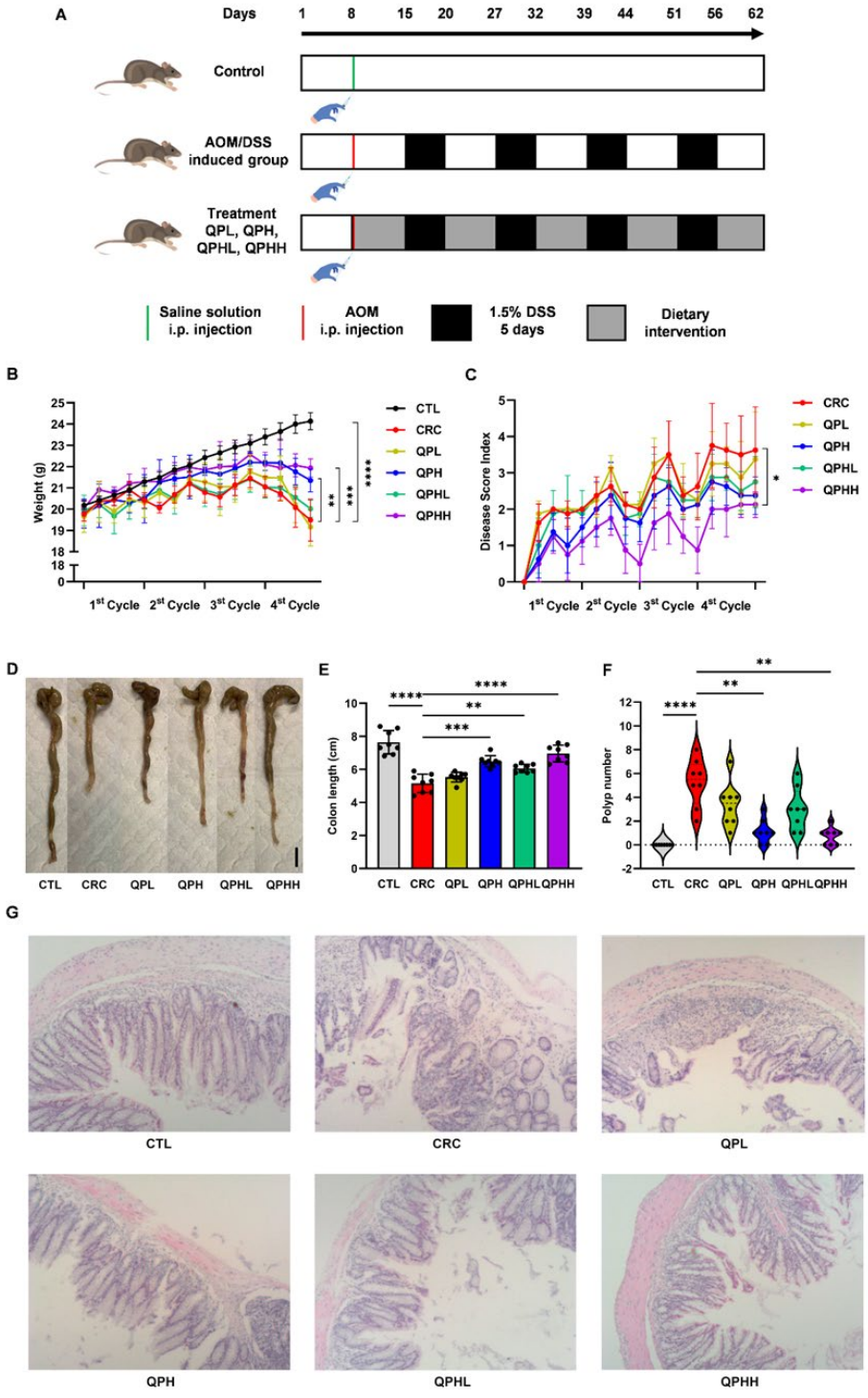
A
Days
1
8
15
20
27
32
39
44
51
56
62
Control
AOM/DSS induced group
Treatment QPL, QPH, QPHL, QPHH
Saline solution i.p. injection
AOM i.p. injection
1.5% DSS 5 days
Dietary intervention
B
Weight (g)
1st Cycle
2st Cycle
3st Cycle
4st Cycle
CTL
CRC
QPL
QPH
QPHL
QPHH
C
Disease Score Index
D
E
Colon length (cm)
F
Polyp number
G
CTL
CRC
QPL
QPH
QPHL
QPHH

Figure 4-1. Ameliorative effect of quinoa protein and its hydrolysate on the development of AOM/DSS-induced colorectal cancer (CRC) mouse model. QPL, low quinoa protein; QPH, high quinoa protein; QPHL, low quinoa protein hydrolysate; QPHH, high quinoa protein hydrolysate. (A) A schematic diagram showing the design of CRC mice model establishment and dietary interventions (QPL, QPH, QPHL, QPHH); AOM, azoxymethane; DSS, dextran sodium sulfate; i.p. injection, intraperitoneal injection. (B) The average body weight (g) of mice in different treatment groups. (C) Disease score index (DAI) of mice in different treatment groups. (D) Representative photographs of colons from mice in different groups, bar=1 cm. (E) Colon length (cm). (F) Polyp number. (G) Pathological changes of tumor tissues by H&E staining (200 × magnification) in mice. Data are presented as mean ± standard deviation (SD) (n=8). $p < 0.05$, *; $p < 0.01$, **; $p < 0.001$, ***; $p < 0.001$, ****.

3.2. SCFAs analysis in colon tissue

Following treatment with AOM/DSS, the levels of acetic acid, propionic acid, butyric acid, isobutyric acid, valeric acid, isovaleric acid, and total SCFAs decreased significantly (Figure 4-2). However, when compared with the CRC group, the levels of total SCFAs increased in the QPL, QPH, QPHL, and the QPHH group by 1.55, 3.89, 3.66, and 3.91 fold, respectively, although the changes were not statistically significant (Figure 4-2). Moreover, when compared with the CRC group, the concentration of acetic acid significantly increased in the QPH group, butyric acid exhibited significantly higher concentrations in the QPH, QPHL, and QPHH groups, and propionic acid remarkedly increased in the QPH and QPHL groups.

In this study, treatment with QPH, QPHL, and QPHH enhanced the production of butyric acid by more than 4 folds when compared with the CRC group. The levels of acetic acid increased significantly by 3.45 fold in the QPH group and by 1.47–3.33 fold in the QPL, QPHL, and QPHH groups compared with the CRC group, although these increases were not significant. When compared with the CRC group, the levels of propionic acid increased by 4–5 fold in the QPH and QPHL groups.

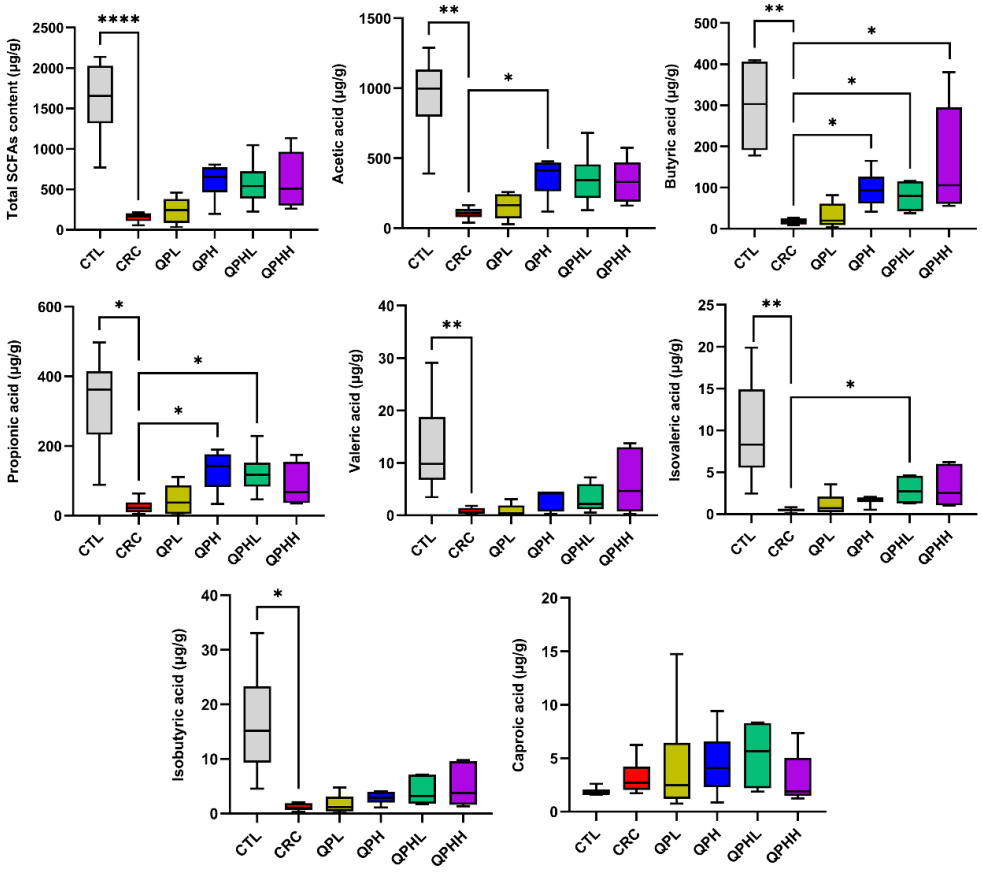

Figure 4-2. Determination of short chain fatty acids (SCFA) in mouse fecal samples using gas chromatography-mass spectrometry (GC-MS). (A) Acetic acid. (B) Butyric acid. (C) Isobutyric acid. (D) Propionic acid. (E) Valeric acid. (F) Isovaleric acid. (G) Caproic acid. Data are presented as mean ± standard deviation (SD) (n=8). $p < 0.05$, *; $p < 0.01$, **; $p < 0.001$, ***, $p < 0.001$, ****.

3.3. Changes in gut microbiota composition

In this study, 16S rDNA high throughput sequencing was performed to investigate the effect of QPH and QPHH on gut microbiota. Analysis of the rarefaction curves of the observed OTUs indicated that the sequencing depth of gut microbiota was sufficient to cover the microbial diversity of samples (Figure 4-3A). Results shown in Figure 4-4A demonstrated that the observed OUTs were significantly decreased in the CRC group, and that QPH as well as QPHH partly prevented the reduction in the number of observed species. The Shannon and Simpson indexes were used to evaluate the community diversity, whereas community richness was estimated based on the Chao1 index. Alpha diversity analysis showed that AOM/DSS significantly reduced

the community diversity, and only QPHH was elevated as revealed by the Shannon and Simpson indices (Figure 4-3B, C). Likewise, the Chao1 index was significantly decreased in the CRC group, and this change was reversed by QPHH (Figure 4-3D). Variations in species diversity was determined through NMDS-beta diversity analysis, and samples were clustered based on Bray–Curtis distance (NMDS Stress = 0.1737) and Unweighted UniFrac distance (NMDS Stress = 0.1100). Data shown in Figure 4-3E and F reveal that there was a significant separation between CTL and CRC groups. Moreover, QPH and QPHH samples overlapped between CTL and CRC groups. These data suggested that QPHH altered gut microbiota structure after tumor induction.

Furthermore, the specific changes in differential taxa disturbed by AOM/DSS treatment and partly recovered by QPH and QPHH interventions were investigated at the phylum level (Figure 4-3G). A heatmap was constructed to display the structural differences among the four groups (Figure 4-4B). At the phylum level, the relative abundance of *Firmicutes* and *Bacteroidetes* was different among the four groups (Figure 4-5A, B). Moreover, the abundance of *Bacteroidetes* was reduced (CTL: 44.02%, CRC: 26.38%) whereas that of *Firmicutes* was not altered (CTL: 49.33%, CRC: 50.50%) in the CRC group compared with the CTL group. Further analysis showed that the abundance of *Firmicutes* was 42.87% and 50.67%, whereas that of *Bacteroidetes* was 44.14% and 41.02% in the QPH group and QPHH group, respectively. However, the abundance of *Firmicutes* was not altered among the four groups. Treatment with AOM/DSS decreased the abundance of *Bacteroidetes* by 17.64%, and this effect was reversed by QPH and QPHH (Figure 4-3G). This indicates that the ratio of F/B was higher in the CRC group compared with the other three groups, although the difference was not statistically significant (Figure 4-5C).

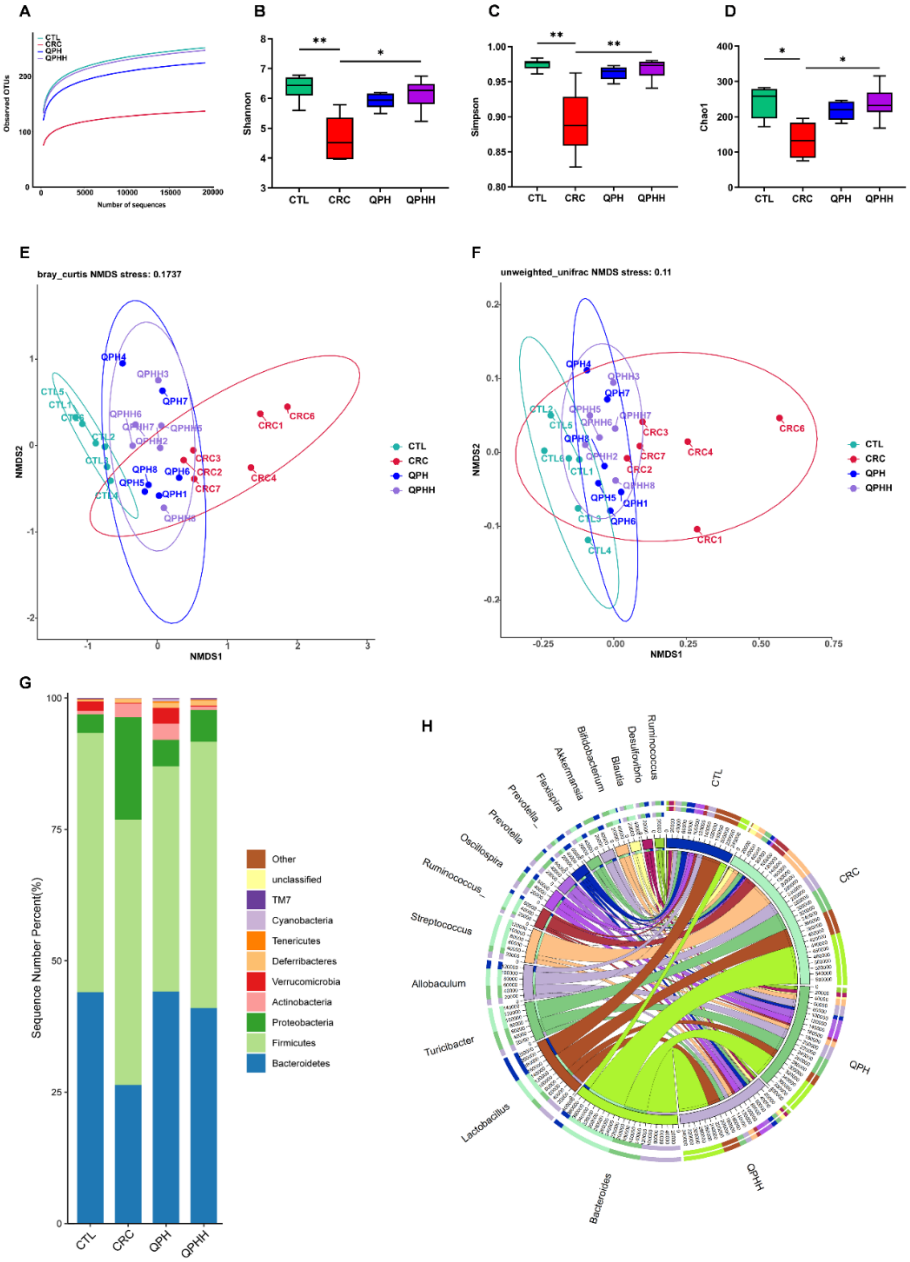

Figure 4-3. The effects of QPH and QPHH on the composition of gut microbiota. (A) Rarefaction curves. Alpha diversity indicators (B) Shannon, (C) Simpson, and (D) Chao1 index. Beta diversity based on (E) Bray–Curtis distance and (F) Unweighted UniFrac distance nonmetric multidimensional scaling (NMDS) analysis. (G) Relative abundance of gut microbiota at the phylum level. (H) Relative abundance of gut microbiota at the genus level. n=6, $p < 0.05$, *; $p < 0.01$, **.

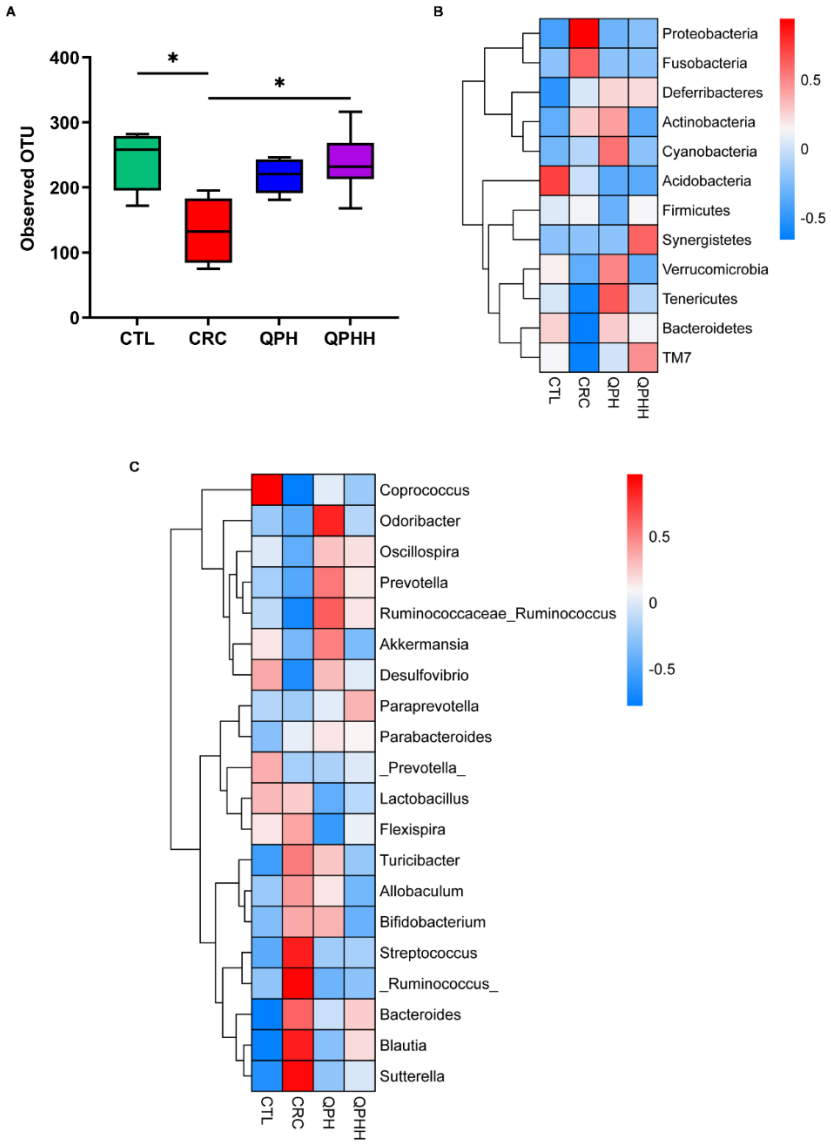

Figure 4-4. The effects of QPH and QPHH on the composition of gut microbiota. (A) Observed OTUs in each group. The heatmap of relative abundance of bacterial community at (B) phylum level and (C) genus level. The value was calculated using the normalization method, Z score = (X−μ)/δ, X for normalized random variables, where μ is the mean of the sample and δ is the standard deviation of the sample.

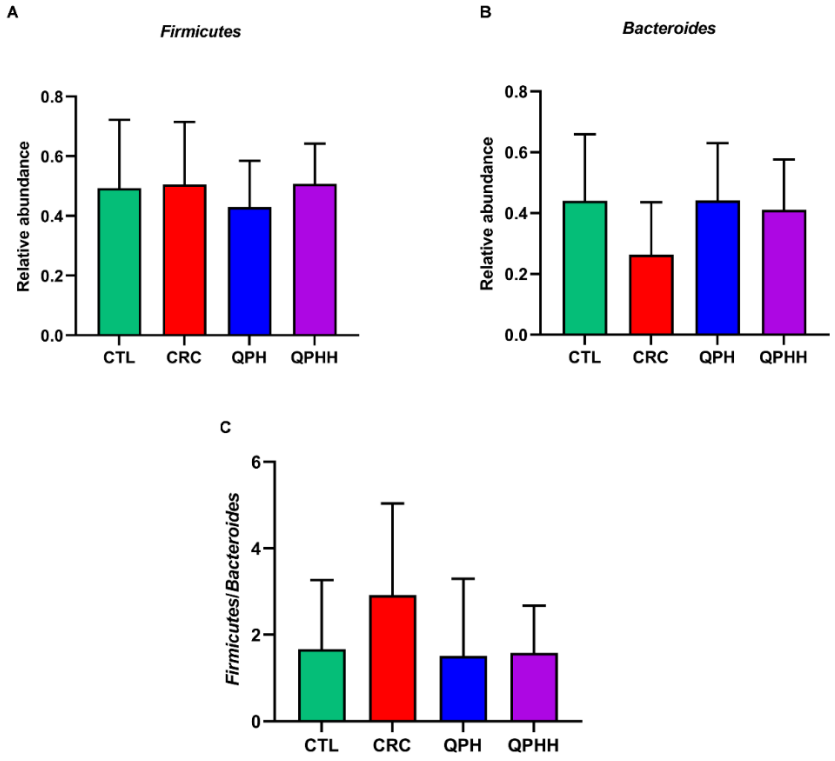

Figure 4-5. The effects of QPH and QPHH on the abundance of gut microbiota at phylum level. (A) Relative abundance of Firmicutes. (B) Relative abundance of Bacteroidetes. (C) Firmicutes/Bacteroidetes ratio. The data are presented as mean ± standard deviation (SD), ns indicates no significant difference.

At the genus level, a circus diagram (Figure 4-3H) and heatmap (Figure 4-4C) were used to display changes in the intestinal microbiota. A comparison of relative abundance of the bacterial taxa provided by the LEfSe (Figure 4-6A) was compared based on DESeq2 results (Table 4-2). As shown in Figure 4-6B, several SCFAs-producing bacteria, such as *Butyricicoccus*, *Prevotella*, *Odoribacter*, *Clostridium*, and *Coprococcus* were detected. The AOM/DSS treatment decreased the abundance of *Butyricicoccus*, *Prevotella*, *Clostridium*, and *Coprococcus* significantly, and the abundance of *Odoribacter* was lower in the treated groups compared with that of the CTL group. Meanwhile, the depletion of *Butyricicoccus*, *Prevotella*, *Odoribacter*, and *Coprococcus* was remarkably recovered with QPH or QPHH supplementation,

Table 4-2. Significantly different genera between groups analyzed by DESeq2 (Padj < 0.05).

CTL group vs CRC group			
Genus	**log2FoldChange**	**pvalue**	**P_{adj}**

Coprococcus	7.676929	4.60E-16	1.89E-14
Turicibacter	-8.90488	8.92E-15	1.83E-13
Blautia	-7.47194	1.73E-11	2.37E-10
Streptococcus	-7.68075	1.23E-07	1.26E-06
Desulfovibrio	4.719964	4.02E-06	3.30E-05
Butyricicoccus	4.718744	5.40E-05	0.000344
Helicobacter	-6.96711	5.87E-05	0.000344
Erysipelotrichaceae_Clostridium	-4.05875	7.67E-05	0.000393
Ruminococcus	3.04534	9.37E-05	0.000427
Akkermansia	5.05601	0.000112	0.00046
Ralstonia	-3.34987	0.000622	0.002318
Bacteroides	-2.42611	0.001083	0.0037
Anaeroplasma	3.490716	0.001991	0.006279
Alistipes	-3.41797	0.002889	0.008376
Dehalobacterium	2.717549	0.003064	0.008376
AF12	3.000871	0.005073	0.012982
Odoribacter	3.126761	0.005383	0.012982
[Eubacterium]	-2.37565	0.006871	0.015351
unclassified	1.288304	0.007114	0.015351
Prevotella	3.672306	0.009814	0.020118
Anaerotruncus	2.659497	0.014035	0.027402
Oscillospira	2.321231	0.014883	0.027736
Sutterella	-2.05258	0.016711	0.029789
[Prevotella]	2.712738	0.031594	0.053973
Coprobacillus	-2.35404	0.045015	0.073824

QPH group vs CRC group			
Genus	**log2FoldChange**	**pvalue**	**P_{adj}**
Coprococcus	-5.9152	4.06E-10	1.66E-08
AF12	-4.29644	5.68E-05	0.00068
Ruminococcus	-3.19883	3.99E-05	0.00068
Flexispira	3.8475	6.64E-05	0.00068
Odoribacter	-4.40426	8.65E-05	0.000709
Akkermansia	-5.00496	0.000131	0.000897
Desulfovibrio	-3.5406	0.000546	0.003197
Anaeroplasma	-3.8207	0.00066	0.003383
Prevotella	-4.30347	0.002469	0.011247
[Eubacterium]	2.201916	0.005108	0.020942

Oscillospira	-2.41923	0.011117	0.037983
Acinetobacter	2.24708	0.010332	0.037983

QPHH group vs CRC group			
Genus	**log2FoldChange**	**pvalue**	**P_{adj}**
Coprococcus	-4.89552	2.36E-07	9.66E-06
Butyricicoccus	-4.35068	0.000188	0.003857
Lactococcus	3.836165	0.001031	0.010653
[Eubacterium]	2.575573	0.001039	0.010653
Acinetobacter	2.842888	0.00162	0.013286
Desulfovibrio	-3.06875	0.002733	0.018676
Ruminococcus	-2.29099	0.00328	0.019214
Bifidobacterium	3.082251	0.008356	0.042825
[Ruminococcus]	2.039129	0.010505	0.047854
Prevotella	-3.57194	0.011991	0.048082
Anaeroplasma	-2.79923	0.0129	0.048082

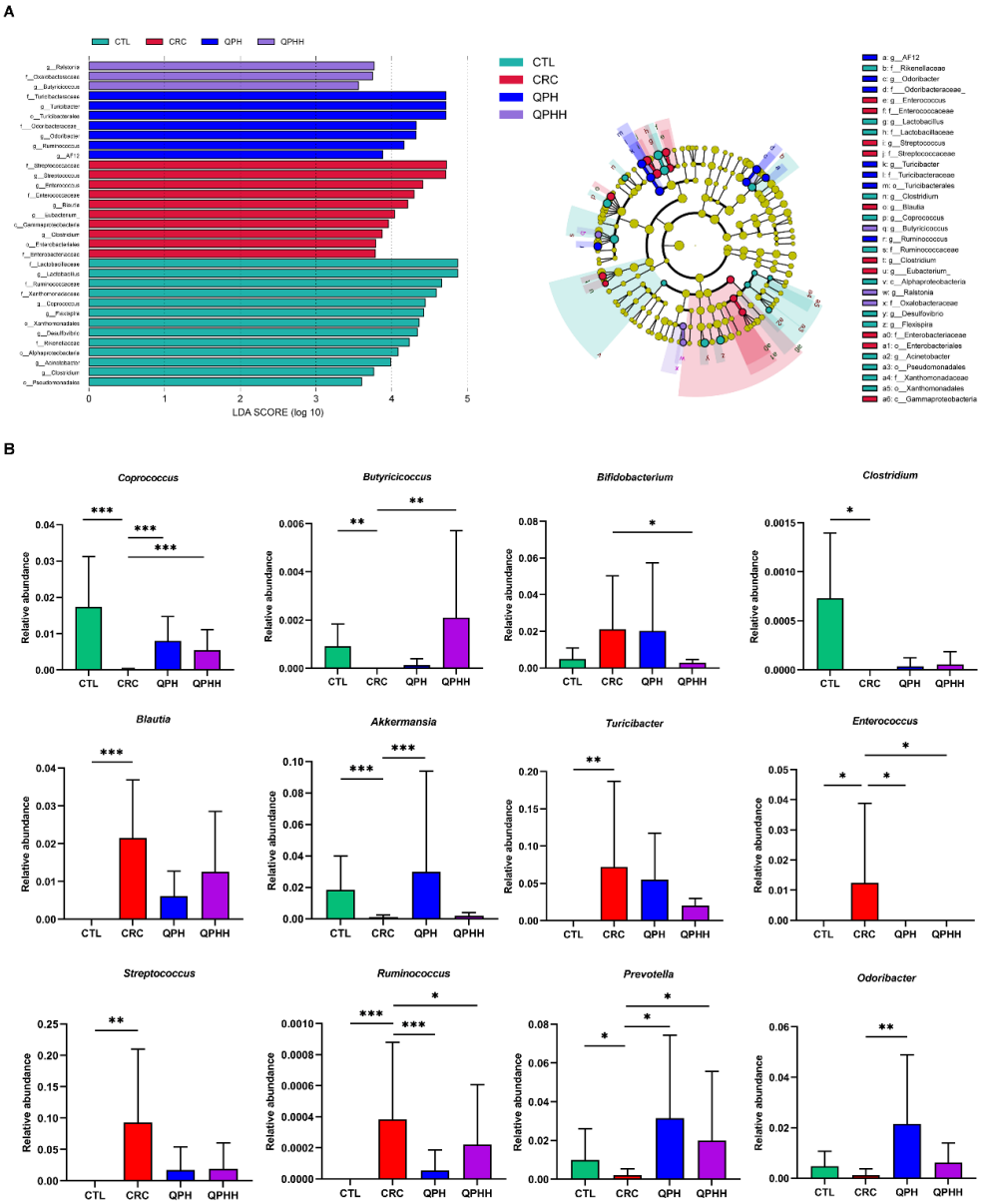

Figure 4-6. The effects of QPH and QPHH on the abundance of gut microbiota. (A) Linear discriminant analysis scores and Cladogram showing taxonomic differences based on LEfSe analysis. (B) Relative abundance of selected gut bacteria at the genus level. P values were determined by DESeq2. n=6, Padj < 0.05, *; Padj < 0.01, **; Padj < 0.001, ***.

As the major products of gut microbiota, SCFAs also play a crucial role in regulating gut microbiota and enhancing intestinal barriers. In this study, Spearman correlation analysis was used to examine the correlation between gut microbiota and SCFAs production. As shown in Figure 4-7, the top 30 taxa in terms of abundance at the genus level were selected for correlation analysis. Result showed that acetic acid, butyric acid, and propionic acid were positively related to the relative abundance of *Coprococcus*. The abundance of *Clostridium* was also positively correlated with acetic acid, whereas the abundance of *Butyricicoccus* was positively correlated with butyric acid.

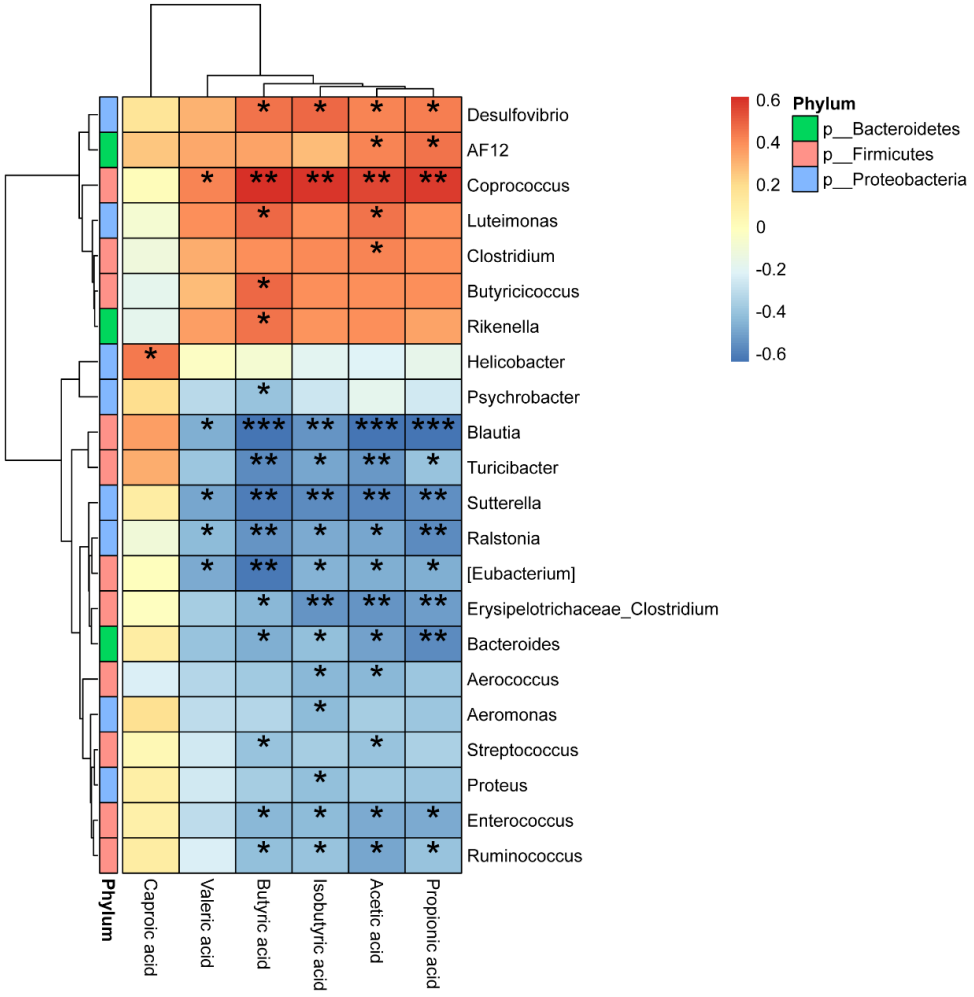

Figure 4-7. Correlation analysis between SCFA and gut microbiota at the genus level. n=6, $p < 0.05$, *; $p < 0.01$, **.

3.4. Functional prediction of bacterial taxa

PICRUSt was used to predict the functional profile of gut microbiota based on changes in the microbial composition between groups. As shown in Figure 4-8A, 36 functional genes were found to be differentially expressed between the CTL group and CRC group. The expression of functional genes related to N-Glycan biosynthesis, glucosinolate biosynthesis, selenocompound metabolism, microRNAs in cancer, and amino acids biosynthesis and metabolism was higher in the CTL group compared with the CRC group, whereas the expression of genes associated with fatty acid metabolism, propanoate metabolism, pyruvate metabolism, vitamin B6 metabolism, glutathione metabolism, fructose and mannose metabolism, carbohydrate digestion and absorption, nicotinate, and nicotinamide metabolism, and glycerophospholipid metabolism were significantly higher in CRC group ($p < 0.05$), which was consistent with findings from previous studies (Cai et al., 2019; Wan et al., 2019). However, QPH or QPHH treatment reversed the CRC-induced effects on the functional genes (Figure 4-8B, C). The expression of genes involved in N-Glycan biosynthesis, arginine biosynthesis, alanine, aspartate and glutamate metabolism, selenocompound metabolism, and microRNAs in cancer was higher in QPH, QPHH, and CTL groups than in CRC group ($p < 0.05$), whereas the abundance of genes involved in propanoate metabolism, vitamin B6 metabolism, fructose, and mannose metabolism, carbohydrate digestion and absorption, nicotinate and nicotinamide metabolism, and glycerophospholipid metabolism was lower in QPH, QPHH, and CTL groups than in CRC group ($p < 0.05$). Treatment with QPH increased the expression of genes associated with PPAR signaling pathway relative to CRC and CTL treatments ($p < 0.05$). Zhou and co-workers revealed that increased PPAR expression was effective to inhibit the progression of CRC (Zhou et al., 2020). Meanwhile, the proportion of functional genes related to RNA transport, AMPK signaling pathway, and NOD-like receptor signaling pathway was significantly increased in QPHH-treated group compared with CTL and CRC-treated groups. AMPK inhibits the growth of cancer cells and tumorigenesis by regulating mitochondrial metabolism (W. Yang et al., 2021). IL-17-dependent and NOD-like receptor signaling pathways play important roles in inflammatory diseases and cancer (Vonderheide, 2014).

A

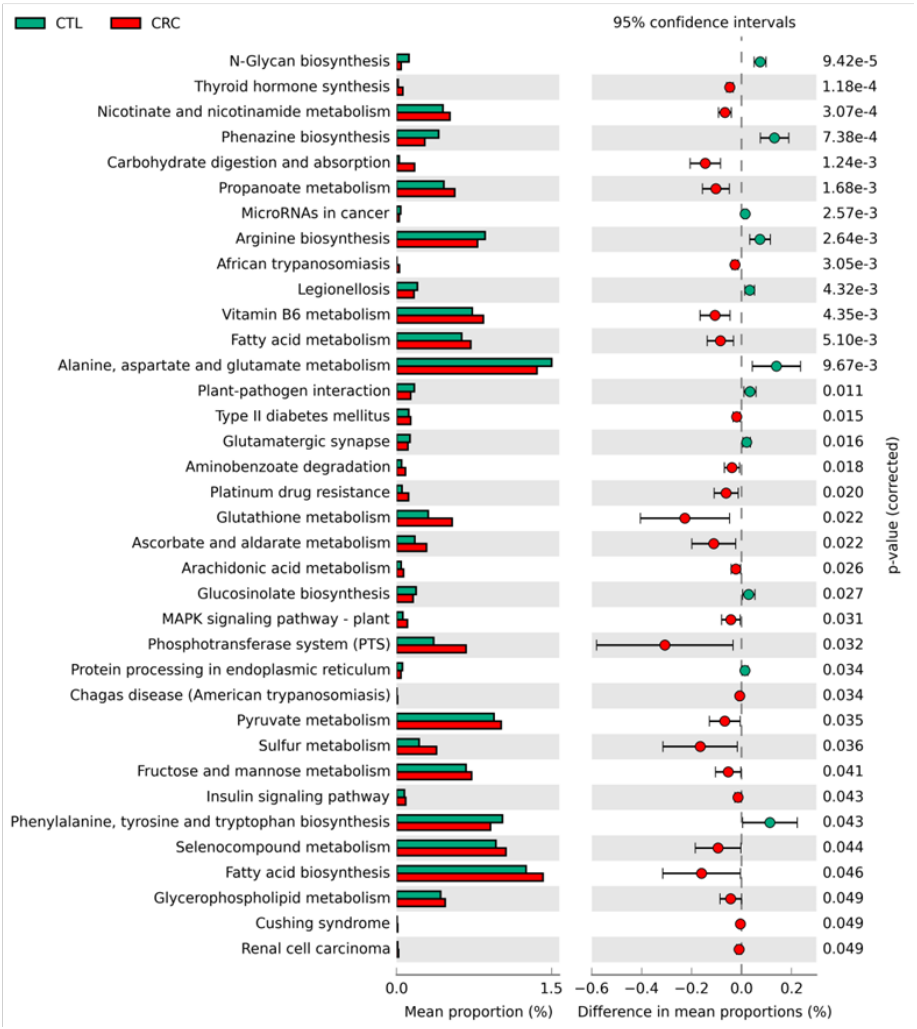

Figure 4-8. Continued

B

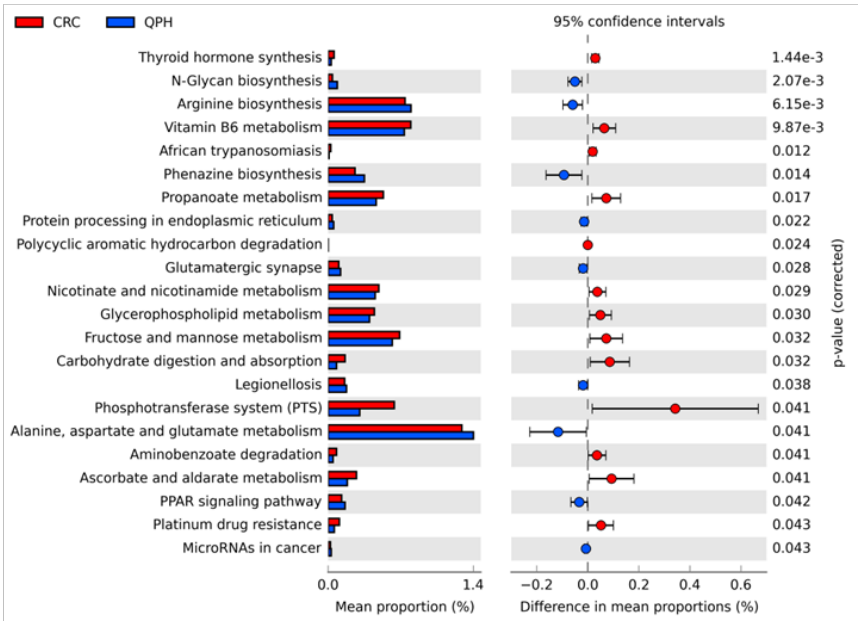

Figure 4-8. Continued

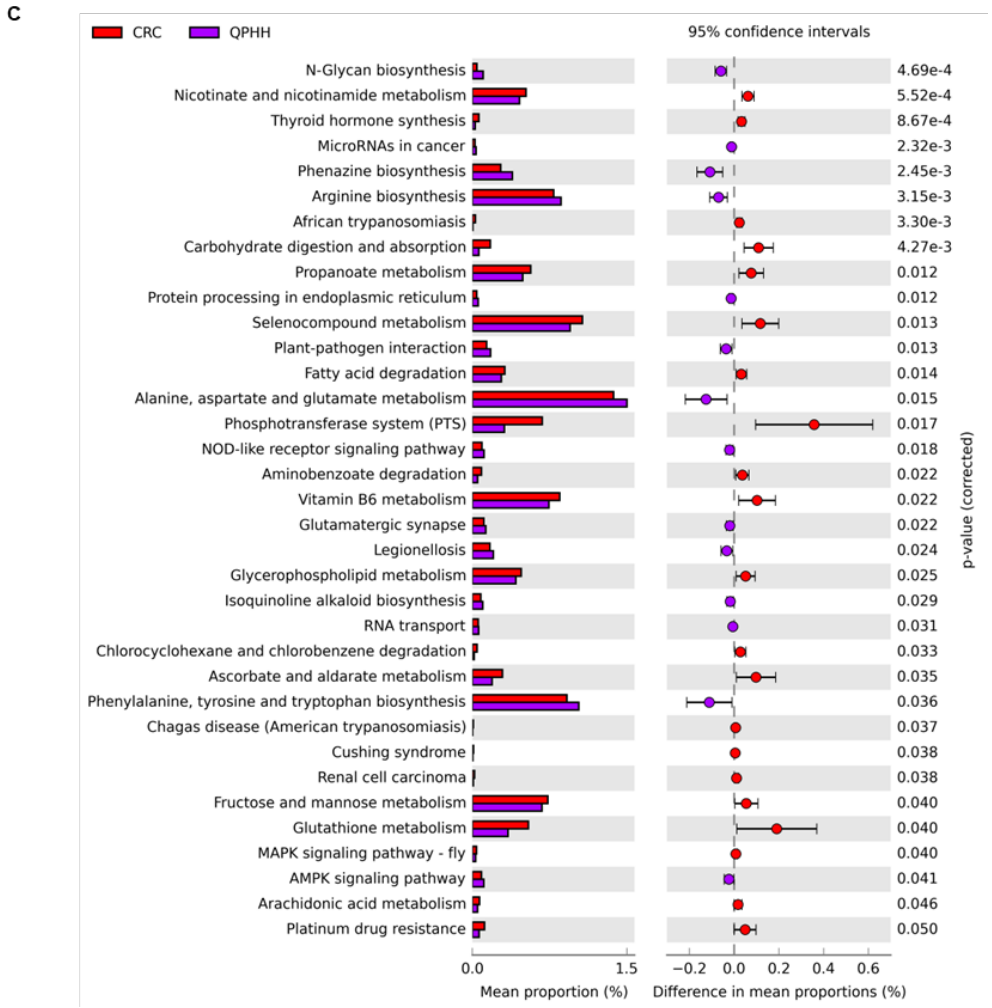

Figure 4-8. Significant differences in relative abundance of predicted meta-genome function between groups: (A) CTL group vs CRC group. (B) CRC group vs QPH group. (C) CRC group vs QPHH group. STAMP was used to measure the function with significant difference. n=6, $p < 0.05$ was considered statistically significant.

5

Chapter V Preparation, physicochemical properties, and formation mechanism of quinoa self-assembled peptide-based hydrogel

Introduction to Chapter 5

According to chapter 4, quinoa proteins and peptides can alleviate colon cancer in vivo. However, compared to quinoa protein (QP), quinoa peptides (QPH) obtained from simulated digestion did not show much stronger activity. We speculate that QPH has experienced a similar degradation process to QP in the digestive tract in vivo, and eventually digested into amino acids. As a result, QPH did not achieve the expected bioactivity as a peptide structure. Moreover, the bioactivities of protein are closely related to its physicochemical properties, especially its bioavailability in vivo. Besides nutritional value and bioactivity, many bioactive peptides exhibit favorable gelation properties, which makes them widely used in food processing and pharmaceutical fields. Therefore, in this chapter, we tried to find a simple and efficient method to improve the physicochemical properties of quinoa protein and peptides, which contributes to maintain their bioavailability in vivo and application value.

This work is an original contribution, adapted from: Fan, X., Guo, H., Richel, A., Zhang, L., Liu, C., Qin, P., Blecker, C., Ren, G. (2023). Preparation, physicochemical properties, and formation mechanism of quinoa self-assembled peptide-based hydrogel. Food hydrocolloids, 145, 109139. DOI: 10.1016/j.foodhyd.2023.109139.

Abstract

Currently, self-assembly peptides with hydrogel properties used in various applications are chemically synthesized. These peptides not only had safety and environmental problems but also were expensive and cumbersome to prepare. The present study established a convenient and efficient method for producing plant-based peptides with decent gel-forming ability from quinoa proteins. After alkaline protease treatment, the hydrogels made with quinoa protein hydrolysis exhibited potent self-assembly capacity, enhanced gel hardness, and improved rheological properties. Moreover, the microstructure results revealed that the quinoa peptide hydrogels had a regular, uniform, and interconnected porous structure. These observations were primarily attributed to the hydrogen bonding force and hydrophobic aggregation caused by hydrophobic group exposure. The amino acid and proteomics analysis suggested that the amino acid composition and sequence of quinoa peptides significantly influenced the formation of self-assembled hydrogels. Overall, this study provided a cost-effective approach to improve the gelling ability of quinoa protein and had the potential to replace the use of chemically synthesized peptides in various applications, laying the theoretical basis for the development of novel natural plant-based foods.

Keywords: quinoa protein; enzymatic hydrolysis; gelation; rheological property; microstructure; molecular characteristics

1. Introduction

With the rapid growth of the human population and intensifying greenhouse effect, plant-based proteins are considered a promising alternative to meet the growing demand for nutritional food and reduce the consumption of animal-origin food. A reasonable combination intake of plant proteins or as a main food ingredient can ensure adequate nutrition for the human body to maintain a healthy state. Soy and pea proteins are the most well-known plant protein sources. To provide more plant proteins with high nutritional value and quality, it is necessary to deepen mining and research on other superior plant proteins. Quinoa—a new food and emerging protein source—has received widespread attention because of its high protein content and well-balanced amino acid compositions (McClements, Newman, & McClements, 2019). Additionally, quinoa has a high content of essential amino acids, primarily lysine, methionine and cysteine, and is gluten-free (Elsohaimy, Refaay, & Zaytoun, 2015), making it highly valuable in plant-based protein products and appealing to broader consumers.

Enzymatic hydrolysis is recognized as a promising and effective approach for improving the functional properties and nutritional value of proteins. Moreover, gelation is believed to be one of the most crucial techno-functionalities of proteins and is extensively used in food processing and pharmaceuticals (Gosal & Ross-Murphy, 2000). Peptides—the main products of protein enzymatic hydrolysis—have the potential to form self-assembled hydrogels, which have attracted widespread interest because of their ease of preparation, reproducibility, biodegradability, biocompatibility, and the availability of various chemical functions and structures (De Leon Rodriguez & Hemar, 2020). However, these gelation-capable peptides are mainly obtained through designed synthesis or microbial recombinant expression (De Leon Rodriguez, et al., 2020). It is still difficult to apply synthetic peptides to practical production applications because of their limitations, including difficulties in purification, low stability, poor dispersion, and safety issues (Yu, et al., 2022). Therefore, a safe, easily accessible, and environmentally friendly method to produce plant-based peptides with gel-forming abilities is imminent.

Although animal proteins have been suggested to have better gelation properties than plant proteins, enzymatic hydrolysis can improve the gelation properties of plant proteins by changing the ionic interactions, hydrogen bonds, and hydrophobic regions (Nieto-Nieto, Wang, Ozimek, & Chen, 2014; G. Zhao, Liu, Zhao, Ren, & Yang, 2011). For instance, oat protein isolates exhibited enhanced gel-forming abilities after hydrolyzing with flavourzyme and trypsin at pH 9 by adjusting the electrostatically repulsive force and the hydrophobic attractive force (Nieto-Nieto, et al., 2014). Similarly, compared to pea protein, the gelling capacity of pea protein hydrolysate increased after alcalase treatment followed by heating at 85℃ for 10 min (Chen & Campanella, 2022). However, in a recent study on the gelation properties of quinoa protein, the quinoa peptide gels were formed in an acidic condition (pH < 3), and their gel strength decreased with the raising pH (Galante, De Flaviis, Boeris, & Spelzini, 2020). Although several plant-based hydrogels have been obtained through enzymatic hydrolysis, the formation conditions require constant adjusting and are cumbersome

to apply in food processing. Furthermore, these studies have mainly focused on the structural properties and did not investigate the effect of small molecular weight plant-based peptides, which are more similar to synthetic self-assembled peptides, on hydrogel formation. Therefore, the present study provided a simple and efficient method for producing self-assembled hydrogels via mild alcalase hydrolysis of quinoa proteins. We determined the physicochemical properties of quinoa peptide hydrogels, including molecular weight, degree of hydrolysis, gel hardness, rheological properties, and surface hydrophobicity. Moreover, the potential gelation mechanism of the quinoa hydrogels was elucidated based on the results of particle size distribution, zeta potential, free sulfhydryls, Fourier transform infrared spectroscopy, scanning electron microscopy, and amino acid and proteomics analysis. Our study provided the rationale for the development of novel, green, and safe plant-based protein foods.

2. Materials and methods

2.1. Materials and Reagents

Quinoa seeds (Mengli-I) were obtained from the Inner Mongolia Yiji Biotechnology Company (Ulanqab, China). Sodium hydroxide (NaOH), hydrochloric acid (HCl), and n-hexane were obtained from Sinopharm Chemical Reagent Co. Ltd. (Shanghai, China). Alcalase (≥200,000 U/g) was obtained from Novozyme (Beijing, China).

2.2. Quinoa protein, quinoa protein hydrolysates, and hydrogel preparation

QP extraction was conducted according to a previous method (Galante, et al., 2020) with some modifications. Quinoa flour was dispersed in distilled water (10%, *w*/*v*). The suspension was stirred for 2 h at room temperature and then centrifuged at 6000 g for 30 min. The supernatant was adjusted to pH 4 by adding 1M HCl to precipitate the proteins and then centrifuged at 6000 g for 30 min. The precipitate was resuspended in water, adjusted to a pH of 7.0, and freeze-dried. The obtained powder was denoted as QP. QP suspension (5%, *w*/*v*) was hydrolyzed with alcalase at a QP:alcalase ratio of 200:3 (*w*/*w*) at pH 8.0 and 55℃. Samples were collected at different hydrolysis intervals (0, 15, 30, 60, 90, 120, 150, and 180 min). The 180-min alcalase hydrolysate was further freeze-dried and termed QPH.

The hydrogel was prepared by mixing the freeze-dried QP or QPH powder with deionized water at a pH of 7.0, completely oscillating for 1 min, and allowed to stand for 10 min at room temperature.

2.3. Degree of hydrolysis determination, sodium dodecyl sulfate-polyacrylamide gel electrophoresis (SDS-PAGE), and molecular weight

In this study, the degree of hydrolysis (DH) was determined according to the method of Adler-Nissen (1979) with slight modifications. QPH samples were added to sodium phosphate buffer (0.2 M, pH 8.2). TNBS reagent (0.1% *w*/*v*) was added to start the reaction and incubated at 50℃ for 1 h. After incubation, 0.1 N HCl was added to stop

the reaction. The absorbance was measured at 340 nm.

The QP hydrolysis was verified using SDS-PAGE. The samples were mixed with a loading buffer (2×, Bio-Rad, USA; 1:1 (*v*/*v*)), boiled at 100℃ for 10 min, and rapidly cooled on ice. The samples were loaded onto a Mini-protein TGX precast gel (Bio-Rad, USA) and the gel was subjected to electrophoresis at 120 V under reducing conditions on a Mini-PROTEAN 3 Cell system (Bio-Rad, USA). The protein bands were visualized by staining with Coomassie R250 brilliant blue (Biorigin, Beijing, China). A colour Prestained Protein Marker (Genstar, Beijing, China) was used as the molecular weight standard.

The molecular weight (Mw) distribution was determined using a Waters high-performance liquid chromatography (Waters, Milford, MA, USA) equipped with a refractive-index detector (Waters 2414). The samples were separated through a PL Aqua gel-OH mixed-H 8 μm column (Agilent Technologies, Santa Clara, CA, USA) at 30℃. The mobile phase consisted of 0.2 M $NaNO_3$ and 0.01 M NaH_2PO_4 aqueous solution (pH 7.0) at a rate of 1 mL/min, and 20 μL of 5 mg/mL sample was injected into the high-performance liquid chromatography system. A calibration curve was obtained using narrow-distribution polyethylene glycol of known molecular weight to obtain the molecular weight calibration curve. Data was analyzed using gel permeation chromatography (GPC) software (Waters, Milford, MA, USA).

2.4. Texture analysis

Texture measurements were conducted using a TMS-PRO series Texture Profile Analyzer (TMS-Pro, FTC, USA). The samples were prepared in cylindrical containers (20 mm diameter × 10 mm height). The cylindrical plunger (5 mm diameter) penetrated 50% into the gel samples at a crosshead speed of 5 mm/s and a return speed of 5 mm/s with a trigger force of 49 mN. The maximum breaking force was defined as the hardness (N) of gels. Four independent replicates were measured for each sample.

2.5. Rheological properties

A Haake Mars60 rotational rheometer (Thermo Fisher, Germany) equipped with a stainless-steel parallel plate (diameter, 40 mm; gap, 1 mm) was used to measure the rheological properties of the hydrogel. The hydrogels were placed on a parallel plate for 2 min to maintain the temperature equilibrated at 25℃ before each measurement. The viscosity was detected using the steady shear mode, and the shear rates ranged from 0.1 to 100 s-1. The frequency sweep measurements were performed at a constant strain of 1%, whereas the frequency varied from 0.01 to 100 Hz. The storage modulus (G′) and loss modulus (G″) were recorded as functions of the frequency. At least three measurements were measured per sample.

2.6. Determination of particle size distribution (PSD)

The particle size distributions of QP and QPH were determined using a Malvern Mastersizer 2000 analyzer (Malvern Instruments, Worcestershire, UK) and static light scattering. The refractive indices (RI) used for the samples and dispersant were 1.52

and 1.33, respectively. The volume-weighted mean D[4, 3] represents the mean particle size. All samples were dissolved in water at a concentration of 1 mg/mL and transferred into a water-filled tank of the instrument filled with water. The samples were homogeneously dispersed in water by continuous stirring and ultrasonic. The mean particle size and particle size distribution were obtained from the software based on the diffraction of laser scattered by the sample particles. Each value was conducted in triplicate on duplicate samples at room temperature.

2.7. Scanning electron microscopic observation

Protein and peptide hydrogel microstructures were observed using scanning electron microscopy (SEM, Hitachi Corporation, Japan). All samples (12%) were frozen at -80℃, freeze-dried using a vacuum freeze-dryer, and cut into small pieces (2 × 2 × 1 mm^3). The fracture surfaces were observed using SEM after being sputter-coated with gold.

2.8. Zeta potential

Zeta-potential was measured using a Dynamic Laser Light Scattering instrument (Zetasizer Nano-Zs, Malvern Instruments, UK) at room temperature. The freeze-dried samples were diluted in 0.1 mol/L sodium phosphate buffer (pH 7.0) at a concentration of 1 mg/mL. Four replicates were performed for each sample.

2.9. Determination of surface hydrophobicity and free sulfhydryl contents

Surface hydrophobicity was measured using 1-anilino-8-naphthalene sulfonate as a hydrophobic probe according to the method of (Zuo, et al., 2022) with minor modifications. Different hydrolysate samples were diluted to 1 mg/mL concentration with phosphate buffer (0.1 M, pH 7.0). Approximately 2 mL of each sample was mixed with 50 μL of 8.0 mM ANS solution and allowed to react for 20 min in the dark. Fluorescence intensity was detected using a Synergy HT spectrofluorometer (BIO-TEK, VT, USA) with a slit width of 5 nm. The excitation and emission wavelengths were 390 and 470 nm, respectively. The slope value of fluorescence intensity versus sample concentration was used as the index of surface hydrophobicity.

The free sulfhydryl (-SH) groups were determined using Ellman's reagent (DTNB, 5,5'-dithio-bis-(2-nitrobenzoic acid) as previously described (Beveridge, Toma, & Nakai, 1974; Yin, Tang, Wen, & Yang, 2010) with some modifications. The samples (50 mg) were dissolved in 10 mL Tris-glycine buffer containing 2 mmol/L ethylenediaminetetraacetic acid (EDTA), and then 100 μL Ellman's reagent was added. The mixed suspension was placed in the dark for 1 h at 25℃. The mixture without a sample was used as the blank control. Absorbance was measured at 412 nm. The SH concentration was calculated using the molar extinction coefficient of 2-nitro-5-thiobenzoateat and the equation is as follows:

$$SH\ (\mu mol/g) = (A_{412} \times 10^6) / [(b \times \varepsilon) \times C],$$

where A_{412} is the absorbance at 412 nm, 10^6 (μmol/mol), b (cm) is the cuvette path length, ε (14150 L mol^{-1} cm^{-1}) is the molar extinction coefficient, and C (g/L) is the

sample concentration.

2.10. Fourier transform infrared spectroscopy (FTIR)

Infrared spectra were recorded using a Shimadzu IRAffinity-1S FTIR-spectrometer (Shimadzu, Tokyo, Japan) equipped with a diamond attenuated total reflectance (ATR) attachment. The sample was mixed with KBr at a ratio of 1:100 (*w*/*w*) and compressed into a tablet. Measurements were performed in the 4000-600 cm^{-1} at a resolution of 4 cm^{-1} with a total of 32 scans. The sample data were analyzed using the OPUS 7.2 spectroscopy software. The secondary structure of the protein was assigned by band fitting the amide I region (1700–1600 cm^{-1}) using Omnic 8.2 software and reported as the percentage of the total peak area.

2.11. Amino acid and proteomics analysis

The amino acid composition of QPH was determined using high-performance liquid chromatography (HPLC, LC20A, Shimadzu, Japan) with pre-column phenylisothiocyanate (PITC) derivatization. Briefly, the QPH sample was dissolved in 6 M HCl and hydrolyzed for 24 h at 110℃. The hydrolysate was dried and derivatized with PITC at room temperature for 30 min. After derivatization, the sample was detected using a reversed-phase HPLC with a UV detector (254 nm).

Mass spectrometry data were collected using an EASY-nLC 1200 HPLC system in series with a Q Exactive HF-X mass spectrometer (Thermo, MA, USA). The QPH sample was dissolved in water and centrifuged at 12000 g for 10 min. The supernatant was filtered through a 5-kD ultrafiltration filter and desalted using a C18 column. Thereafter, the desalted peptides solution was concentrated using a centrifugal concentrator and allowed to undergo further detection. The peptide sample was loaded onto the pre-column via an autosampler and then separated through an analytical column (C18, 2 μm, 75 μm × 25 cm). The liquid chromatography method was set as follows: mobile phase A (0.1% formic acid), mobile phase B (0.1% formic acid), flow rate (300 nL/min), and the gradient employed was a 100 min linear gradient. Mass spectrometry data acquisition was performed in DAA mode with a full-scan MS (Resolution: 60000, automatic gain control (AGC) target value: 3e6, scan range: 350–1800 m/z, maximum injection time: 20 ms) and 25 MS/MS scans (Resolution: 15000, automatic gain control (AGC) target value: 2e5, maximum injection time: 50 ms). The isolation window was set to 1.6 m/z, the high-energy dissociation (HCD) normalized collision energy was set to 28%, and the dynamic exclusion time of repeated ion acquisition was set to 35 s.

Raw MS and MS/MS data were analyzed using Maxquant software (version 1.6.6). The database searches against the UniProt protein database were carried out using the search engine Andromeda. The search parameters were as follows: carbamidomethyl (C) was set as a fixed modification; oxidation (M) and acetyl (protein N-term) were used as variable modifications; the mass tolerance in MS was set to 20 ppm, the main search tolerance was set to 4.5 ppm; the MS/MS tolerance was set to 20 ppm; the identifications were filtered to acquire a 1% false discovery rate (FDR).

2.12. Differential Scanning Calorimetry (DSC)

Thermal properties of QP and QPH were measured using differential scanning calorimeter (DSC) Q1000 TA Instruments (New Castle, Delaware, USA). Approximately 2 mg sample powder was weighed and sealed in the aluminum hermetic pan. Samples were heated from 20 to 250 ℃ at a rate of 10 ℃/min in an inert environment using nitrogen with the gas flow at 50 mL/min. An empty pan is used as a reference. Protein denaturation temperature and enthalpy were calculated using Universal analysis software.

2.13. Dynamic surface tension

The adsorption of QP and QPH at air-water interface (25 ℃) was measured using maximum bubble pressure method. The contents of QP and QPH samples were about 0.8 mg/mg, and 1mg/mL sample solutions were prepared by adding Milli-Q water. Using an S180 capillary (diameter 0.2 mm) and a Bubble Pressure Tensiometer BP100 (Krüss GmbH - Hamburg, Germany), air bubbles were generated at a constant speed through the protein solution (1 mg/ml). The pressure reached its maximum when the bubble radius reached the capillary radius. The surface tension was continuously monitored from bubble formation until bubble pressure reached the maximum value. The adsorption kinetic curve was established by plotting surface tension versus surface age (10 ms to 230 s).

2.14. Statistical analysis

All measurements were conducted in duplicate or triplicate, and the experimental results were presented as mean ± standard deviations (SD). Statistical differences among means were determined using GraphPad Prism (version 9.3.0) through one-way or two-way ANOVA, and significant differences were considered at $p < 0.05$.

3. Results

3.1. Quinoa protein and its hydrolysates

According to a previously reported method, the quinoa protein yield and purity were determined to be 6.85% and 86.02%, respectively. The SDS-PAGE protein pattern showed that QP had many bands with varying levels of intensity (Figure 5-1A). According to previous literature, the band with a molecular weight above 65 kDa corresponded to 7S Globulin, and the band around 45-55 kDa was assigned to 11S globulin (Brinegar & Goundan, 1993; Shen, Tang, & Li, 2021). Under reduced conditions, the disulfide bonds of 11S globulin are broken to form acidic (AS) and basic (BS) polypeptide subunits with the molecular mass of 32-39 kDa and 20-23 kDa, respectively (Abugoch, Romero, Tapia, Silva, & Rivera, 2008; Brinegar, et al., 1993). Additionally, the band at approximately 10 kDa corresponded to 2S albumin (Brinegar, Sine, & Nwokocha, 1996).

To obtain quinoa peptides, QP was digested with alcalase for 180 min. The extent of protein degradation is represented by DH (Figure 5-1B). QP experienced steady hydrolysis from 0 of DH at the beginning to 15% in 90 min, the 11S globulin band quickly degraded, and the alkaline subunit of 11S globulin gradually disappeared. As

the hydrolysis degree increased, the intensity of high-molecular-weight bands decreased. When DH reached 18% after 180 min, all subunits partially disappeared. These results demonstrated that the peptide fragments were released during the hydrolysis and these quinoa peptides were less than 10 kDa. GPC results depicted that the 180-min hydrolysate had a mean Mw of 5.01 kDa, demonstrating that the peptides were released during the hydrolysate process.

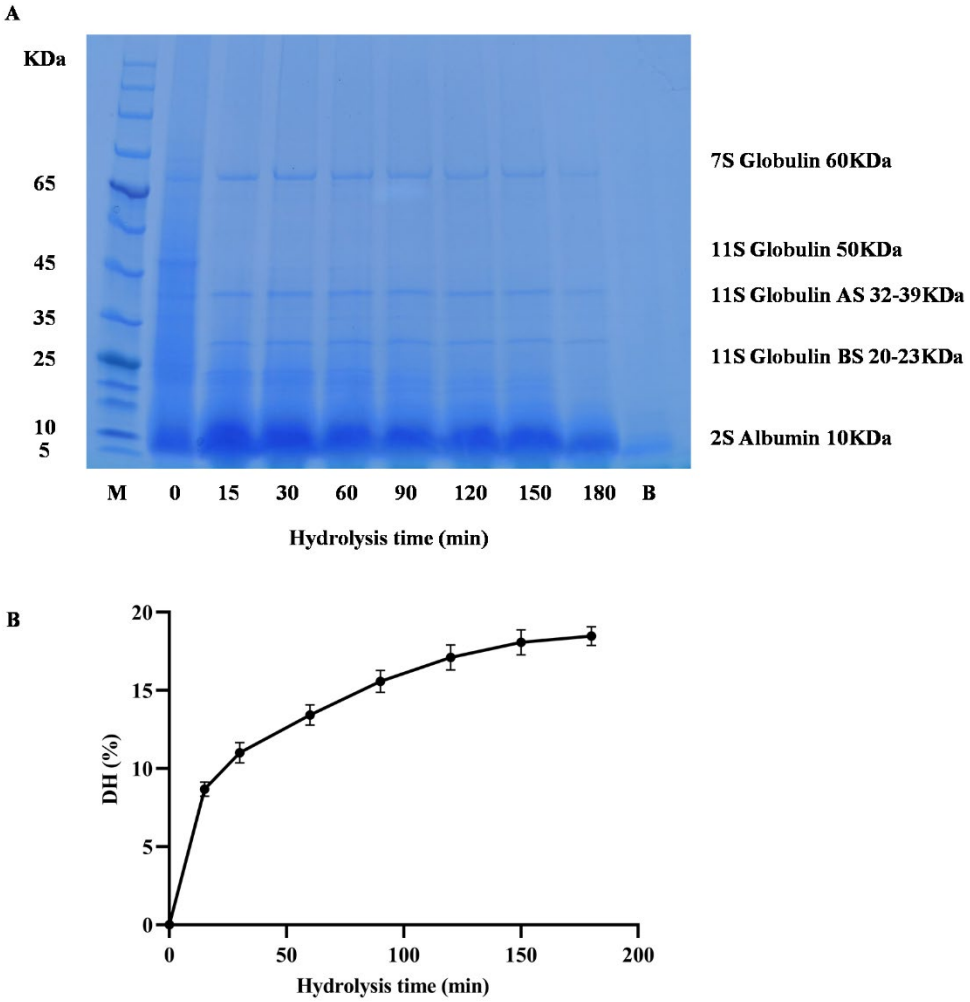

Figure 5-1. (A) SDS-PAGE profiles of quinoa protein (QP) and its hydrolysates (QPH) resulting from alcalase hydrolysis at various incubation times. M: molecular weight marker; B: blank; (B) Degree of hydrolysis of QP under alcalase treatment.

3.2. Gelation of QP and its hydrolysates

According to previous studies, pH adjustment and heat treatment are identified as

the main factors affecting the gelation property of QP (Galante, et al., 2020; Ruiz, Xiao, van Boekel, Minor, & Stieger, 2016). Moreover, the gel formation of QP was induced and affected by salt addition (Yang, et al., 2022). In the present study, QP did not exhibit gel-forming properties before adding alcalase. However, as hydrolysis proceeded, the solution became slightly viscous after 60 min, suggesting that the peptides might have formed organized microstructures. Subsequently, the gel properties of QPH were examined, and 10%–15% (*w*/*v*) of QP and QPH suspensions were prepared. As shown in Figure 5-2A, no hydrogels formed of QP within the concentration range of 10%–15%. Notably, QPH formed hydrogels at 11%–15%, and 10% was the critical concentration of hydrosol to hydrogel. In contrast to a previous study, QPH with potent hydrogel-forming capacity was prepared through excessive hydrolysis. Moreover, QPH hydrogels could be obtained by dissolving QPH in water at a suitable ratio without other chemical induction steps.

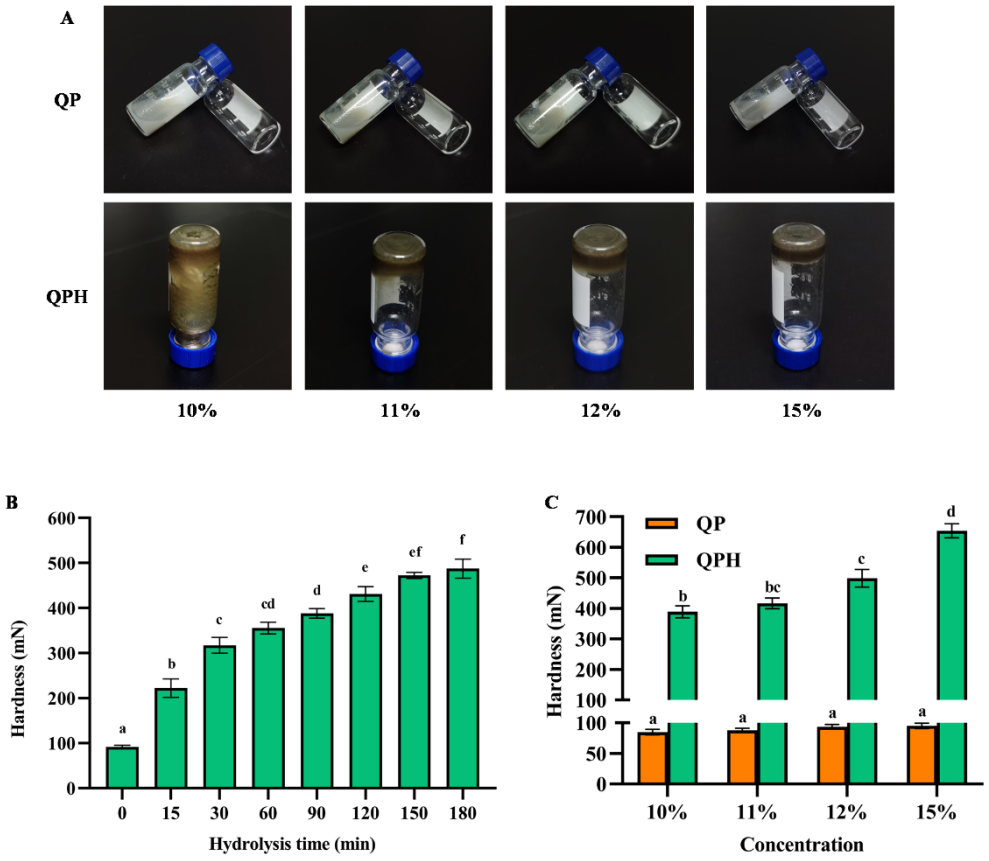

Figure 5-2. Hardness of hydrogel/hydrosol formed by QP and QPH at various concentrations. (A) hydrogel forming ability; (B) changes in the hardness of 12% QP hydrogel with alcalase hydrolysis time; (C) hardness of 10%-15% QP (orange bars) and 10%-15% QPH (green bars). Mean value of three determinations ± SD, and values with different letters are significantly different ($p < 0.05$).

As previously mentioned, QP gradually exhibited gel-forming properties with increasing DH. Therefore, the hardness variation of 12% QP during hydrolysis was determined (Figure 5-2B). There was a rising trend in hardness as hydrolysis time increased. In the beginning, the hardness significantly increased more than doubled from 91.86 mN (4.68 kPa) of QP to 222.07 mN (11.31 kPa) of 15-min QPH. After that, there was a smooth uptrend of its hardness, which increased significantly to 487.52 mN (24.83 kPa) at 180 min. Furthermore, the hardness of QP and QPH at different concentrations was also measured. As shown in Figure 5-2C, the texture test results showed that the hardness of QPH presented an upward trend with the increased concentration, and the breaking force was from 388.83 mN (19.20 kPa) of 10% hydrosol to 654.22 mN (33.32 kPa) of 15% hydrogel. Conversely, QP did not show appreciable changes in hardness (84.74–95.03 mN (4.32–4.84 kPa)) at each concentration of 10%–15% (Figure 5-2C). These results indicated that excessive hydrolysis was an effective approach to produce quinoa peptides with potent hydrogel-forming abilities.

3.3. Rheological properties of QPH hydrogels

Rheological properties can directly reflect the formation and transformation of hydrogel structure, thereby facilitating the exploration of the mechanism of gel formation. For the viscosity test, both QP and QPH displayed an increasing trend as the sample concentration increased from 10%–15%, whereas the viscosity of all samples decreased at each concentration with an increasing shear rate (0.1 to 100 s-1) (Figures 5-3A-B). Moreover, we found that all QPH samples exhibited a higher viscosity than QP samples at each share rate, implying that the structure of QP itself could not occur in sol-to-gel transition, whereas the structure of QPH generated by enzymatic degradation was more prone to interaction.

The values of G' and G'' were used to indicate the viscoelasticity of materials, indicating whether they behaved as an elastic solid ($G' > G''$) or as a viscous liquid ($G' < G''$). As shown in Figures 5-3C-D, the frequency sweep test was conducted at 1% strain within the Linear Viscoelastic Region. For all QP samples at each concentration, the G' value was lower than the G'' value throughout the entire frequency range (0.1-100 Hz), and both G' and G'' values slightly increased as the frequency increased (Figure 5-3C). Moreover, the G' values of all QP samples were lower than 10 Pa. These observations indicated that QP was weak in gelation properties and more inclined to exhibit fluid properties as hydrosol. In contrast, there were completely different trends between G' and G'' at each QPH concentration with increasing frequency. For 10% QPH, similar to the QP samples, its G' value was lower than the G'' value, but the difference between them was narrowed (Figure 5-3D). When the concentration of QPH reached 11%, the gap between G' and G'' shrunk, and as the frequency increased, the G' value exceeded the G'' value, implying that 11% was the critical concentration for the sol-to-gel transition of QPH. Furthermore, the G' value thoroughly surpassed the G'' value as the concentration of QPH reached 12% or 15%, indicating that elasticity was dominant in the QPH structure and a stable hydrogel network was formed. Similar results, regarding the viscoelasticity of protein, have been reported in previous studies (Luo, Cheng, Zhang, & Yang, 2022; Yu, et al., 2022).

Furthermore, the enhanced gel strength may be due to the smaller particle size and unfolded protein structure, which improves the interactions between proteins or peptide molecules. Moreover, non-covalent bonds, including hydrogen bonds, disulfide bonds, and hydrophobic interactions, can influence the formation of plant protein gels (Galante, et al., 2020; Luo, Zhang, Palmer, Hemar, & Yang, 2021).

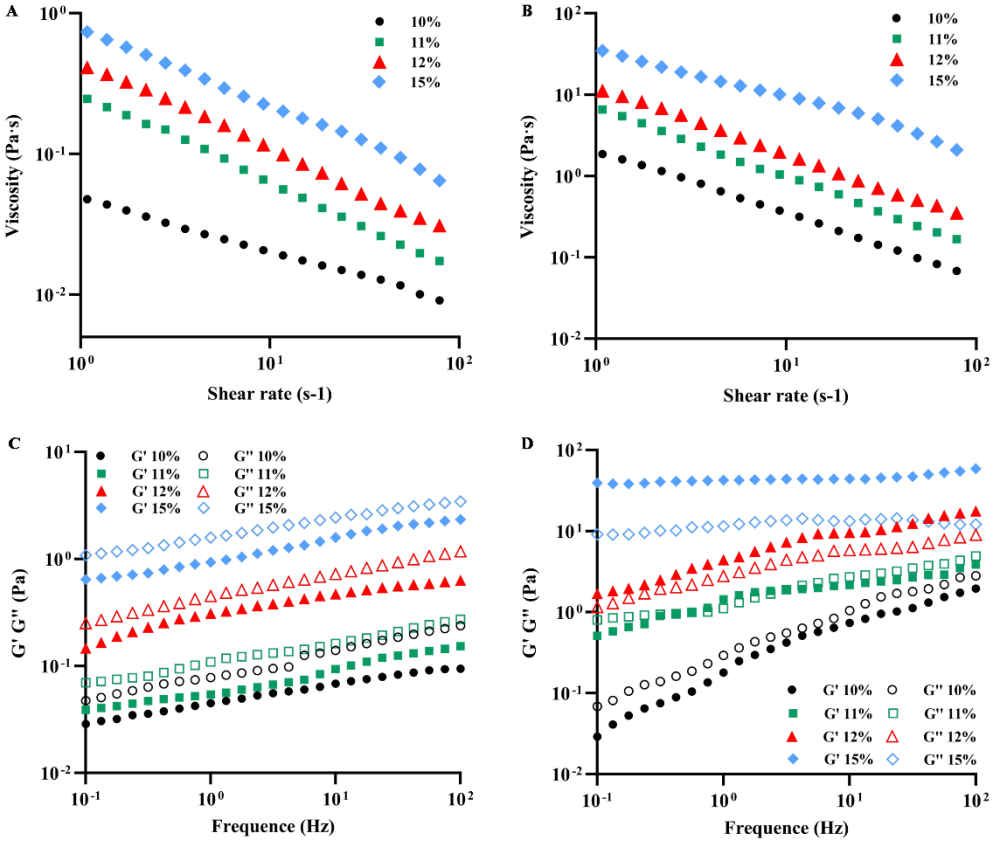

Figure 5-3. Rheological properties of QP and QPH at various concentrations (10%-15%). Viscosity profile of QP (A) and QPH (B); storage modulus (G′) and loss modulus (G″) of QP (C) and QPH (D).

3.4. Microstructure analysis

Particle size is one of the main factors that affect the functional properties of proteins (Wang, et al., 2022). The particle size distribution and mean particle size were shown in Figure 5-4A. The mean particle size of QP suspension was 46.25 μm, and its particle size distribution ranged from 2.35–677.70 μm. QP suspensions without treatment displayed large aggregates ranging from 0.06–100 μm, consistent with the QP sample in the present study (Shen, et al., 2021). After alcalase hydrolysis, the mean particle size of QPH was decreased than that of QP. However, the particle size

distribution of QPH revealed a bimodal distribution. Most of the particles were in the 0.51–112.47 μm, with a smaller distribution between 148.26 and 778.1 μm.

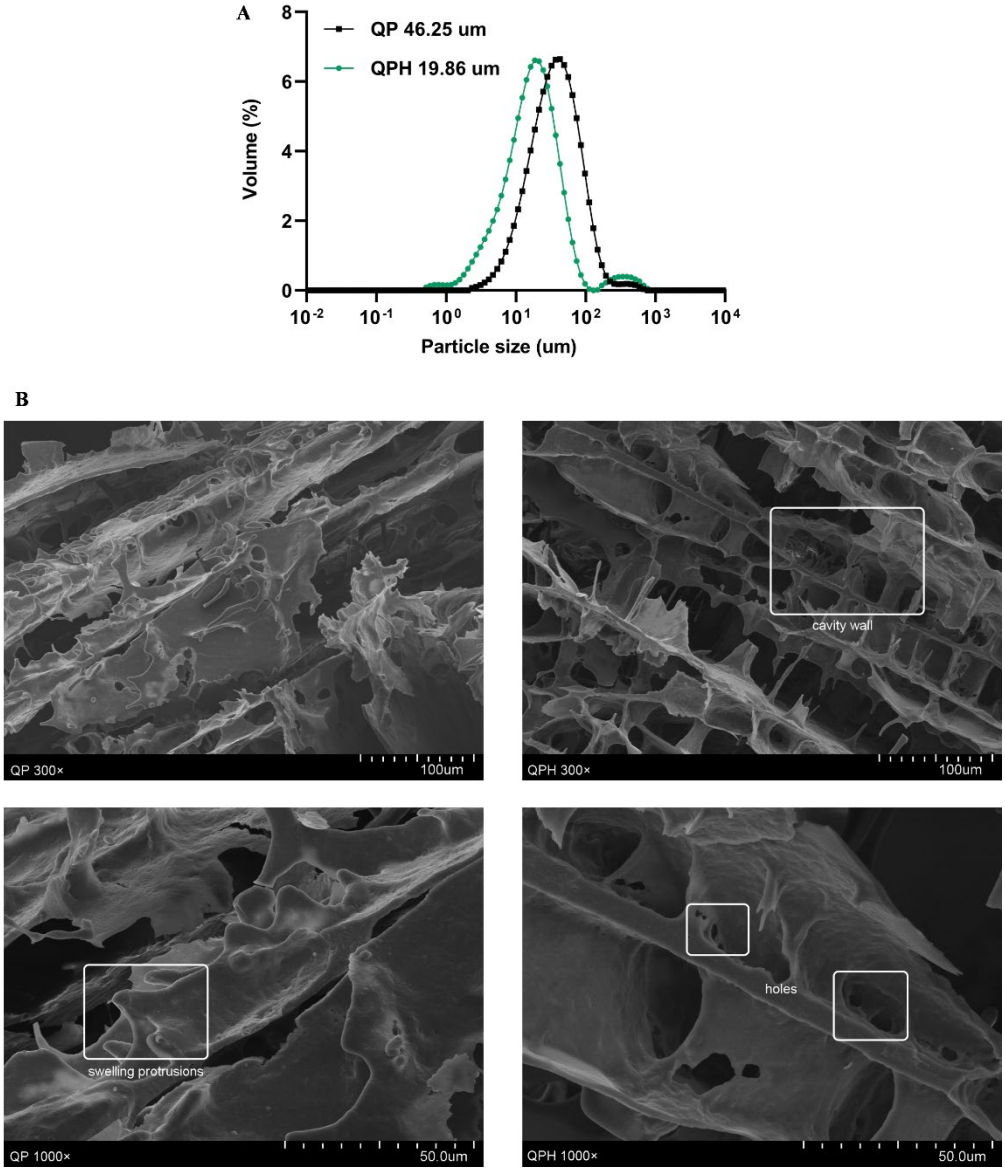

Figure 5-4. (A) Particle size distributions of QP and QPH; (B) SEM images of 12% QP and 12% QPH hydrogels; the upper panel represent pictures at 300× magnification and the lower panel represent pictures at 1000× magnification; the white words represent the structure in the white box.

SEM was performed to visually assess the network gel structure and particle shape of 12% QP and QPH. As illustrated in Figure 5-4B, QP hydrogel displayed irregular and compactly stacked lamella, suggesting that it may be less capable of entrapping water molecules through hydrogen bonds. Moreover, the lamella surface was smooth with swelling protrusions stretching out, and there were also some protein particles on the lamellar surface. These results implied that the cross-linking of QP hydrogel was limited. In contrast, a regular, uniform, and interconnected porous structure was observed in the SEM image of QPH hydrogel. Meanwhile, its cavity wall thickness was very thin, and there were holes in the connection of adjacent cavities, with little or no protrusions and protein particles linked to the cavity wall. This change might be caused by the hydrolysis effect of alcalase, as mentioned previously, which decreased the particle size and resulted in the exposure of SH groups and hydrophobic groups (Yu, et al., 2022). These results indicated that QPH could form a strong self-assembled hydrogel and have a potent ability to capture water molecules through hydrogen bonds. Furthermore, the microstructural changes between QP and QPH are related to the functional properties, which is consistent with our results of gel hardness, rheological properties, and particle size.

3.5. Molecular interactions of QPH aggregation

The surface hydrophobicity and free sulfhydryl content were determined and displayed in Figure. 5. The hydrophobicity of QP and its hydrolysates increased from 477 (QP) to 645 (QPH). The hydrophobicity of the 150-min hydrolysate was close to that of QPH, implying that the hydrophobic groups buried in QP were gradually exposed to enzymatic hydrolysis, and the exposure of the hydrophobic groups almost reached the maximum at 150 min. Conversely, the content of SH groups decreased with increasing DH, reaching a final value of 7.09 μmol/g. However, during the first 15 min, the concentration of SH groups was increased from 10.65 μmol/g of QP to 16.78 μmol/g of 15-min hydrolysate. Afterwards, the SH groups exhibited a continuous reduction from 16.78 μmol/g to 7.09 μmol/g of QPH. Similar results were also observed in a previous study, where the content of free SH groups of QP elevated from 10.9 μmol/g to 17.7 μmol/g at pH 8.5 during the first 5 min (Mäkinen, Zannini, Koehler, & Arendt, 2016), which suggested that enzymatic hydrolysis not only broke down proteins into short peptides but also disulfide bonds in the initial stage. These peptides may re-aggregate because of the interactions of exposed reactive groups, which were considered to contribute to the self-aggregation forming capacity and formation of the mesh-like structure of QPH. Furthermore, zeta potential was measured, and the zeta potential of QPH (-23.40 mV) was significantly lower than that of QP (-17.35 mV). A highly negative zeta potential is conducive to gel formation and stability (Yu, et al., 2022).

FTIR measurements were performed to further investigate the self-assembled ability of QPH. The FTIR spectra of QP and QPH were presented in Figure. 6, and both exhibited the typical FTIR absorbance spectrum of the protein. The characteristic peaks of QP appeared at 3293 cm−1 (amide A), 2961 cm−1, 2931 cm−1 (amide B), 1656 cm−1 (amide I), 1542 cm−1 (amide II), and 1240 cm−1 (amide III). However, after hydrolysis treatment with alcalase, the same characteristic peaks of QPH were

shifted to 3294 cm−1, 2959 cm−1, 2928 cm−1, 1651 cm−1, 1547 cm−1, and 1243 cm−1. Amide A represented the O–H and N–H stretching vibrations (Yu, et al., 2022), and it was found that the major peaks at 3293 cm−1 differed between QP and QPH. In particular, the relative intensity of the absorption peak of QPH at 3371 cm−1 was lower than that of QP. Moreover, the band at 1656 cm−1 (amide I) for the C=O stretching vibration of QP shifted to a lower frequency at 1651 cm−1 of QPH (Daliri, et al., 2021). Generally, the bands at amide A and amide I were mainly mixed peaks of chemical bonds subject to hydrogen bonding and non-hydrogen bonding, and the absorption peaks of chemical bonds are affected by hydrogen bonds shifting to the lower band (Liang, et al., 2022). Therefore, the change of the peaks at 3371 cm−1 indicated that the hydrogen bonding of QPH was stronger than that of QP, improving the gelation ability of QPH.

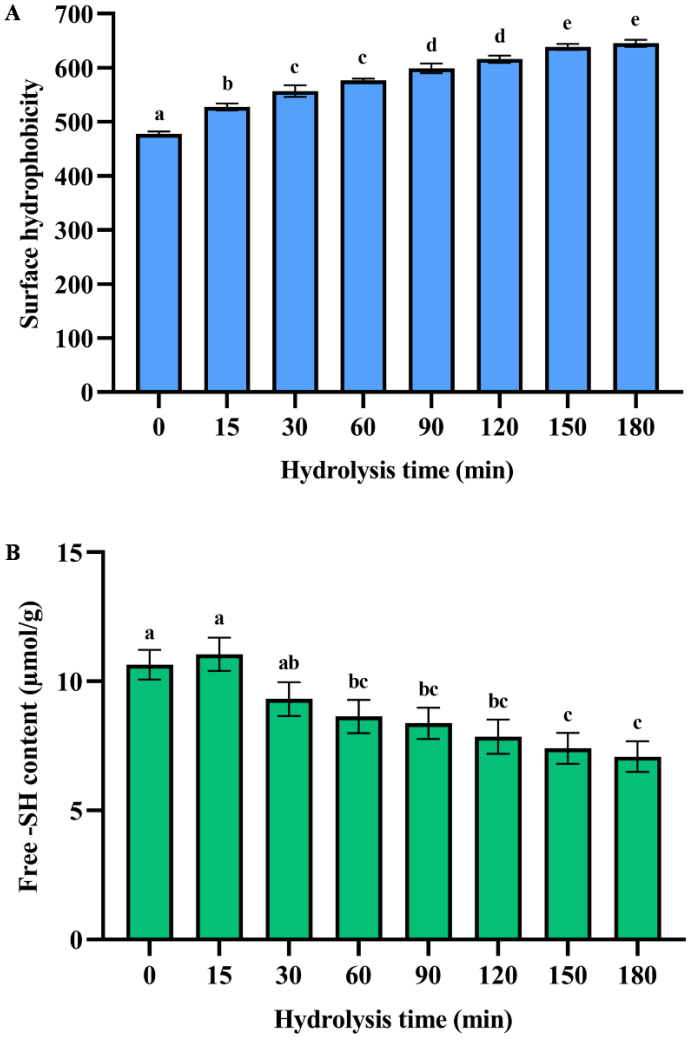

Figure 5-5. Surface hydrophobicity (A) and free sulphydryl content (B) of QP and QPH samples. Mean value of three determinations ± SD, and values with different letters are significantly different ($p < 0.05$).

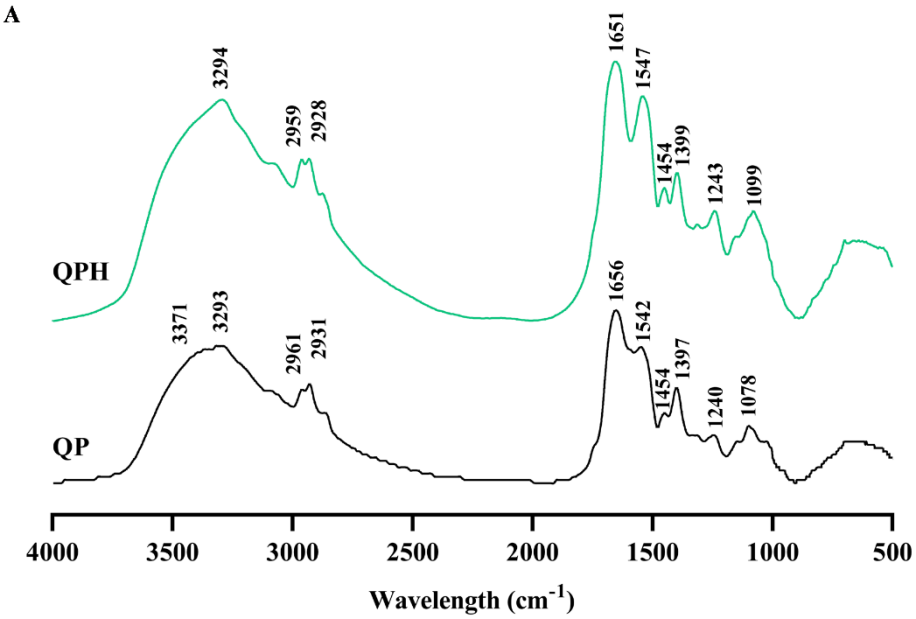

B

	β-sheet (%)	Random (%)	α-helix (%)	β-turn (%)
QP	27.64 ± 0.47 [a]	24.63 ± 0.74 [b]	15.82 ± 0.55 [a]	31.91 ± 0.88 [a]
QPH	27.36 ± 1.26 [a]	27.09 ± 1.10 [a]	15.61 ± 1.02 [a]	29.94 ± 1.11 [b]

Figure 5-6. FTIR spectroscopy (A) and secondary structures (B) of QP and QPH. Mean value of three determinations ± SD, and values with different letters in the same column are significantly different ($p < 0.05$).

Fourier self-deconvolution (FSD) method was conducted in the amide I region (1700–1600 cm−1) to analyze the secondary structure of quinoa peptides, and the proportions of α-helix, β-sheet, β-turn, and the random coil were calculated. As depicted in Figure. 6, compared with QP, the contents of α-helix and β-sheet were similar, whereas the random coil content increased significantly, and the β-turn

content decreased in QPH, implying that enzymatic hydrolysis did affect the secondary structure of QP. Similarly, a previous study found that the contents of α-helix and β-sheet were decreased, whereas the random coil content increased after alcalase hydrolysis (Ma, et al., 2022). Moreover, α-helix, β-turn, and β-sheet rely on specific forms of hydrogen bond interactions to form a relatively ordered structure, whereas random coil has a disordered structure because of the differences in hydrogen bond interactions (Xu & Wang, 2019). In our study, the breakage of the peptide and disulfide bonds of QP under alcalase treatment caused α-helix, β-turn, and β-sheet to unfold and form a random coil structure, resulting in an increased disordered secondary structure and exposed reactive groups of QPH. Overall, the enzymatic hydrolysis of QPH resulted in an increase in the disordered secondary structure and the exposure of hydrogen-bonded groups, which had a significant effect on the formation of self-assembling peptide hydrogels.

3.6. Thermal properties and interfacial Properties

The thermal denaturation properties of QP and QPH were analyzed by DSC to measure their thermal transitions. The denaturation temperature and enthalpy change can reflect the thermostability and tertiary structural property. As shown in Figure 5-7, no characteristic crystallization peak and melting peak observed both in QP and QPH samples, and only a weak glass transition peak found in QPH, indicating QP and QPH were denatured in the preparation process. Previous study reported that extreme pH values led to the denaturation of quinoa protein (Ruiz, Opazo-Navarrete, et al., 2016). In this study, quinoa protein underwent acid precipitation during the extraction, which could lead the lack of DSC peaks at high temperature.

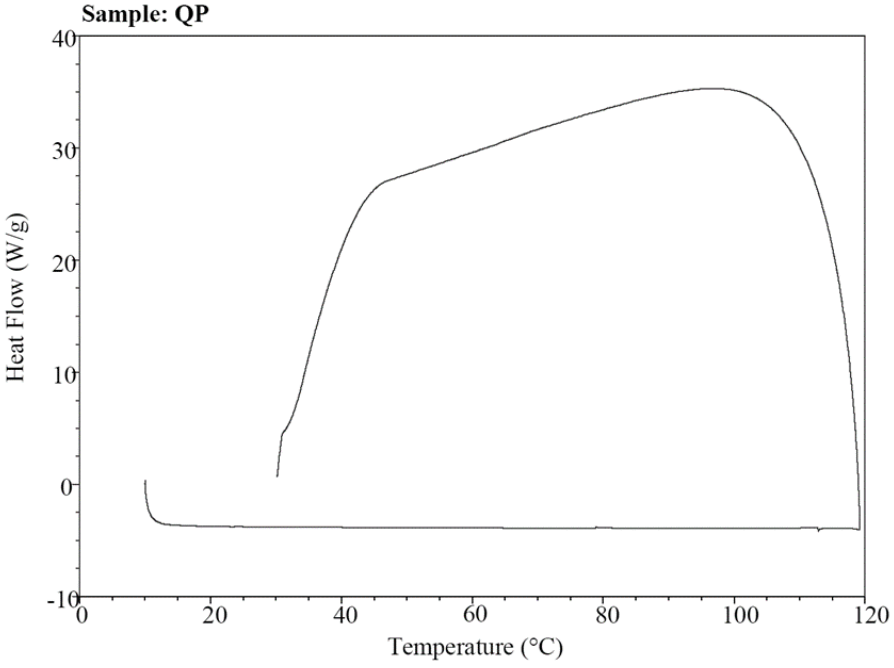

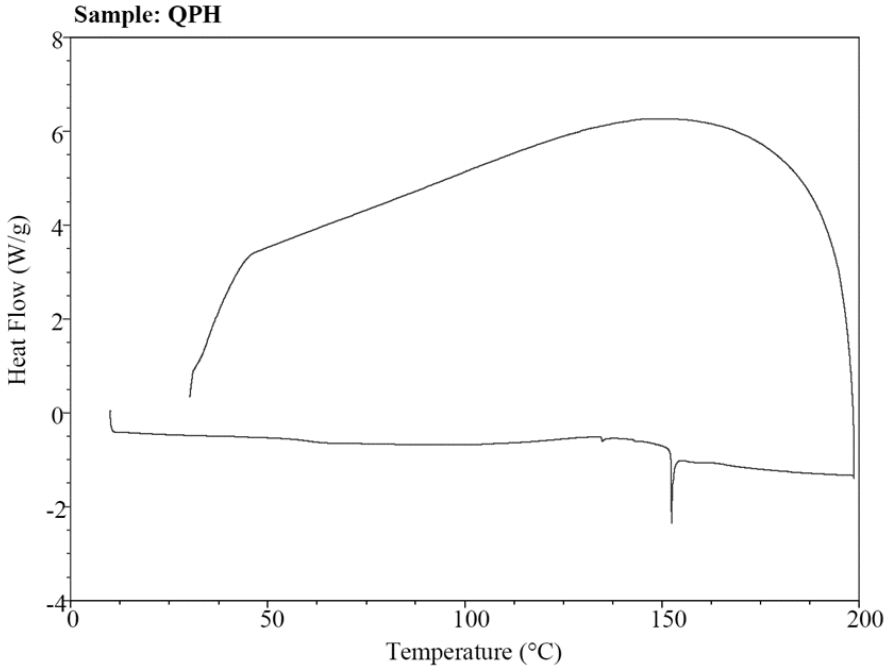

Figure 5-7. DSC thermograms of QP and QPH.

The changes in the adsorption kinetics of samples at the air-water interface were assessed via dynamic surface tension measurements. Surface tension can be instantly measured at the initial stage of adsorption using the maximum bubble pressure method. The lag time and the initial adsorption rate were obtained from the adsorption kinetic results. As shown in figure 5-8A, the surface tension curves of QP and QPH have similar changing trends at pH 7, and there is no difference in their lag time and initial adsorption rate (figure 5-8B). However, after the initial stage, it is worth noting that the surface tension of QPH was higher than that of QPH, which may be related to the exposure of hydrophobic groups as the surface age increased.

A

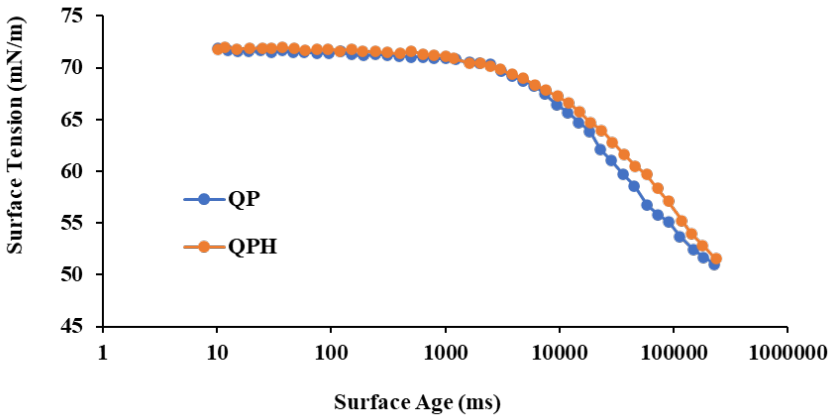

B

Sample	Lag time (s)	Adsorption rate (mN/(m ms))
QP	6.0236 ± 0.0282	0.0113 ± 0.0000
QPH	6.0675 ± 0.0055	0.0112 ± 0.0000

Figure 5-8. Adsorption kinetics at air-water interface (A) and adsorption kinetic parameters: lag time, rate of adsorption (B) of QP and QPH.

3.7. Molecular characteristics of QPH hydrogels

In the present study, 17 different amino acids were detected in QPH (Table 5-1), and previous studies have indicated that different amino acids contribute differently to the interactions between molecules. For QPH, the hydrophilic amino acids (Asp, Thr, Ser, Tyr, Glu, His, Lys, Arg, and Cys-Cys) made up 56.91%, and the hydrophobic amino acids (Leu, Ile, Phe, Gly, Ala, Val, Pro, and Met) made up 43.09%, suggesting that QPH represented an amphipathic nature and preferred to form aggregates spontaneously in solution, which was consistent with the results of surface hydrophobicity. Amino acid residues that could easily form hydrogen bonds because of the particular carboxyl, amino, or guanidyl groups were found among Asp, Glu, Lys, and Arg, accounting for 40.57% of the total amino acids (Yu, et al., 2022). Notably, the contents of Glu and Arg accounted for 13.85% and 10.17%, respectively. A previous study reported that the hydroxyl group of glutamic acid promoted the peptide-peptide interaction through hydrogen bonds, and the guanidine side group facilitated the interaction among peptide chains through hydrogen bonds, electrostatic interactions, and salt bridges, which ultimately alters the topology of the network formed and the final mechanical properties of the hydrogels (Gao, et al., 2017). Phe, Tyr, and His, which accounted for 11.56% of the total amino acids, were thought to contribute to peptide self-assembly due to the presence of phenyl rings or imidazole

rings that can form π-π stacking (Yu, et al., 2022). In addition, it has been demonstrated that high helicity amino acids, particularly Ala and Leu, were considered to aid in stabilizing the network of peptide hydrogels (Fu, et al., 2021). In our study, over 10% of Ala and Leu presented in QPH.

Table 5-1. The percentage of 17 amino acids determined in quinoa protein hydrolysate (QPH).

Amino acid	QPH(%)	Amino acid	QPH(%)
Asp	9.00	Ile	5.64
Thr	3.89	Leu	6.97
Ser	4.34	Tyr	4.11
Glu	13.85	Phe	4.82
Gly	4.45	His	3.59
Ala	3.57	Lys	7.55
Cys-Cys	0.41	ArG	10.17
Val	4.59	Pro	9.87
Met	3.19	Total	100

Aside from the amino acid content, the effect of the peptide chain sequence of QPH on gel formation was investigated using ultra-high-performance liquid chromatography-tandem spectrometry. The data files were analyzed using the Andromeda scoring algorithm of MaxQuant software, along with the uniport-taxonomy_63459 (*Chenopodium quinoa*).fasta database search. The identification results were summarized in Table 5-2, and a total of 97 peptide sequences were identified in QPH. It was observed that 76 peptides have molecular weights greater than 1 kDa, with peptide chain length in the range of 9 to 25 residues and molecular weight in the range of 1016.49 to 2721.37 kDa, whereas the molecular weight of the remaining 19 peptides was less than 1 kDa, with peptide chain lengths ranging from 6 to 10 residues and molecular weight ranging from 613.34 to 997.62 kDa. These findings agreed with those of a previous study (Yu, et al., 2022), implying that the middle-length peptides that are similar to synthetic peptides (480 Da–6 kDa) contributed to the hydrogel formation via self-assembly.

Protein electrostatic and hydrophobic interactions influence gelation behaviour. Whether the amphiphilic peptides displayed (XZXZ)n sequence of alternating hydrophobic (X) and hydrophilic (Z) residues or the peptides made up of alternating uncharged (U) and charged (C) residues known as the (UCUC)n sequence, both of which demonstrated potent gel aggregation capacity to self-assemble into hydrogels (Bowerman & Nilsson, 2012; Saiani, et al., 2009). The analysis of the identified peptides revealed that QPH is primarily composed of amphipathic peptides and most of these identified peptides displayed the (XZXZ)n sequence in general, for instance, IGPQKPIPDVVVILPPKEDDVYAR, KLEPTPGDMIR, and RLNLEAVGVELDQTGAVK (Table 5-2). In total, 69 identified peptides with (XZXZ)n similar sequence comprised 33.33% to 77.78% hydrophobic residues. In terms of the (UCUC)n sequence, a previous study reported that AEAEAKAKAEAEAKAK (yeast Zuotin peptides), AEAKAEAK, and FEFKFEFK

(synthesized peptides) could obtain the robust gel aggregation capability through self-assembly (Saiani, et al., 2009). In this study, the charged residues of most peptides could reach or surpass 50% of total residues and presented a common sequence (UCUC)n, for example, EDPKDDYLK, DLKEDPKDDYLK, and RMPDDLDYAK (Table 5-2). These observations suggested that the amino acid sequence and composition of QPH were critical for the final achievement of its hydrogel-forming ability, which may be attributed mostly to compliance with the hydrogel-forming rules of synthetic self-assembled peptides.

Table 5-2. Peptides identified in QPH.

Feature	Peptide sequence	m/z	Mass (Da)	Protein accession	Position
$(XZXZ)_n$	IGPQKPIPDVVVILPPKEDDVYAR	886.83	2657.48	A0A803MWB7	198-221
	IGPQKPIPDVVVILPPK	604.04	1809.11	A0A803MWB7	198-214
	AYADDDLIR	526.26	1050.50	A0A803KXN1	125-133
	DTFPDDLLAPVLK	722.39	1442.77	A0A803KQI7	72-84
	KLEPTPGDMIR	636.83	1271.65	A0A803KU86	330-340
	TVPDGLPDDHPR	659.82	1317.63	A0A803L525	71-82
	FIIDMPGLK	517.29	1032.57	A0A803LB63	68-76
	EIPEDGRVPK	570.31	1138.60	A0A803LS32	12-21
	NNPVLIGEPGVGK	647.36	1292.71	A0A803LSG5	214-236
	QAVSPL	614.35	613.34	A0A803LSG5	905-910
	IEFPLPDRR	381.55	1141.62	A0A803MPE1	328-336
	ELLPPGSVDNTTR	699.86	1397.72	A0A803MRI3	138-150
	LNLEAVGVELDQTGAVK	878.48	1754.94	A0A803MUE8	303-320
	RLNLEAVGVELDQTGAVK	638.02	1911.04	A0A803MUE8	302-320
	FPSPGSEDDAQK	639.29	1276.56	A0A803MW84	376-387
	VEIPPYR	437.25	872.48	A0A803MW84	1050-1067
	AVDEEDLLK	516.27	1030.52	A0A803KPS8	579-587
	ATLLPSDPYHR	635.33	1268.65	A0A803KRP4	66-76
	HWVLDPIDGTK	640.84	1279.66	A0A803KX23	167-177
	LEPLPDGSMNPK	657.32	1312.63	A0A803L2M5	1041-1052
	IEDVTPIPTDSTR	722.37	1442.73	A0A803L2X3	128-140
	FTNPDLR	431.72	861.43	A0A803L3C1	871-877
	FPTLPFIPK	530.32	1058.62	A0A803L4E2	136-144
	GEIVEPDNDPPQK	719.35	1436.68	A0A803L6G6	58-70
	MMEFAEKIGWK	693.33	1384.65	A0A803L6T6	208-218
	TIYIPQPTWGNHPK	826.43	1650.85	A0A803LBT5	213-226
	GVLPDSKPIVVK	626.39	1250.76	A0A803LEZ0	113-124

IVQQPNEKPALR	464.94	1391.79	A0A803LI84	107-118
VFEMEMGIFK	631.79	1261.57	A0A803LIU4	27-36
LPYLLK	373.74	745.47	A0A803LP38	102-107
IEEEPVPEPPK	632.33	1262.64	A0A803LSH2	556-566
RPYPEDSYAPR	675.83	1349.64	A0A803M4L5	520-530
DLDYIEEPFLR	705.35	1408.69	A0A803M8T5	1131-1141
DLEKILK	429.77	857.52	A0A803M8V6	554-560
GEIVEPDNDAPQK	706.34	1410.66	A0A803MCT4	58-70
VGETVDIVGMVDTR	753.88	1505.74	A0A803MFX4	216-229
ETVQYPVEHPEK	728.36	1454.70	A0A803MG10	47-58
IVDFIK	367.73	733.44	A0A803MK45	151-156
LVFKDDEGNSMK	699.83	1397.65	A0A803MWY1	42-53
RSAEETPQDPVDD	729.82	1457.63	A0A803MZ16	164-176
AVDSLVPIGR	513.80	1025.59	A0A803MZD3	7-16
IEFPLPDIK	536.31	1070.60	A0A803N4I6	322-330
LPVDQVIQPVIR	688.92	1375.82	A0A803NAD8	197-209
KSLQNSNILSR	631.34	1260.67	A0A803KWR9	319-329
VNEPLNI	800.40	799.40	A0A803L533	866-872
LDIQQQ	746.36	745.35	A0A803L5M9	597-602
WNVTLK	381.21	760.41	A0A803LGI9	788-793
VENLVSER	473.75	945.48	A0A803LGJ9	383-390
LKDQVQENNFLLK	796.41	1590.81	A0A803LHY8	293-305
QFFDNSNEVNR	687.28	1372.54	A0A803LI90	517-528
IWTPPEDLRK	418.90	1253.68	A0A803LQF4	323-332
QVSEEEVMK	548.25	1094.48	A0A803LWQ2	323-331
QVIGPDDNGVK	571.30	1140.58	A0A803LX46	26-36
TPSPGIEIPEEWSAAAYTIAKSFTR	454.57	2721.37	A0A803M3Y3	10-34
INNIFR	389.22	776.42	A0A803M7Q1	208-213
HNMAGIIMEYIDGFEVR	997.98	1993.94	A0A803MA62	374-390
TWFNQPAR	510.26	1018.50	A0A803MCX4	23-30

	TLGKFNPFK	526.79	1051.57	A0A803MEW5	547-555
	GALDGGLDIPHSDK	697.85	1393.68	A0A803MPQ9	164-177
	FGTPEDLK	453.73	905.45	A0A803MQJ5	353-360
	IDDIVTVR	465.77	929.52	A0A803MR68	527-534
	VGLSLENNQLK	609.32	1216.62	A0A803MSD7	224-234
	VQSPIRNANTVR	679.36	1356.70	A0A803MW56	362-373
	FDGTVPEPR	509.25	1016.49	A0A803N231	278-286
	ARFDGTVPEPR	415.55	1243.63	A0A803N231	276-286
	VQIVPR	356.72	711.43	A0A803N291	51-56
	EFADDVLPR	531.27	1060.52	A0A803N5C3	241-249
	GLQNEMEVMK	590.27	1178.53	A0A803N5K3	321-330
	LDVNLPVDR	521.28	1040.55	A0A803NDP1	186-194
	SHIPDGPGYEEK	644.81	1327.60	A0A803MW32	119-130
	DSPLLPPDTR	555.79	1109.57	A0A803N201	703-712
	GHAVGDIPGVR	539.29	1076.57	A0A803LZW3	49-59
	GGVIDEDALVR	572.30	1142.59	A0A803MP37	87-97
$(UCUC)_n$	EDPKDDYLK	561.77	1121.52	A0A803KXN1	164-172
	DLKEDPKDDYLK	493.58	1477.73	A0A803KXN1	161-172
	RWEIPDDILHR	483.92	1448.75	A0A803M049	95-105
	RMPDDLDYAK	612.29	1222.57	A0A803M3Q4	133-142
	KPDTDFDFYK	638.30	1274.58	A0A803MPE1	406-415
	VLEDDDSLR	531.26	1060.50	A0A803MS48	1332-1340
	ILSSDEGKK	976.53	975.52	A0A803L215	44-52
	DDSMNDYITK	609.25	1216.49	A0A803L6C7	64-73
	NLDDTIDDDKLK	702.85	1403.68	A0A803LGZ0	292-303
	KIWDDITVR	573.32	1144.62	A0A803LRN3	230-238
	KSMDDPGR	905.41	904.41	A0A803M212	540-547
	VEIDDDQKLR	615.82	1229.63	A0A803MEA7	16-25
	DGFIIR	360.71	719.40	A0A803NDX4	47-52
None	NNNPASSKK	959.49	958.48	A0A803MS48	438-446
	TQVIPPLPEDR	632.85	1263.68	A0A803L206	698-708

VPPALPLPPPPITK	718.95	1435.88	A0A803M8F1	67-80
IQQQQQTNK	559.77	1117.53	A0A803KQY4	335-343
VFGPTSQQR	511.25	1020.49	A0A803L2W5	55-63
LPPVWK	370.23	738.44	A0A803MEN6	135-140
IVPGNNNSYDK	611.29	1220.57	A0A803MQJ5	609-619
LVLLPR	355.75	709.49	A0A803MUJ6	209-214
FDDSEQQTPGWK	719.32	1436.62	A0A803MZ46	352-363
VLIGEIGLGK	499.82	997.62	A0A803MNP0	2-11
NGGVFPR	374.19	746.37	A0A803N4A8	41-47

The letters marked in shades represent hydrophobic amino acids, underlines represent positively charged amino acids, and wavy lines represent negatively charged amino acids.

6

Chapter VI General discussion

1. General discussion

1.1. Anti-Colon Cancer Activity of Novel Peptides Isolated from In Vitro Digestion of Quinoa Protein in Caco-2 Cells

Colon cancer is a common malignant tumor in the digestive system and is difficult to detect in the early stages. Many risk factors are affecting the occurrence and progress of colon cancer, including age, chronic alcohol, unhealthy diet, and so on. Although some synthetic drugs are currently utilized for the treatment of colon cancer, which is insufficient and may have side effects. Recently, dietary and microbial components are expected as therapeutic adjuvants to inhibit the occurrence of colon cancer (Wyatt & Greathouse, 2021). Compared to other cereals, quinoa was rich in protein with excellent nutritional value, which can release bioactive peptides after enzymatic hydrolysis (Vilcacundo et al., 2018; Montserrat-de la Paz, Martinez-Lopez, Villanueva-Lazo, Pedroche, Millan, & Millan-Linares, 2021). Moreover, quinoa protein and its derived peptides have shown certain antihypertensive activity and the greatest anti-cancer effects (Vilcacundo et al., 2018; Guo et al., 2020).

In this study, the antiproliferative activities of different samples were evaluated in colon cancer Caco-2 cells. Vilcacundo and co-workers have proved that sequential incubation with pepsin and pancreatin result in the complete degradation of quinoa protein while incubation with pepsin resulted in the partial hydrolysis of quinoa protein. They also demonstrated that the antiproliferative activity of gastroduodenal digests significantly increased than that exhibited by gastric digest (Vilcacundo et al., 2018). We followed their digestion conditions to prepare QPH and found that QPH exhibited an increasing antiproliferative activity while QP did not show obvious anticancer ability in the concentration range from 0-4 g/L, which is consistent with a previous study (Vilcacundo et al., 2018). This result suggests that more peptides of quinoa protein were released by pepsin and pancreatin after in vitro simulation digestion.

To investigate the effect of the molecular weight of quinoa peptides on the proliferation of Caco-2 cells, QPH was separated into two parts: fraction > 5 kDa and fraction < 5 kDa. Compared to fraction > 5 kDa, fraction < 5 kDa showed a dose-dependent proliferation inhibitory activity, indicating that low molecular weight quinoa peptides possess more effective antiproliferative activity than high molecular weight peptides. Jumeri et al. have reported the greater molecular mobility and diffusivity of low molecular weight peptides were identified to improve interactions with cancer cell components and enhance antiproliferative activity (Jumeri & Kim, 2011). There have been several studies about the peptides derived from different crops as nutraceuticals in the prevention or the treatment of cancer. Kannan and co-workers found the fraction < 5 kDa of rice bran protein hydrolyzates imparts a stronger anti-cancer activity against Caco-2 and HepG2 cells than fraction 5-10 kDa and fraction > 5 kDa (Kannan, Hettiarachchy, Johnson, & Nannapaneni, 2008). Similar results were also observed in the study of González-Montoya et al., the fraction < 10 kDa of germinated soybean digests showed a higher ability to inhibit Caco-2 proliferation than fraction >10 kDa (Gonzalez-Montoya, Hernandez-Ledesma, Silvan, Mora-

Escobedo, & Martinez-Villaluenga, 2018). However, there was a difference in soybean digests, Rayaprolu and co-workers identified that fraction 10–50 kDa extracted from soybean meal protein was the most potent component inhibiting human liver and colon cells viability (Rayaprolu, Hettiarachchy, Chen, Kannan, & Mauromostakos, 2013). Besides, the antiproliferative activity of quinoa peptides in human colon cancer cells has been measured in a recent study, and the fraction > 5 kDa exhibited more suppressive activity than fraction < 5 kDa (Vilcacundo et al., 2018). Although the hydrolyzates were obtained from the same crop, the same molecular weight fractions may have different anti-cancer activities, which can be attributed to several factors including crop cultivars, environment areas, enzymatic hydrolysis conditions, amino acid composition, and peptide hydrophobicity.

To identify the potential peptides responsible for the antiproliferative activity, fraction < 5 kDa was analyzed by LC-MS/MS. The bioactivity of identified peptides was predicted using PeptideRanker and the peptides with predicted scores over 0.7 were listed in Table 1. And the shorter sequences have higher inhibitory activity compared to the other similar sequence, which is consistent with the Jumeri' conclusion mentioned above. The result of the antiproliferation experiment showed that quinoa peptides FHPFPR, NWFPLPR, and HYNPYFPG were more active in inhibiting the proliferation of colon cancer cells. It has been previously reported that antioxidant peptides have the potential to prevent and treat reactive oxygen species-related diseases, especially some forms of cancer (Sheih, Fang, Wu, & Lin, 2010). These antioxidant peptides can be used as anticancer compounds to reduce genetic alterations such as mutation and chromosome rearrangement by inhibiting oxidative stress (Jumeri et al., 2011). Furthermore, amino acids tyrosine (Y), tryptophan (W), methionine (M), cysteine (C), histidine (H), and phenylalanine (F) were considered as the main contributor to the radical-scavenging activities of peptides (Hernandez-Ledesma, Davalos, Bartolome, & Amigo, 2005). The quinoa peptides with MW < 5 kDa also have exhibited antihypertensive activity via inhibiting the activity of ACE, and the ACE inhibitors have been shown to be associated with the colorectal cancer risk in a duration-response manner (Cheung, Chan, Seto, Wong, & Leung, 2020; Guo et al., 2020). In a recent study, the quinoa peptides containing sequences PR and FP have been demonstrated to have ACE inhibitory activity (Guo et al., 2020). Combined with previous studies and our experimental results, the quinoa peptides with antioxidant and antihypertensive activities played significant roles in alleviating colon cancer.

The molecular docking analysis further explained the possible inhibition mechanism. Structural analysis showed that the active site of HDAC1 protein crystal structure was a long tunnel that leads to the cavity of the catalytic machinery containing zinc ions. The tunnel is mainly hydrophobic and consists of amino acids His140, His141, Gly149, Asp176, His178, His179, Phe205, and Asp264 (Krishna et al., 2020). The HDAC1 inhibitors, suberoylanilide hydroxamic acid (SAHA), and the macrocyclic peptide FK228, were investigated in previous studies (Krishna et al., 2020; Y. Zhang et al., 2020). The re-docking complex of the inhibitor SAHA and HDAC1 showed that SAHA had hydrogen bonds with His178, Asp176, and hydrophobic interactions with His140, His141, and Tyr303 of HDAC1 (Krishna et al., 2020). Moreover, the docking

conformations of FK228 in the binding pockets of HDAC1 proved that the hydrophobic interaction and hydrogen bonding of Glu91, Asp92 in the Loop2 and His 21, Pro22 in the Loop1 of HDAC1 were associated with HDAC1 activity (Zhang et al., 2020). In this study, the molecular docking result showed that HYNPYFPG had hydrogen bonds with Glu98, Asp99, His28, His141, and Phe205. The different positions of amino acid Glu, Asp, and His were due to the reconstruction of FK228 in HDAC1 that leads to the rearrangement of amino acid numbers. These binding sites between HYNPYFPG and HDAC1 were considered to inhibit the enzyme activity. Although FHPFPR and NWFPLPR were also bound in the active pocket of HDAC1, only His28 and Asp99 were reported to inhibit HADC1 activity. However, it should be mentioned that both FHPFPR and NWFPLPR displayed direct interactions with residues Arg270 and Leu271, which might be responsible for their HDAC1 inhibitory activity. Meanwhile, it has been demonstrated that the inhibitory peptides based on a non-competitive inhibition mechanism could not bind to the active residue of receptor-enzyme (Yuan, Sun, & Zhuang, 2018). Thus, FHPFPR, NWFPLPR and HYNPYFPG have potential as the novel HDAC1 inhibitors.

Although quinoa peptides have been demonstrated to possess various bioactivities, the mechanism by which these anti-cancer peptides exert their inhibitory effect in human colon cancer cells are not fully understood. Histone acetylation and deacetylation have been revealed as important factors for the regulation of cancer progression (West & Johnstone, 2014). Studies have shown that abnormal histone deacetylation is associated with malignant tumors and HDACi can inhibit cancer progression through remodeling histone acetylation (Zhou et al., 2021). Until recently, the inhibitory effect of HDAC1 has been proved in different types of cancer cells, including breast cancer, gastric cancer, pancreatic cancer, non-small cell lung cancer, and colon cancer. In addition to the drugs with inhibitory effects, the soybean peptide lunasin can induce apoptosis in cancer cells by regulating histone acetylation. In this study, the mRNA expression of HDAC1 in quinoa peptides treatment group was decreased while EP300 displayed no significant effect. Similar to previous studies, the mRNA expression of IL-8, Bcl-2 was significantly inhibited, and caspase3 was upregulated compared to the control group. Tang and co-workers demonstrated that HDAC1 can positively regulate the transcription and promoter activities of IL-8, while not IL-6, in breast cancer cells (Tang et al., 2017). And they suggested that NF-κB and MAPK signals were not involved regulation of IL-8. However, we found that the expression of NF-κB, IL-6 was also significantly repressed after treatment, which is supported by prior studies. It has been proved that HDACi vorinostat can suppress the activation of IL-8 promoter in Caco-2 cells via NF-κB-independent pathways (Hoshimoto, Suzuki, Katsuno, Nakajima, & Saito, 2002). Moreover, Choi et al. have indicated that vorinostat can inhibit the expression of IL-6 and IL-8 in peripheral blood mononuclear cells (PBMCs) from treated patients (Choi et al., 2015). In our previous study, lunasin of transgenic wheat also had inhibitory effect on colon cancer cells by modulating apoptosis pathway, and the expression of Bax and caspase3 was increased while Bcl-2 was decreased (Fan et al., 2020). Furthermore, TNF-α, VEGFA, and c-Myc were considered to serve important roles in tumorigenesis and tumor development, which can be regulated by HDAC1 (Zhu et al., 2010; Liu et al., 2018;

Chen et al., 2020). Among these genes, only TNF-α was significantly downregulated in this study, which was proved that mitochondrial reactive oxygen species (ROS) induces HDAC activation through c-Src signaling in LPS-stimulated cardiomyocytes, and HDAC activation and mitochondrial ROS promote LPS-stimulated TNF-α expression in cardiomyocytes (Zhu et al., 2010). One possible explanation for these discrepancies is that HDAC1 activity was inhibited by use of siRNAs to knockdown its expression. However, the quinoa peptides were not highly specific for inhibiting HDAC1. Therefore, our results suggested that the quinoa peptides inhibit cell proliferation by regulating various pathways in colon cancer Caco-2 cells.

1.2. Supplementation of quinoa peptides alleviates colorectal cancer and restores gut microbiota in AOM/DSS-treated mice

Quinoa protein hydrolysate has been demonstrated to exert anti-cancer effects in colon cancer cell lines, including HT-29, HT-116, and Caco-2 (Vilcacundo et al., 2018). However, the anti-colon cancer activity of quinoa protein and its hydrolysate has not been investigated in vivo, which is significant and necessary for early detection and appropriate treatment strategies for colon cancer. In this study, using a mouse model of AOM/DSS-induced CRC, we examined the anti-colon cancer activity of quinoa protein and its hydrolysate. Administration of different doses of quinoa protein or its hydrolysate prevented severe body weight loss and improved the DAI index to different extents. They also prevented colon shortening and reduced the polyp number caused by AOM/DSS treatment. Moreover, H&E-stained colorectal sections showed that different degrees of recovery was observed after being administrated with quinoa protein or its hydrolysate. These results are similar to previous results on the effects of bioactive compounds on DSS-induced colitis and AOM/DSS-induced colon cancer (Feng et al., 2020; Zeng et al., 2021). Thus, QPH and QPHH mitigated the clinical signs of colon cancer and exhibited protection against AOM/DSS-induced colon cancer.

SCFAs, key metabolites produced by gut microbiota and absorbed by colonic cells, possess many benefits against intestinal disease (Hager et al., 2019). In contrast, reduced production of SCFAs may aggravate disease severity (Singh et al., 2020). In this study, AOM/DSS treatment significantly decreased acetic acid, propionic acid, butyric acid, isobutyric acid, valeric acid, isovaleric acid, and total SCFA concentration. However, these reductions in SCFAs were recovered to varying degrees, especially in QPH and QPHH groups. At present, as the most studied SCFA, butyric acid not only facilitates the growth of the colonic epithelium, it also effectively inhibits colorectal cancer (Bergman, 1990). Recent studies indicated that cancerous colonocytes utilize anaerobic glycolysis for energy supply despite ample oxygen supply, thereby limiting fatty acid oxidation. Therefore, butyric acid begins to accumulate in the cytoplasm instead of being used as an energy source in cancerous colonocytes, which allows butyric acid to act as a histone deacetylase inhibitor (HDACi), eventually leading to the death of cancerous colonocytes through modulating the apoptosis process (Bates, 2012; Encarnacao, Abrantes, Pires, & Botelho, 2015). Moreover, butyric acid was reported to play a key role in enhancing the integrity of the gut barrier and reshaping host metabolic health (Liu et al., 2020).

Notably, inflammatory bowel disease (IBD) is a main risk factor for colon cancer development. It was reported that acetic acid and propionic acid can treat IBD and that butyric acid may inhibit the release of proinflammatory cytokines by regulating the NF-κB signaling pathway (Maslowski et al., 2009). It was found that administration of QPH or QPHH exhibited a better phenotype in the colon and higher increases of SCFAs than that in QPL group or QPHL group. Moreover, acetic acid, butyric acid, and propionic acid were the dominant SCFAs in colon tissue, and their significant reduction was consistent with the poor clinical phenotype of colon tissues. Therefore, the SCFAs contents were restored upon treatment with quinoa protein and its hydrolysate, which may indirectly reflect the health condition of the colon.

Gut microbiota influences host's health and pathological conditions. Growing evidence indicates that changes in gut microbiota can contribute to the development of CRC (Song & Chan, 2019). Moreover, recent studies have shown that some dietary components can alleviate CRC by modulating gut microbiota composition. A higher ratio of *Firmicutes/Bacteroidetes* may be an indicator of colitis-associated colon cancer (He, Han, Li, Qian, & Hou, 2021), and the ratio of F/B was higher in the CRC group compared with the CTL group. However, QPH and QPHH reversed the reduction of *Bacteroidetes*. Therefore, the F/B ratio was lower than that in the CRC group and much closer to the CTL group. At the genus level, as we speculated, the beneficial bacteria, such as *Butyricicoccus*, *Prevotella*, *Odoribacter* and *Coprococcus* significantly reversed with QPH or QPHH supplementation, which may help to produce SCFAs and is consistent with increased production of acetic acid, butyric acid, and propionic acid. In contrast, compared to the CTL group, the relative abundance of *Ruminococcus*, *Blautia*, *Turicibacter*, *Streptococcus*, and *Enterococcus* was significantly increased in the CRC group. Similarly, QPH and QPHH treatments reversed the CRC-induced changes. Generally, *Blautia* is considered a probiotic based on its ability to prevent the occurrence of inflammation, promote the production of SCFAs, and inhibit intestinal colonization by pathogenic bacteria in the intestine (Liu et al., 2021). However, a reduction of *Blautia* was observed after QPH and QPHH treatments compared with the CRC treatment. Another study proposed that some *Blautia* could be harmful, and converted primary bile acids to secondary bile acids (deoxycholic acid and lithocholic acid) through the 7-α-dehydroxylation reactions, which was indicated as carcinogens in colon cancer (Vaughn et al., 2019). Likewise, similarly to the study of Feng et al. (2020), the abundance of *Bifidobacterium* in the CRC group was higher than that in other groups. In contrast, a recent study revealed that an increased abundance of *Bifidobacterium* can prevent and attenuate CRC initiation by regulating oncomiRs and tumor suppressor miRNAs, and CRC patients had a lower abundance of *Bifidobacterium* (Fahmy et al., 2019).

In addition, as mentioned in results above, the abundance of *Coprococcus* and *Butyricicoccus* was significantly increased QPH and QPHH-treated groups compared with the CRC-treated group. In contrast, the abundance of *Ruminococcus*, *Blautia*, *Turicibacter*, *Streptococcus*, and *Enterococcusin* was negatively related with SCFAs. According to a previous study, *Coprococcus* was capable of producing butyrate and exerting immunomodulatory and anti-inflammatory effects (Yang et al., 2019). *Clostridium* and *Butyricicoccus* were SCFAs-producing genera and hence are

beneficial to the health of gastrointestinal tract functioning. The abundance of these genera was reduced in ulcerative colitis patients and individuals with inflammatory diseases (Wu, Song, Pei, & Ling, 2021). In comparison, *Ruminococcus*, *Turicibacter*, and *Streptococcus* were associated with IBD or CRC, and these genera contributed to the development of CRC (Ward et al., 2016; Wu et al., 2018; Alrafas, Busbee, Chitrala, Nagarkatti, & Nagarkatti, 2020). The correlation analysis results showed that the changes in gut microbiota at the genus level were significantly correlated with the content of SCFAs in the colon. Evidence from previous studies demonstrated that SCFAs can reduce the pH, inhibit pathogen growth, and influence intestinal functions in the colon (Sanders, Merenstein, Reid, Gibson, & Rastall, 2019). Moreover, as the primary products of intestinal microbial metabolism, SCFAs also play critical roles in regulating the composition and homeostasis of gut microbiota. Therefore, correlation analysis between SCFA and gut microbiota can be used as a basis for investigating the underlying mechanisms of CRC development.

Furthermore, based on the results of changes in the relative abundance of gut flora, we also found that QPHH and QPH exhibited a slightly different effect on the flora. For instance, QPHH has more beneficial effects on the abundance of *Butyricicoccus*, *Bifidobacterium*, *Clostridium*, and *Turicibacter*, whereas the significant alterations in the abundance of *Coprococcus*, *Blautia*, *Ruminococcus*, *Prevotella*, and *Odoribacter* were observed under QPH treatment. These discrepancies may result from the different states of the quinoa protein in the two treatments. QPHH obtained by in vitro digestion contains peptides with small molecular weights which can be easily absorbed and assimilated. However, in some cases, proteins may function without being digested or degraded because the structural conformation of the functional domains is important for exerting their functional role (Reza et al., 2021), which might be responsible for the different alterations in the QPH group. Of note, most of these investigations focused on the genus level, but not at species or strain levels. Moreover, different species of the bacterium may exert beneficial and adverse effects on host health, and the potential mechanisms of most bacteria in diseases have not been defined yet.

Notably, according to the results of functional predictions, QPH or QPHH treatment significantly restored the changes in gene expression induced by AOM/DSS. The changes in the structure of gut microbiota in QPH and QPHH treated groups corresponded to functional differences between these two groups. Consequently, we hypothesized that an improvement in the makeup of the intestinal microbiota would result in an increase in SCFA synthesis, which would then change the expression profile of genes that are associated and ultimately prevent the formation of CRC.

1.3. Preparation, physicochemical properties, and formation mechanism of quinoa self-assembled peptide-based hydrogel

In this study, we provided a convenient and efficient method for producing plant-based self-assembly peptides with hydrogel-forming ability from quinoa proteins and studied the mechanism of hydrogel formation. It has been mentioned above that quinoa proteins and peptides can alleviate colon cancer. However, compared to QP, QPH obtained from simulated digestion did not show much stronger activity. We

speculate that QPH has experienced a similar degradation process to QP in the digestive tract in vivo and is eventually digested into amino acids. As a result, QPH did not achieve the expected bioactivity as a peptide structure. In a previous study, after pancreatin hydrolysis, QP exhibited high emulsion and foam stability and improved antioxidant activity (Daliri, et al., 2021). Another research reported that Album (*Chenopodium album*) proteins with trypsin treatment showed higher surface hydrophobicity, antioxidant activity and improved flow properties, whereas particle size and turbidity of pepsin treated album proteins was lower than that of trypsin treated proteins (Islam, Mir, & Gani, 2023). Moreover, Galante et al. (2020) proved that the antioxidant activity of QP was also increased in the presence of a peptidase from *Aspergillus niger*, but its gelling ability was reduced. These results indicated that neither the use of pepsin or pancreatin alone, nor the combined use of these two enzymes improved the gelation ability of proteins. Therefore, we compared the gelling ability of quinoa proteins and their enzymatic hydrolysates, and found that QP did not form a hydrogel, and it also did not form a hydrogel after pepsin and pancre hydrolysis. This may be the main reason why quinoa peptides did not show high anti-colon cancer activity in mice. However, QP exhibited hydrogel properties after hydrolyzed by alcalase.

After alcalase hydrolysis, quinoa peptides derived from quinoa protein self-assembled into hydrogels that exhibited increased gel hardness and improved rheological properties. During the hydrolysate process, the SDS-PAGE and GPC results proved that quinoa protein subunits with large molecular weights converted into low molecular weight quinoa peptides with a mean Mw of 5.01 kDa as DH increased to 18%. In previous studies, heating, pH, and ionic strength are recognized to be the main factors affecting gel formation. However, QPH hydrogels were easily obtained by mixing QPH powder and water in a certain ratio without adding hazardous chemicals, which could protect heat-sensitive active substances and reduce energy consumption. Moreover, the formation and modification of the hydrogel structure can be directly reflected by rheological characteristics. At the same shear rate, QPH samples possessed a higher viscosity than QP samples, which is consistent with the results for gel hardness, suggesting that enzymatically produced QPH has a higher interaction-prone structure. Since the G' value was lower than the G'' value and lower than 10 Pa over the entire frequency range for all QP samples, QP had poor gelation capabilities and was more prone to exhibit fluid properties as a hydrosol. By contrast, QPH hydrogels exhibited the sol-to-gel transition when the G' value exceeded the G'' value at the concentration of 11%, which indicated the hydrogel network structure was formed in QPH hydrogels.

A previous study indicated that enzymatic hydrolysis could disrupt the intermolecular interactions of proteins and change the protein structure, thereby changing the aggregated state and particle size of protein (Ma, et al., 2022). However, excessive enzymatic hydrolysis or ultrasound treatment could lead to the interaction between exposed active groups, which may cause the reaggregation of protein/peptide molecules and an increase in particle size (Zhao, et al., 2021). These agreed with our experimental results that the mean particle size of QPH was smaller than that of QP. Moreover, the particle size distribution of QPH was spread in two regions, with the

majority of them in the 0.51–112.47 μm and the remainder in 148.26–778.1 μm. The SEM results showed that QP might be less effective at entangling water molecules with hydrogen bonds. However, QPH hydrogel exhibited a regular, uniform, connected porous structure, which implied that QPH could self-assemble into a robust hydrogel and possess a significant capacity to bind water molecules via hydrogen bonding. Moreover, the porous structure of QPH hydrogel could facilitate the diffusion and sustained release of bioactive substances.

As previously reported, enzymatic hydrolysis-induced changes in hydrophobicity and SH groups directly correlated with gel formation (Zhao, et al., 2011). The hydrophobicity of the 150-min hydrolysate was comparable to that of QPH, suggesting that the hydrophobic groups hidden in QP were gradually revealed during enzymatic hydrolysis. Although the content of SH groups reduced as DH increased, SH groups displayed a shift that initially grew before decreasing, which indicated that the disulfide bonds were initially broken down by enzymatic hydrolysis along with the protein into short peptides. Therefore, the exposure of these hydrophobic groups facilitated the self-aggregation ability and the formation of the hydrogel network. FTIR results further demonstrated that the hydrogen bonding of QPH was enhanced after hydrolysis. Moreover, the β-turn content reduced while the random coil content increased significantly in QPH, indicating enzymatic hydrolysis did have an impact on the secondary structure and led to the increase in disordered secondary structure, which influenced the formation of self-assembled hydrogels.

The thermal properties of quinoa protein are essential for effective improvement and better application. However, the DSC results showed that neither QP nor QPH had the exothermic and endothermic peaks during heating, which may be caused by the extreme extraction pH as previous studies reported (Ruiz, Opazo-Navarrete, et al., 2016; Ruiz, Xiao, et al., 2016). Moreover, the DSC analysis provides more information on the tertiary structure of the protein (Li, Blecker, & Karboune, 2021). Therefore, we supposed that most of the tertiary structure of QP was disrupted due to acid precipitation during extraction, and the reason for changes in the hydrophobicity and SH groups was the production of short peptide fragments by enzymatic hydrolysis.

For surface tension, lag time reflects the process of enough protein being adsorbed at the interface to enable molecular interactions, and this process is related to how flexible and susceptible protein molecules are to conformational changes (Pizones Ruíz-Henestrosa, Carrera Sánchez, & Rodríguez Patino, 2007). Moreover, the initial adsorption is affected by the competition between the protein net charge and exposed hydrophobicity (Schmidt, Damgaard, Greve-Poulsen, Larsen, & Hammershøj, 2018). However, in this study, there was no significant difference in surface tension, lag time and adsorption rate between QP and QPH in the initial stage. After the lag phase, although the initial adsorption rates of QP and QPH were similar, the adsorption rate of QPH was slightly higher than that of QP as the surface age increased. This is mainly because the exposed hydrophobicity was offset by the increase in net charge, and the adsorption rate of QPH increased with the increase of exposed hydrophobic groups.

Amino acid composition, sequence, and spatial location are essential for the formation and properties of peptide hydrogels. The proportion of the hydrophilic

amino acids and the hydrophobic amino acids in QPH proved that QPH had an amphipathic character and preferred to aggregate spontaneously in solution. In addition, the different amino acid residues in the dominant proportion in QPH also contributed to the formation of self-assembled hydrogels. Asp, Glu, Lys, and Arg were found to include amino acid residues that were able to make hydrogen bonds with other amino acids or guanidyl groups. Due to the existence of phenyl rings or imidazole rings that can form π-π stacking, Phe, Tyr, and His were assumed to contribute to peptide self-assembly. Moreover, Ala and Leu were considered to assist stabilize the network of peptide hydrogels because of their potent helicity. The identification of the peptide chain sequence of QPH showed that QPH primarily comprised middle-length peptides, which also contributed to the hydrogels' formation. Furthermore, the amphiphilic peptides contained in QPH were mainly presented in $(XZXZ)_n$ and $(UCUC)_n$ sequences that are highly capable of self-assembly.

But overall, in terms of hardness, QPH hydrogels formed at 11%–15% can only be regarded as soft hydrogels. Similarly, soybean protein isolate (SPI) was modified by papain hydrolysis to improve gel properties. The gel hardness of the samples treated at different times was 2.5 to 3 times higher than that of the control group (Zhao et al., 2021). Notably, the hardness of SPI hydrogels (about 2–2.6 N) was much greater than that of QPH hydrogels. Moreover, they used the combined treatment of enzyme and ultrasound to modify SPI, and the gel properties of SPI were further enhanced (Zhao et al., 2021). Therefore, under the premise of retaining nutrients and active substances as much as possible, more optimized modifications, such as combined multi-enzymatic treatment, combined ultrasonic and enzymatic treatment, combined cold-set and enzymatic treatment, etc., are necessary to be further explored.

7

Chapter VII Conclusion and perspectives

1. General conclusion and perspectives

1.1. Anti-Colon Cancer Activity of Novel Peptides Isolated from In Vitro Digestion of Quinoa Protein in Caco-2 Cells

The aim of this chapter was to investigate the anti-colon cancer activity of quinoa peptides in Caco-2 colon cancer cells. Firstly, the combination of LC–MS/MS, cell antiproliferative assay and PeptideRanker effectively screened quinoa bioactive peptides with anti-colon cancer activity. Moreover, it was found that the shorter peptides possessed higher bioactivity, especially the novel peptides FHPFPR, NWFPLPR and HYNPYFPGGA, identified from QPH, which were proved to exert a promising antiproliferative activity. The results of molecular docking further showed the best binding mode between peptides and HDAC1, and stated the presence of specific amino acids in the peptide sequence may contribute to the binding interaction. At last, the results of RT-qPCR and Western blot indicated that these peptides may serve their function by inhibiting HDAC1 activity and modulating cancer-related gene expression. However, the effects of quinoa peptides were only verified in Caco-2 cells, and it is unknown how these peptides will work in other cell lines. More research is needed to further investigate their molecular mechanism in related markers and signaling pathways, and to study the anti-colon cancer activity in vivo. This study lays the groundwork for future research. Various emerging omics technologies should be fully utilized to explore their bioactive mechanism and compare the differences in bioactive functions in vivo and in vitro.

1.2. Supplementation of quinoa peptides alleviates colorectal cancer and restores gut microbiota in AOM/DSS-treated mice

As mentioned above, most of the experiments on the anti-colon cancer activity of quinoa proteins and peptides are cell experiments conducted in vitro. In this chapter, it is demonstrated that quinoa protein or its hydrolysate ameliorated the AOM/DSS induced CRC in mice by altering intestinal flora and increasing the production of beneficial SCFAs. Some minor differences in microbiota function were observed between QPH and QPHH groups. The discrepancies were ascribed to the differential digestion extent of quinoa protein. Therefore, this study provides a preliminary understanding of the potential mechanism of quinoa protein and its hydrolysate on CRC. However, QPH did not exhibit higher anti-colon cancer activity compared with QP. Future studies are necessary to investigate the specific mechanistic interactions among quinoa proteins, CRC, and gut microbiota. In addition, the effect of different processing methods on the bioactivity of quinoa protein needs to be explored to find the optimal processing conditions for quinoa food to maintain its functional activity. Notably, during the digestion process in vivo, the physiochemical properties of quinoa proteins and peptides would be affected and changed, which may cause changes in their bioactivities. Therefore, studying and improving their physiochemical properties provides a basis for their development and application in functional foods.

1.3. Preparation, physicochemical properties, and formation

mechanism of quinoa self-assembled peptide-based hydrogel

We described a method for producing spontaneous self-assembly peptides with hydrogel-forming capability from quinoa proteins using moderate enzyme hydrolysis without the use of hazardous chemicals or crosslinkers. Moreover, the experiment results revealed that alcalase hydrolysis significantly affected the structure and gel-forming properties of quinoa proteins. Quinoa peptides generated by hydrolysis were observed with an Mw of 5.01 kDa and could self-assemble into hydrogels with favourable physical and rheological properties, resulting from changes in the driving forces such as hydrophobic aggregation and hydrogen bonding. Furthermore, the amino acid analysis revealed that amino acids such as Arg and Glu contribute to forming self-assembled hydrogels. Proteomics analysis indicated that most identified quinoa peptides possessed the typical molecular properties of self-assembled peptides (including peptides with alternate charged and uncharged residues) and amphiphilic peptides (composed of alternate hydrophilic and hydrophobic residues). This chapter proposed a simple, low-cost, efficient, and environmentally friendly technique for the large-scale manufacture of plant-based self-assembled hydrogels in factories, as well as a novel idea for the system that has long relied on synthetic peptides to produce peptide hydrogels. However, as described above, the bioactivities of QP and QPH were related to their physicochemical properties, and different treatments lead to changes in the physicochemical properties, thereby affecting their bioactivities. Moreover, neither the quinoa variety nor the synergistic effects of multiple enzymes were considered in our study. Therefore, future work should further investigate the effects of various quinoa protein types and enzyme combinations on the characteristics of quinoa peptide hydrogels. In addition, with the aid of in vivo bioactivity experiments and computer simulation technology, we can improve the physicochemical properties of bioactive peptides while preserving their bioactivities.

References

Abugoch, L. E., Romero, N., Tapia, C. A., Silva, J., & Rivera, M. (2008). Study of Some Physicochemical and Functional Properties of Quinoa (Chenopodium Quinoa Willd) Protein Isolates. Journal of Agricultural and Food Chemistry, 56(12), 4745-4750.http://doi.org/10.1021/jf703689u

Akimoto, N., Ugai, T., Zhong, R., Hamada, T., Fujiyoshi, K., Giannakis, M., Wu, K. A., Cao, Y., Ng, K., & Ogino, S. (2021). Rising incidence of early-onset colorectal cancer - a call to action. Nature Reviews Clinical Oncology, 18 (4), 230-243 https://doi.org/10.1038/s41571-020-00445-1

Aleksandrova, K., Romero-Mosquera, B., & Hernandez, V. (2017). Diet, Gut Microbiome and Epigenetics: Emerging Links with Inflammatory Bowel Diseases and Prospects for Management and Prevention. Nutrients, 9 (9) https://doi.org/10.3390/nu9090962

Alrafas, H. R., Busbee, P. B., Chitrala, K. N., Nagarkatti, M., & Nagarkatti, P. (2020). Alterations in the Gut Microbiome and Suppression of Histone Deacetylases by Resveratrol Are Associated with Attenuation of Colonic Inflammation and Protection Against Colorectal Cancer. Journal of Clinical Medicine, 9 (6) https://doi.org/10.3390/jcm9061796

Aluko, R. E., & Monu, E. (2003). Functional and bioactive properties of quinoa seed protein hydrolysates. Journal of Food Science, 68 (4), 1254-1258 https://doi.org/10.1111/j.1365-2621.2003.tb09635.x

Amanda, G., Moreno, Y., & Carciofi, B. (2020). Plant proteins as high-quality nutritional source for human diet. Trends in Food Science & Technology, 97(170–184), 97. https://doi.org/10.1016/j.tifs.2020.01.011

Antognoni, F., Potente, G., Biondi, S., Mandrioli, R., & Ruiz, K. B. (2021). Free and conjugated phenolic profiles and antioxidant activity in quinoa seeds and their relationship with genotype and environment. Plants, 10(6), 1046. https://doi.org/10.3390/plants10061046

Bai, J. Y., Zhao, J. J., AL-Ansi, W., Wang, J., Xue, L. M., Liu, J. X., Wang, Y., Fan, M. C., Qian, H. F., Li, Y., & Wang, L. (2021). Oat beta-glucan alleviates DSS-induced colitis via regulating gut microbiota metabolism in mice. Food & Function.http://doi.org/10.1039/d1fo01446c

Balakrishnan, G., & Schneider, R. G. (2020). Quinoa flavonoids and their bioaccessibility during in vitro gastrointestinal digestion. Journal of Cereal Science, 95, Article 103070. https://doi.org/10.1016/j.jcs.2020.103070

Bates, S. E. (2012). Reinventing Cancer Cell Metabolism. Clinical Cancer Research, 18 (20), 5536-5536 https://doi.org/10.1158/1078-0432.Ccr-12-2884

Bergman, E. N. (1990). Energy contributions of volatile fatty acids from the gastrointestinal tract in various species. Physiol Rev, 70 (2), 567-590 https://doi.org/10.1152/physrev.1990.70.2.567

Beveridge, T., Toma, S. J., & Nakai, S. (1974). DETERMINATION OF SH- AND

SS-GROUPS IN SOME FOOD PROTEINS USING ELLMAN'S REAGENT. Journal of Food Science, 39(1), 49-51. https://doi.org/10.1111/j.1365-2621.1974.tb00984.x

Bowerman, C. J., & Nilsson, B. L. (2012). Review self-assembly of amphipathic β-sheet peptides: Insights and applications. Peptide Science, 98(3), 169-184.https://doi.org/10.1002/bip.22058

Brinegar, C., & Goundan, S. (1993). Isolation and characterization of chenopodin, the 11S seed storage protein of quinoa (Chenopodium quinoa). Journal of Agricultural and Food Chemistry, 41(2), 182-185.http://doi.org/10.1021/jf00026a006

Brinegar, C., Sine, B., & Nwokocha, L. (1996). High-Cysteine 2S Seed Storage Proteins from Quinoa (Chenopodium quinoa). Journal of Agricultural and Food Chemistry, 44(7), 1621-1623.http://doi.org/10.1021/jf950830+

Cai, X. K., Han, Y. H., Gu, M., Song, M. Y., Wu, X., Li, Z. Z., Li, F., Goulette, T., & Xiao, H. (2019). Dietary cranberry suppressed colonic inflammation and alleviated gut microbiota dysbiosis in dextran sodium sulfate-treated mice. Food & Function, 10 (10), 6331-6341 https://doi.org/10.1039/c9fo01537j

Cao, Y., Zou, L., Li, W., Song, Y., Zhao, G., & Hu, Y. (2020). Dietary quinoa (Chenopodium quinoa Willd.) polysaccharides ameliorate high-fat diet-induced hyperlipidemia and modulate gut microbiota. International Journal of Biological Macromolecules, 163, 55–65. https://doi.org/10.1016/j.ijbiomac.2020.06.241

Castro, A. V., Lazarte, C. E., Perez-Rea, D., Carlsson, N., Almgren, A., Bergenståhl, B., et al. (2019). Fermentation of pseudocereals quinoa, canihua, and amaranth to improve mineral accessibility through degradation of phytate. Journal of the science of Food and Agriculture, 99(11), 5239–5248. https://doi.org/10.1002/jsfa.9793

Chakrabarti, S., Jahandideh, F., & Wu, J. P. (2014). Food-Derived Bioactive Peptides on Inflammation and Oxidative Stress. Biomed Research International, 2014. https://doi.org/10.1155/2014/608979

Chen, C., Wei, M., Wang, C., Sun, D. P., Liu, P., Zhong, X., He, Q. S., & Yu, W. B. (2020). The histone deacetylase HDAC1 activates HIF1 alpha/VEGFA signal pathway in colorectal cancer. Gene, 754. https://doi.org/10.1016/j.gene.2020.144851

Chen, D., & Campanella, O. H. (2022). Limited enzymatic hydrolysis induced pea protein gelation at low protein concentration with less heat requirement. Food Hydrocolloids, 128, 107547. https://doi.org/10.1016/j.foodhyd.2022.107547

Cheung, K. S., Chan, E. W., Seto, W. K., Wong, I. C. K., & Leung, W. K. (2020). ACE (Angiotensin-Converting Enzyme) Inhibitors/Angiotensin Receptor Blockers Are Associated With Lower Colorectal Cancer Risk A Territory-Wide Study With Propensity Score Analysis. Hypertension, 76(3), 968-975. https://doi.org/10.1161/Hypertensionaha.120.15317

Choi, S. W., Gatza, E., Hou, G. Q., Sun, Y. P., Whitfield, J., Song, Y. H., Oravecz-Wilson, K., Tawara, I., Dinarello, C. A., & Reddy, P. (2015). Histone deacetylase inhibition regulates inflammation and enhances Tregs after allogeneic hematopoietic cell transplantation in humans. Blood, 125(5), 815-819. https://doi.org/10.1182/blood-2014-10-605238

Dakhili, S., Abdolalizadeh, L., Hosseini, S. M., Shojaee-Aliabadi, S., &

Mirmoghtadaie, L. (2019). Quinoa protein: Composition, structure and functional properties. Food Chemistry, 299, Article 125161. https://doi.org/10.1016/j.foodchem.2019.125161

Daliri, H., Ahmadi, R., Pezeshki, A., Hamishehkar, H., & Ghorbani, M. (2021). Quinoa bioactive protein hydrolysate produced by pancreatin enzyme functional and antioxidant properties. LWT- Food Science and Technology, 150(4), Article 111853. https://doi.org/10.1016/j.lwt.2021.111853

Daliri, H., Ahmadi, R., Pezeshki, A., Hamishehkar, H., Mohammadi, M., Beyrami, H., Khakbaz Heshmati, M., & Ghorbani, M. (2021). Quinoa bioactive protein hydrolysate produced by pancreatin enzyme- functional and antioxidant properties. LWT, 150, 111853.https://doi.org/10.1016/j.lwt.2021.111853

De Leon Rodriguez, L. M., & Hemar, Y. (2020). Prospecting the applications and discovery of peptide hydrogels in food. Trends in Food Science & Technology, 104, 37-48. https://doi.org/10.1016/j.tifs.2020.07.025

Dia, V. P., & de Mejia, E. G. (2010). Lunasin promotes apoptosis in human colon cancer cells by mitochondrial pathway activation and induction of nuclear clusterin expression. Cancer Letters, 295(1), 44-53. https://doi.org/10.1016/j.canlet.2010.02.010

Dia, V. P., & Gonzalez de Mejia, E. (2011). Lunasin induces apoptosis and modifies the expression of genes associated with extracellular matrix and cell adhesion in human metastatic colon cancer cells. Molecular Nutrition & Food Research, 55 (4), 623-634 https://doi.org/10.1002/mnfr.201000419

Dia, V. P., & Mejia, E. G. (2010). Lunasin promotes apoptosis in human colon cancer cells by mitochondrial pathway activation and induction of nuclear clusterin expression. Cancer Letters, 295 (1), 44-53 https://doi.org/10.1016/j.canlet.2010.02.010

Donaldson, G.P., S.M. Lee, and S.K. Mazmanian. (2016). Gut biogeography of the bacterial microbiota. Nature Reviews Microbiology, 14(1), 20-32. https://doi.org/10.1038/nrmicro3552

Drzewiecki, J., Martinez-Ayala, A. L., Lozano-Grande, M. A., Leontowicz, H., Leontowicz, M., & Jastrzebski, Z. (2018). In vitro screening of bioactive compounds in some gluten-free plants. Applied Biochemistry and Biotechnology, 186, 847–860. https://doi.org/10.1007/s12010-018-2772-9

Elsohaimy, S. A., Refaay, T. M., & Zaytoun, M. A. M. (2015). Physicochemical and functional properties of quinoa protein isolate. Annals of Agricultural Sciences, 60(2), 297-305.https://doi.org/10.1016/j.aoas.2015.10.007

Encarnacao, J. C., Abrantes, A. M., Pires, A. S., & Botelho, M. F. (2015). Revisit dietary fiber on colorectal cancer: butyrate and its role on prevention and treatment. Cancer and Metastasis Reviews, 34 (3), 465-478 https://doi.org/10.1007/s10555-015-9578-9

Eshelman, M. A., Shah, M., Raup-Konsavage, W. M., Rennoll, S. A., & Yochum, G. S. (2017). TCF7L1 recruits CtBP and HDAC1 to repress DICKKOPF4 gene expression in human colorectal cancer cells. Biochemical and Biophysical Research

Communications, 487(3), 716-722. https://doi.org/10.1016/j.bbrc.2017.04.123

Fahmy, C. A., Gamal-Eldeen, A. M., El-Hussieny, E. A., Raafat, B. M., Mehanna, N. S., Talaat, R. M., & Shaaban, M. T. (2019). Bifidobacterium longum Suppresses Murine Colorectal Cancer through the Modulation of oncomiRs and Tumor Suppressor miRNAs. Nutrition and Cancer-an International Journal, 71 (4), 688-700 https://doi.org/10.1080/01635581.2019.1577984

Fan, X., Guo, H. M., Teng, C., Zhang, B., Blecker, C., & Ren, G. X. (2022). Anti-Colon Cancer Activity of Novel Peptides Isolated from In Vitro Digestion of Quinoa Protein in Caco-2 Cells. Foods, 11 (2) https://doi.org/10.3390/foods11020194

Fan, X., Qin, P. Y., Hao, Y. Q., Guo, H. M., Blecker, C., Everaert, N., & Ren, G. X. (2020). Overexpression of Soybean-Derived Lunasin in Wheat and Assessment of Its Anti-Proliferative Activity in Colorectal Cancer HT-29 Cells. International Journal of Molecular Sciences, 21(24). https://doi.org/10.3390/ijms21249594

Fardet, A. (2010). New hypotheses for the health-protective mechanisms of whole-grain cereals: what is beyond fibre? Nutrition Research Reviews, 23(1), 65-134.http://doi.org/10.1017/S0954422410000041

Fathi, A., & Kardoni, F. (2020). The importance of quinoa (Chenopodium quinoa willd.) cultivation in developing countries: A review. Cercetari Agronomice In Moldova, 337–356. https://doi.org/10.46909/cerce-2020-030

Feng, W. W., Liu, J., Tan, Y. Z., Ao, H., Wang, J., & Peng, C. (2020). Polysaccharides from Atractylodes macrocephala Koidz. Ameliorate ulcerative colitis via extensive modification of gut microbiota and host metabolism. Food Research International, 138 https://doi.org/10.1016/j.foodres.2020.109777

Fernandez-Tome, S., et al. (2019). Role of food proteins and bioactive peptides in inflammatory bowel disease. Trends in Food Science & Technology, 88, 194-206. https://doi.org/10.1016/j.tifs.2019.03.017

Fu, K., Wu, H., & Su, Z. (2021). Self-assembling peptide-based hydrogels: Fabrication, properties, and applications. Biotechnology Advances, 49, 107752.https://doi.org/10.1016/j.biotechadv.2021.107752

G´omez, M. J. R., Prieto, J. M., Sobrado, V. C., & Magro, P. C. (2021). Nutritional characterization of six quinoa (Chenopodium quinoa willd.) varieties cultivated in southern europe. Journal of Food Composition and Analysis, 99(3), Article 103876. https://doi.org/10.1016/j.jfca.2021.103876

Galante, M., De Flaviis, R., Boeris, V., & Spelzini, D. (2020). Effects of the enzymatic hydrolysis treatment on functional and antioxidant properties of quinoa protein acid-induced gels. LWT, 118, 108845 https://doi.org/10.1016/j.lwt.2019.108845.

Galante, M., De Flaviis, R., Boeris, V., & Spelzini, D. (2020). Effects of the enzymatic hydrolysis treatment on functional and antioxidant properties of quinoa protein acid-induced gels. LWT, 118, 108845.https://doi.org/10.1016/j.lwt.2019.108845

Galvez, A. F., Chen, N., Macasieb, J., & de Lumen, B. O. (2001). Chemopreventive property of a soybean peptide (lunasin) that binds to deacetylated histones and inhibits

acetylation. Cancer Research, 61(20), 7473-7478. <Go to ISI>://WOS:000171707400020

Gao, J., Tang, C., Elsawy, M. A., Smith, A. M., Miller, A. F., & Saiani, A. (2017). Controlling Self-Assembling Peptide Hydrogel Properties through Network Topology. Biomacromolecules, 18(3), 826-834.http://doi.org/10.1021/acs.biomac.6b01693

García-Parra, M., Roa-Acosta, D., García-Londo˜no, V., Moreno-Medina, B., & Bravo-Gomez, J. (2021). Structural Characterization and Antioxidant Capacity of Quinoa Cultivars Using Techniques of FT-MIR and UHPLC/ESI-Orbitrap MS Spectroscopy. Plants, 10, 2159. https://doi.org/10.3390/plants10102159

Gassull, M.A. (2006). Review article: the intestinal lumen as a therapeutic target in inflammatory bowel disease. Alimentary Pharmacology & Therapeutics, 24, 90-95. https://doi.org/10.1111/j.1365-2036.2006.03067.x

Gonzalez, J. A., Y. Konishi, M. Bruno, M. Valoy, and F. E. Prado. 2012. Interrelationships among seed yield, total protein and amino acid composition of ten quinoa (Chenopodium quinoa) cultivars from two different agroecological regions. Journal of the Science of Food and Agriculture 92 (6):1222–9. https://doi.org/10.1002/jsfa.4686

Gonzalez-Montoya, M., Hernandez-Ledesma, B., Silvan, J. M., Mora-Escobedo, R., & Martinez-Villaluenga, C. (2018). Peptides derived from in vitro gastrointestinal digestion of germinated soybean proteins inhibit human colon cancer cells proliferation and inflammation. Food Chemistry, 242, 75-82. https://doi.org/10.1016/j.foodchem.2017.09.035

Gosal, W. S., & Ross-Murphy, S. B. (2000). Globular protein gelation. Current Opinion in Colloid & Interface Science, 5(3), 188-194.https://doi.org/10.1016/S1359-0294(00)00057-1

Graf, B. L., Poulev, A., Kuhn, P., Grace, M. H., Lila, M. A., & Raskin, I. (2014). Quinoa seeds leach phytoecdysteroids and other compounds with anti-diabetic properties. Food Chemistry, 163, 178–185. https://doi.org/10.1016/j.foodchem.2014.04.088

Guo, H. M., Hao, Y. Q., Fan, X., Richel, A., Everaert, N., Yang, X. S., & Ren, G. X. (2021). Administration with Quinoa Protein Reduces the Blood Pressure in Spontaneously Hypertensive Rats and Modifies the Fecal Microbiota. Nutrients, 13 (7) https://doi.org/10.3390/nu13072446

Guo, H. M., Hao, Y. Q., Richel, A., Everaert, N., Chen, Y. N., Liu, M. J., Yang, X. S., & Ren, G. X. (2020). Antihypertensive effect of quinoa protein under simulated gastrointestinal digestion and peptide characterization. Journal of the Science of Food and Agriculture, 100(15), 5569-5576. https://doi.org/10.1002/jsfa.10609

Guo, H., Hao, Y., Fan, X., Richel, A., & Ren, G. (2021). Administration with quinoa protein reduces the blood pressure in spontaneously hypertensive rats and modifies the fecal microbiota. Nutrients, 13(7), 2446. https://doi.org/10.3390/nu13072446

Hager, J., Bang, H., Hagen, M., Frech, M., Trager, P., Sokolova, M. V., Steffen, U., Tascilar, K., Sarter, K., Schett, G., Rech, J., & Zaiss, M. M. (2019). The Role of Dietary Fiber in Rheumatoid Arthritis Patients: A Feasibility Study. Nutrients, 11 (10)

https://doi.org/10.3390/nu11102392

Hartman, Z. C., Poage, G. M., den Hollander, P., Tsimelzon, A., Hill, J., Panupinthu, N., Zhang, Y., Mazumdar, A., Hilsenbeck, S. G., Mills, G. B., & Brown, P. H. (2013). Growth of Triple-Negative Breast Cancer Cells Relies upon Coordinate Autocrine Expression of the Proinflammatory Cytokines IL-6 and IL-8. Cancer Research, 73(11), 3470-3480. https://doi.org/10.1158/0008-5472.Can-12-4524-T

He, R., Han, C., Li, Y., Qian, W., & Hou, X. (2021). Cancer-Preventive Role of Bone Marrow-Derived Mesenchymal Stem Cells on Colitis-Associated Colorectal Cancer: Roles of Gut Microbiota Involved. Front Cell Dev Biol, 9, 642948 https://doi.org/10.3389/fcell.2021.642948

Hernandez-Ledesma, B., Davalos, A., Bartolome, B., & Amigo, L. (2005). Preparation of antioxidant enzymatic hydrolysates from (alpha-lactalbumin and beta-lactoglobulin. Identification of active peptides by HPLC-MS/MS. Journal of Agricultural and Food Chemistry, 53(3), 588-593. https://doi.org/10.1021/jf048626m

Hoshimoto, A., Suzuki, Y., Katsuno, T., Nakajima, H., & Saito, Y. (2002). Caprylic acid and medium-chain triglycerides inhibit IL-8 gene transcription in Caco-2 cells: comparison with the potent histone deacetylase inhibitor trichostatin A. British Journal of Pharmacology, 136(2), 280-286. https://doi.org/10.1038/sj.bjp.0704719

Hsieh, C. C., Martinez-Villaluenga, C., de Lumen, B. O., & Hernandez-Ledesma, B. (2018). Updating the research on the chemopreventive and therapeutic role of the peptide lunasin. Journal of the Science of Food and Agriculture, 98(6), 2070-2079. https://doi.org/10.1002/jsfa.8719

Hu, Y., Zhang, J., & Zou, L. (2017). Chemical characterization, antioxidant, immune-regulating and anticancer activities of a novel bioactive polysaccharide from Chenopodium quinoa seeds. International Journal of Biological Macromolecules, 99, 622–629. https://doi.org/10.1016/j.ijbiomac.2017.03.019

Hwang, W. L., Yang, M. H., Tsai, M. L., Lan, H. Y., Su, S. H., Chang, S. C., Teng, H. W., Yang, S. H., Lan, Y. T., Chiou, S. H., & Wang, H. W. (2011). SNAIL Regulates Interleukin-8 Expression, Stem Cell-Like Activity, and Tumorigenicity of Human Colorectal Carcinoma Cells. Gastroenterology, 141(1), 279-U382. https://doi.org/10.1053/j.gastro.2011.04.008

Islami, F., Sauer, A. G., Miller, K. D., Siegel, R. L., Fedewa, S. A., Jacobs, E. J., McCullough, M. L., Patel, A. V., Ma, J., Soerjomataram, I., Flanders, W. D., Brawley, O. W., Gapstur, S. M., & Jemal, A. (2018). Proportion and Number of Cancer Cases and Deaths Attributable to Potentially Modifiable Risk Factors in the United States. Ca-a Cancer Journal for Clinicians, 68 (1), 31-54 https://doi.org/10.3322/caac.21440

Islam, Z.-u., Mir, N. A., & Gani, A. (2023). Effect of controlled enzymatic treatment on the physicochemical, structural and functional properties of high-intensity ultrasound treated album (Chenopodium album) protein. Food Hydrocolloids, 144, 108940.http://doi.org/https://doi.org/10.1016/j.foodhyd.2023.108940

Jairath, V., Jeyarajah, J., Zou, G. Y., Parker, C. E., Olson, A., Khanna, R., D'Haens, G. R., Sandborn, W. J., & Feagan, B. G. (2019). A composite disease activity index for early drug development in ulcerative colitis: development and validation of the

UC-100 score. Lancet Gastroenterology & Hepatology, 4 (1), 63-70 https://doi.org/10.1016/S2468-1253(18)30306-6

Jumeri, & Kim, S. M. (2011). Antioxidant and Anticancer Activities of Enzymatic Hydrolysates of Solitary Tunicate (Styela clava). Food Science and Biotechnology, 20(4), 1075-1085. https://doi.org/10.1007/s10068-011-0146-y

Kannan, A., Hettiarachchy, N., Johnson, M. G., & Nannapaneni, R. (2008). Human Colon and Liver Cancer Cell Proliferation Inhibition by Peptide Hydrolysates Derived from Heat-Stabilized Defatted Rice Bran. Journal of Agricultural and Food Chemistry, 56(24), 11643-11647. https://doi.org/10.1021/jf802558v

Kaspchak, E., Oliveira, M. A. S. d., Simas, F. F., Franco, C. R. C., Silveira, J. L. M., Mafra, M. R., & Igarashi-Mafra, L. (2017). Determination of heat-set gelation capacity of a quinoa protein isolate (Chenopodium quinoa) by dynamic oscillatory rheological analysis. Food Chemistry, 232, 263-271. https://doi.org/10.1016/j.foodchem.2017.04.014

Keum, N., & Giovannucci, E. (2019). Global burden of colorectal cancer: emerging trends, risk factors and prevention strategies. Nature Reviews Gastroenterology & Hepatology, 16 (12), 713-732 https://doi.org/10.1038/s41575-019-0189-8

Kheravii, S. K., Swick, R. A., Choct, M., & Wu, S. B. (2018). Effect of oat hulls as a free choice feeding on broiler performance, short chain fatty acids and microflora under a mild necrotic enteritis challenge. Animal Nutrition, 4(1), 65-72. http://doi.org/10.1016/j.aninu.2017.11.003

Krishna, S., Lakra, A. D., Shukla, N., Khan, S., Mishra, D. P., Ahmed, S., & Siddidi, M. I. (2020). Identification of potential histone deacetylase1 (HDAC1) inhibitors using multistep virtual screening approach including SVM model, pharmacophore modeling, molecular docking and biological evaluation. Journal of Biomolecular Structure & Dynamics, 38(11), 3280-3295. https://doi.org/10.1080/07391102.2019.1654925

Larussa, T., M. Imeneo, and F. Luzza. (2017). Potential role of nutraceutical compounds in inflammatory bowel disease. World Journal of Gastroenterology, 23(14), 2483-2492. https://doi.org/10.3748/wjg.v23.i14.2483

Lee, D., Albenberg, L., Compher, C., Baldassano, R., Piccoli, D., Lewis, J. D., & Wu, G. D. (2015). Diet in the Pathogenesis and Treatment of Inflammatory Bowel Diseases. Gastroenterology, 148(6), 1087-1106 https://doi.org/10.1053/j.gastro.2015.01.007.

Li, D. T., Feng, Y., Tian, M. L., Ji, J. F., Hu, X. S., & Chen, F. (2021). Gut microbiota-derived inosine from dietary barley leaf supplementation attenuates colitis through PPAR gamma signaling activation. Microbiome, 9(1). http://doi.org/10.1186/s40168-021-01028-7

Li, M., Blecker, C., & Karboune, S. (2021). Molecular and air-water interfacial properties of potato protein upon modification via laccase-catalyzed cross-linking and conjugation with sugar beet pectin. Food Hydrocolloids, 112, 106236.http://doi.org/https://doi.org/10.1016/j.foodhyd.2020.106236

Li, X. T., Liu, Y. L., Wang, Y., Li, X., Liu, X. R., Guo, M. R., Tan, Y. W., Qin, X. F.,

Wang, X. H., & Jiang, M. S. (2020). Sucralose Promotes Colitis-Associated Colorectal Cancer Risk in a Murine Model Along With Changes in Microbiota. Frontiers in Oncology, 10 https://doi.org/10.3389/fonc.2020.00710

Li, Y., Li, W., Wang, X., Ding, C., Liu, J. Z., Li, Y., Li, W. J., & Sun, Y. D. (2020). High-Salt Diet-Induced Gastritis in C57BL/6 Mice is Associated with Microbial Dysbiosis and Alleviated by a Buckwheat Diet. Molecular Nutrition & Food Research, 64(8). http://doi.org/10.1002/mnfr.201900965

Liang, R., Zhang, H., Wang, Y., Ye, J., Guo, L., He, L., Li, X., Qiu, T., & Tuo, X. (2022). Dual dynamic network system constructed by waterborne polyurethane for improved and recoverable performances. Chemical Engineering Journal, 442, 136204.https://doi.org/10.1016/j.cej.2022.136204

Lingiardi, N., Galante, M., de Sanctis, M., & Spelzini, D. (2022). Are quinoa proteins a promising alternative to be applied in plant-based emulsion gel formulation? Food Chemistry, 394, 133485. https://doi.org/10.1016/j.foodchem.2022.133485

Liu, W., Zhang, Y., Qiu, B., Fan, S. J., Ding, H. F., & Liu, Z. H. (2018). Quinoa whole grain diet compromises the changes of gut microbiota and colonic colitis induced by dextran Sulfate sodium in C57BL/6 mice. Scientific Reports, 8. http://doi.org/10.1038/s41598-018-33092-9

Liu, X. F., Yu, Y., Zhang, J. N., Lu, C. X., Wang, L. M., Liu, P., & Song, H. (2018). HDAC1 Silencing in Ovarian Cancer Enhances the Chemotherapy Response. Cellular Physiology and Biochemistry, 48(4), 1505-1518. https://doi.org/10.1159/000492260

Liu, X. M., Mao, B. Y., Gu, J. Y., Wu, J. Y., Cui, S. M., Wang, G., Zhao, J. X., Zhang, H., & Chen, W. (2021). Blautia-a new functional genus with potential probiotic properties? Gut Microbes, 13 (1) https://doi.org/10.1080/19490976.2021.1875796

Liu, Z. G., Dai, X. S., Zhang, H. B., Shi, R. J., Hui, Y., Jin, X., Zhang, W. T., Wang, L. F., Wang, Q. X., Wang, D. N., Wang, J., Tan, X. T., Ren, B., Liu, X. N., Zhao, T., Wang, J. M., Pan, J. R., Yuan, T., Chu, C. Q., Lan, L., Yin, F., Cadenas, E., Shi, L., Zhao, S. C., & Liu, X. B. (2020). Gut microbiota mediates intermittent-fasting alleviation of diabetes-induced cognitive impairment. Nature Communications, 11 (1) https://doi.org/10.1038/s41467-020-14676-4

Luo, L., Cheng, L., Zhang, R., & Yang, Z. (2022). Impact of high-pressure homogenization on physico-chemical, structural, and rheological properties of quinoa protein isolates. Food Structure, 32, 100265.https://doi.org/10.1016/j.foostr.2022.100265

Luo, L., Zhang, R., Palmer, J., Hemar, Y., & Yang, Z. (2021). Impact of High Hydrostatic Pressure on the Gelation Behavior and Microstructure of Quinoa Protein Isolate Dispersions. ACS Food Science & Technology, 1(11), 2144-2151.http://doi.org/10.1021/acsfoodscitech.1c00332

Ma, Z., Li, L., Wu, C., Huang, Y., Teng, F., & Li, Y. (2022). Effects of combined enzymatic and ultrasonic treatments on the structure and gel properties of soybean protein isolate. LWT, 158, 113123.https://doi.org/10.1016/j.lwt.2022.113123

Mäkinen, O. E., Zannini, E., & Arendt, E. K. (2015). Modifying the Cold Gelation Properties of Quinoa Protein Isolate: Influence of Heat-Denaturation pH in the

Alkaline Range. Plant Foods for Human Nutrition, 70(3), 250-256. https://doi.org/10.1007/s11130-015-0487-4

Mäkinen, O. E., Zannini, E., Koehler, P., & Arendt, E. K. (2016). Heat-denaturation and aggregation of quinoa (Chenopodium quinoa) globulins as affected by the pH value. Food Chemistry, 196, 17-24. https://doi.org/10.1016/j.foodchem.2015.08.069

Mariadason, J. M. (2008). HDACs and HDAC inhibitors in colon cancer. Epigenetics, 3(1), 28-37. https://doi.org/10.4161/epi.3.1.5736

Maslowski, K. M., Vieira, A. T., Ng, A., Kranich, J., Sierro, F., Yu, D., Schilter, H. C., Rolph, M. S., Mackay, F., Artis, D., Xavier, R. J., Teixeira, M. M., & Mackay, C. R. (2009). Regulation of inflammatory responses by gut microbiota and chemoattractant receptor GPR43. Nature, 461 (7268), 1282-U1119 https://doi.org/10.1038/nature08530

McClements, D. J., Newman, E., & McClements, I. F. (2019). Plant-based Milks: A Review of the Science Underpinning Their Design, Fabrication, and Performance. Comprehensive Reviews in Food Science and Food Safety, 18(6), 2047-2067.https://doi.org/10.1111/1541-4337.12505

Menon, R., Gonzalez, T., Ferruzzi, M., Jackson, E., Winderl, D., & Watson, J. (2016). Oats-From Farm to Fork. Adv Food Nutr Res, 77, 1-55. http://doi.org/10.1016/bs.afnr.2015.12.001

Michon, C., Cuvelier, G., & Launay, B. (1993). Concentration dependence of the critical viscoelastic properties of gelatin at the gel point. Rheologica Acta, 32(1), 94-103.http://doi.org/10.1007/BF00396681

Mohamed, D. A., Fouda, K. A., & Mohamed, R. S. (2019). In vitro anticancer activity of quinoa and safflower seeds and their preventive effects on non-alcoholic fatty liver. Pakistan Journal of Biological Sciences, 22(8), 383–392. https://doi.org/10.3923/pjbs.2019.383.392

Montales, M. T., Simmen, R. C., Ferreira, E. S., Neves, V. A., & Simmen, F. A. (2015). Metformin and soybean-derived bioactive molecules attenuate the expansion of stem cell-like epithelial subpopulation and confer apoptotic sensitivity in human colon cancer cells. Genes Nutr, 10 (6), 49 https://doi.org/10.1007/s12263-015-0499-6

Montserrat-de la Paz, S., Martinez-Lopez, A., Villanueva-Lazo, A., Pedroche, J., Millan, F., & Millan-Linares, M. C. (2021). Identification and Characterization of Novel Antioxidant Protein Hydrolysates from Kiwicha (Amaranthus caudatus L.). Antioxidants, 10(5). https://doi.org/10.3390/antiox10050645

Montserrat-de la Paz, S., Martinez-Lopez, A., Villanueva-Lazo, A., Pedroche, J., Millan, F., & Millan-Linares, M. C. (2021). Identification and Characterization of Novel Antioxidant Protein Hydrolysates from Kiwicha (Amaranthus caudatus L.). Antioxidants, 10 (5) https://doi.org/10.3390/antiox10050645

Mudgil, P., Kilari, B. P., Kamal, H., Olalere, O. A., & Maqsood, S. (2020). Multifunctional bioactive peptides derived from quinoa protein hydrolysates: Inhibition of α-glucosidase, dipeptidyl peptidase-IV and angiotensin I converting enzymes. Journal of Cereal Science, 96, Article 103130. https://doi.org/10.1016/j.jcs.2020.103130

Muenchau, S., Deutsch, R., de Castro, I. J., Hielscher, T., Heber, N., Niesler, B., Lusic, M., Stanifer, M. L., & Boulant, S. (2019). Hypoxic Environment Promotes Barrier Formation in Human Intestinal Epithelial Cells through Regulation of MicroRNA 320a Expression. Molecular and Cellular Biology, 39(14). https://doi.org/10.1128/MCB.00553-18

Nadeem, M. S., Kumar, V., Al-Abbasi, F. A., Kamal, M. A., & Anwar, F. (2020). Risk of colorectal cancer in inflammatory bowel diseases. Seminars in Cancer Biology, 64, 51-60. http://doi.org/10.1016/j.semcancer.2019.05.001

Neri-Numa, I. A., Carvalho-Silva, L. B., Morales, J. P., Malta, L. G., Muramoto, M. T., Ferreira, J. E. M., de Carvalho, J. E., Ruiz, A. L. T. G., Marostica, M. R., & Pastore, G. M. (2013). Evaluation of the antioxidant, antiproliferative and antimutagenic potential of araca-boi fruit (Eugenia stipitata Mc Vaugh - Myrtaceae) of the Brazilian Amazon Forest. Food Research International, 50(1), 70-76. https://doi.org/10.1016/j.foodres.2012.09.032

Nieto-Nieto, T. V., Wang, Y. X., Ozimek, L., & Chen, L. (2014). Effects of partial hydrolysis on structure and gelling properties of oat globular proteins. Food Research International, 55, 418-425.https://doi.org/10.1016/j.foodres.2013.11.038

Nongonierma, A. B., Le Maux, S., Dubrulle, C., Barre, C., & FitzGerald, R. J. (2015). Quinoa (Chenopodium quinoa Willd.) protein hydrolysates with in vitro dipeptidyl peptidase IV (DPP-IV) inhibitory and antioxidant properties. Journal of Cereal Science, 65, 112-118 https://doi.org/10.1016/j.jcs.2015.07.004

Pereira, E., Cadavez, V., Barros, L., Encina-Zelada, C., & Ferreira, I. (2020). Chenopodium quinoa willd. (quinoa) grains: A good source of phenolic compounds. Food Research International, 137, Article 109574. https://doi.org/10.1016/j.foodres.2020.109574

Phuagkhaopong, S., Ospondpant, D., Kasemsuk, T., Sibmooh, N., Soodvilai, S., Power, C., & Vivithanaporn, P. (2017). Cadmium-induced IL-6 and IL-8 expression and release from astrocytes are mediated by MAPK and NF-kappa B. Neurotoxicology, 60, 82-91. https://doi.org/10.1016/j.neuro.2017.03.001

Piawah, S., & Venook, A. P. (2019). Targeted therapy for colorectal cancer metastases: A review of current methods of molecularly targeted therapy and the use of tumor biomarkers in the treatment of metastatic colorectal cancer. Cancer, 125 (23), 4139-4147 https://doi.org/10.1002/cncr.32163

Pizones Ruíz-Henestrosa, V., Carrera Sánchez, C., & Rodríguez Patino, J. M. (2007). Formulation Engineering Can Improve the Interfacial and Foaming Properties of Soy Globulins. Journal of Agricultural and Food Chemistry, 55(15), 6339-6348.http://doi.org/10.1021/jf070918a

Rayaprolu, S. J., Hettiarachchy, N. S., Chen, P. Y., Kannan, A., & Mauromostakos, A. (2013). Peptides derived from high oleic acid soybean meals inhibit colon, liver and lung cancer cell growth. Food Research International, 50(1), 282-288. https://doi.org/10.1016/j.foodres.2012.10.021

Ren, G., Zhu, Y., & Shi, Z. (2017). Detection of lunasin in quinoa (Chenopodium quinoa Willd) and the in vitro evaluation of its antioxidant and anti-inflammatory

activities. Journal of the Science of Food and Agriculture, 97(12), 4110–4116. https://doi.org/10.1002/jsfa.8278

Ritva, R. C. V., Hellstroem, J. K., Pihlava, J. M., & Mattila, P. H. (2010). Flavonoids and other phenolic compounds in andean indigenous grains: Quinoa (Chenopodium quinoa), kafiiwa (Chenopodium pallidicaule) and kiwicha (Amaranthus caudatus). Food Chemistry, 120(1), 128–133. https://doi.org/10.1016/j.foodchem.2009.09.087

Rose, D. J. (2014). Impact of whole grains on the gut microbiota: the next frontier for oats? British Journal of Nutrition, 112, S44-S49.http://doi.org/10.1017/S0007114514002244

Ruales, J., & Nair, B. M. (1992). Nutritional quality of the protein in quinoa (Chenopodium quinoa, Willd) seeds. Plant Foods Hum Nutr, 42(1), 1-11. https://doi.org/10.1007/BF02196067

Ruiz, G. A., Opazo-Navarrete, M., Meurs, M., Minor, M., Sala, G., van Boekel, M., Stieger, M., & Janssen, A. E. M. (2016). Denaturation and in Vitro Gastric Digestion of Heat-Treated Quinoa Protein Isolates Obtained at Various Extraction pH. Food Biophysics, 11(2), 184-197.http://doi.org/10.1007/s11483-016-9429-4

Ruiz, G. A., Xiao, W., van Boekel, M., Minor, M., & Stieger, M. (2016). Effect of extraction pH on heat-induced aggregation, gelation and microstructure of protein isolate from quinoa (Chenopodium quinoa Willd). Food Chemistry, 209, 203-210.https://doi.org/10.1016/j.foodchem.2016.04.052

Ruiz, K. B., Biondi, S., Oses, R., Acu˜na-Rodriguez, I. S., Antognoni, F., Martinez-Mosqueira, E. A., et al. (2014). Quinoa biodiversity and sustainability for food security under climate change. A review. Agronomy for Sustainable Development, 34(2), 1–11. https://doi.org/10.1007/s13593-013-0195-0

Saiani, A., Mohammed, A., Frielinghaus, H., Collins, R., Hodson, N., Kielty, C. M., Sherratt, M. J., & Miller, A. F. (2009). Self-assembly and gelation properties of α-helix versus β-sheet forming peptides. Soft Matter, 5(1), 193-202.http://doi.org/10.1039/B811288F

Sanders, M. E., Merenstein, D. J., Reid, G., Gibson, G. R., & Rastall, R. A. (2019). Probiotics and prebiotics in intestinal health and disease: from biology to the clinic (vol 16, pg 605, 2019). Nature Reviews Gastroenterology & Hepatology, 16 (10), 642-642 https://doi.org/10.1038/s41575-019-0199-6

Saus, E., Iraola-Guzman, S., Willis, J. R., Brunet-Vega, A., & Gabaldon, T. (2019). Microbiome and colorectal cancer: Roles in carcinogenesis and clinical potential. Molecular Aspects of Medicine, 69, 93-106 https://doi.org/10.1016/j.mam.2019.05.001

Schmidt, J. M., Damgaard, H., Greve-Poulsen, M., Larsen, L. B., & Hammershøj, M. (2018). Foam and emulsion properties of potato protein isolate and purified fractions. Food Hydrocolloids, 74, 367-378.http://doi.org/https://doi.org/10.1016/j.foodhyd.2017.07.032

Selokar, N. L., St John, L., Revay, T., King, W. A., Singla, S. K., & Madan, P. (2013). Effect of Histone Deacetylase Inhibitor Valproic Acid Treatment on Donor Cell Growth Characteristics, Cell Cycle Arrest, Apoptosis, and Handmade Cloned Bovine

Embryo Production Efficiency. Cellular Reprogramming, 15(6), 531-542. https://doi.org/10.1089/cell.2013.0018

Sheih, I. C., Fang, T. J., Wu, T. K., & Lin, P. H. (2010). Anticancer and Antioxidant Activities of the Peptide Fraction from Algae Protein Waste. Journal of Agricultural and Food Chemistry, 58(2), 1202-1207. https://doi.org/10.1021/jf903089m

Shen, Y., Tang, X., & Li, Y. (2021). Drying methods affect physicochemical and functional properties of quinoa protein isolate. Food Chemistry, 339, 127823. https://doi.org/10.1016/j.foodchem.2020.127823

Shen, Y., Tang, X., & Li, Y. (2021). Drying methods affect physicochemical and functional properties of quinoa protein isolate. Food Chemistry, 339, 127823.https://doi.org/10.1016/j.foodchem.2020.127823

Sheng, Z., Xin, M., Wang, Z., Peng, Z., & Li, Z. (2019). Production of transgenic cattle expressing lysine-rich polypeptide in milk by somatic cell nuclear transfer. Transgenic Research, 28(3–4), 1–9. https://doi.org/10.1007/s11248-019-00124-7

Siegel, R. L., Miller, K. D., & Jemal, A. (2019). Cancer statistics, 2019. CA Cancer J Clin, 69 (1), 7-34 https://doi.org/10.3322/caac.21551

Singh, H., Miyamoto, S., Darshi, M., Torralba, M. G., Kwon, K., Sharma, K., & Pieper, R. (2020). Gut Microbial Changes in Diabetic db/db Mice and Recovery of Microbial Diversity upon Pirfenidone Treatment. Microorganisms, 8 (9) https://doi.org/10.3390/microorganisms8091347

Singh, J. K., Simoes, B. M., Howell, S. J., Farnie, G., & Clarke, R. B. (2013). Recent advances reveal IL-8 signaling as a potential key to targeting breast cancer stem cells. Breast Cancer Research, 15(4). https://doi.org/10.1186/bcr3436

Song, M., & Chan, A. T. (2019). Environmental Factors, Gut Microbiota, and Colorectal Cancer Prevention. Clinical Gastroenterology and Hepatology, 17 (2), 275-289 https://doi.org/10.1016/j.cgh.2018.07.012

Srdic, M., Ovcina, I., Fotschki, B., Haros, C. M., & Llopis, J. M. L. (2020). C. quinoa and S. hispanica L. Seeds Provide Immunonutritional Agonists to Selectively Polarize Macrophages. Cells, 9(3). https://doi.org/10.3390/cells9030593

Stiki, R. I., Milini, D. D., Kosti, A., Jovanovi, Z. B., & Pei, M. B. (2020). Polyphenolic profiles, antioxidant and in vitro anticancer activities of the seeds of puno and titicaca quinoa cultivars. Cereal Chemistry, 97(3), 626–633. https://doi.org/10.1002/cche.10278

Stikic, R., Glamoclija, D., Demin, M., Vucelic-Radovic, B., Jovanovic, Z., & Milojkovic-Opsenica, D. (2012). Agronomical and nutritional evaluation of quinoa seeds (Chenopodium quinoa willd.) as an ingredient in bread formulations. Journal of Cereal Science, 55(2), 132–138. https://doi.org/10.1016/j.jcs.2011.10.010

Swieca, M., Seczyk, L., Gawlik-Dziki, U., & Dziki, D. (2014). Bread enriched with quinoa leaves - the influence of protein-phenolics interactions on the nutritional and antioxidant quality. Food Chem, 162, 54-62. https://doi.org/10.1016/j.foodchem.2014.04.044

Tang, Y., Li, X., Zhang, B., Chen, P. X., Liu, R., & Tsao, R. (2015). Characterisation

of phenolics, betanins and antioxidant activities in seeds of three chenopodium quinoa willd. Genotypes. Food Chemistry, 166, 380–388. https://doi.org/10.1016/j.foodchem.2014.06.018

Tang, Z. H., Ding, S. J., Huang, H. L., Luo, P. F., Qing, B. H., Zhang, S. Y., & Tang, R. T. (2017). HDAC1 triggers the proliferation and migration of breast cancer cells via upregulation of interleukin-8. Biological Chemistry, 398(12), 1347-1356. https://doi.org/10.1515/hsz-2017-0155

Teng, C., Qin, P., Shi, Z., Zhang, W., & Ren, G. (2020). a). Structural characterization and antioxidant activity of alkali-extracted polysaccharides from quinoa. Food Hydrocolloids, 113, Article 106392. https://doi.org/10.1016/j.foodhyd.2020.106392

Teng, C., Shi, Z., Yao, Y., & Ren, G. (2020). Structural Characterization of Quinoa Polysaccharide and Its Inhibitory Effects on 3T3-L1 Adipocyte Differentiation. Foods, 9(10), 1511. https://doi.org/10.3390/foods9101511

Tian, M. L., Li, D. T., Ma, C., Feng, Y., Hu, X. S., & Chen, F. (2021). Barley Leaf Insoluble Dietary Fiber Alleviated Dextran Sulfate Sodium-Induced Mice Colitis by Modulating Gut Microbiota. Nutrients, 13(3). http://doi.org/10.3390/nu13030846

Trott, O., & Olson, A. J. (2010). Software News and Update AutoDock Vina: Improving the Speed and Accuracy of Docking with a New Scoring Function, Efficient Optimization, and Multithreading. Journal of Computational Chemistry, 31(2), 455-461. https://doi.org/10.1002/jcc.21334

Vaughn, B. P., Kaiser, T., Staley, C., Hamilton, M. J., Reich, J., Graiziger, C., Singroy, S., Kabage, A. J., Sadowsky, M. J., & Khoruts, A. (2019). A pilot study of fecal bile acid and microbiota profiles in inflammatory bowel disease and primary sclerosing cholangitis. Clinical and Experimental Gastroenterology, 12, 9-19 https://doi.org/10.2147/Ceg.S186097

Vieira, A. R., Abar, L., Chan, D. S. M., Vingeliene, S., Polemiti, E., Stevens, C., Greenwood, D., & Norat, T. (2017). Foods and beverages and colorectal cancer risk: a systematic review and meta-analysis of cohort studies, an update of the evidence of the WCRF-AICR Continuous Update Project. Annals of Oncology, 28(8), 1788-1802. https://doi.org/10.1093/annonc/mdx171

Vilcacundo, R., Miralles, B., Carrillo, W., & Hernandez-Ledesma, B. (2018). In vitro chemopreventive properties of peptides released from quinoa (Chenopodium quinoa willd.) protein under simulated gastrointestinal digestion. Food Research International, 105, 403–411. https://doi.org/10.1016/j.foodres.2017.11.036

Vilcacundo, R., Miralles, B., Carrillo, W., & Hernandez-Ledesma, B. (2018). In vitro chemopreventive properties of peptides released from quinoa (Chenopodium quinoa Willd.) protein under simulated gastrointestinal digestion. Food Research International, 105, 403-411. https://doi.org/10.1016/j.foodres.2017.11.036

Vilcacundo, R., Miralles, B., Carrillo, W., & Hernandez-Ledesma, B. (2018). In vitro chemopreventive properties of peptides released from quinoa (Chenopodium quinoa Willd.) protein under simulated gastrointestinal digestion. Food Research International, 105, 403-411 https://doi.org/10.1016/j.foodres.2017.11.036

Vital, D. A. L., de Mejia, E. G., Dia, V. P., & Loarca-Pina, G. (2014). Peptides in common bean fractions inhibit human colorectal cancer cells. Food Chemistry, 157, 347-355 https://doi.org/10.1016/j.foodchem.2014.02.050

Vonderheide, R. H. (2014). Tumor-Promoting Inflammatory Networks in Pancreatic Neoplasia: Another Reason to Loathe Kras. Cancer Cell, 25 (5), 553-554 https://doi.org/10.1016/j.ccr.2014.04.020

Wan, P., Peng, Y. J., Chen, G. J., Xie, M. H., Dai, Z. Q., Huang, K. Y., Dong, W., Zeng, X. X., & Sun, Y. (2019). Modulation of gut microbiota by Ilex kudingcha improves dextran sulfate sodium-induced colitis. Food Research International, 126 https://doi.org/10.1016/j.foodres.2019.108595

Wang, L., Dong, J.-l., Zhu, Y.-y., Shen, R.-l., Wu, L.-g., & Zhang, K.-y. (2021). Effects of microwave heating, steaming, boiling and baking on the structure and functional properties of quinoa (Chenopodium quinoa Willd.) protein isolates. International Journal of Food Science & Technology, 56(2), 709-720. https://doi.org/10.1111/ijfs.14706

Wang, Q. M., He, R. Z., Tan, T., Li, J., Hu, Z., Luo, W. H., Duan, L. L., Luo, W. N., & Luo, D. X. (2019). A novel long non-coding RNA-KAT7 is low expressed in colorectal cancer and acts as a tumor suppressor. Cancer Cell International, 19. https://doi.org/10.1186/s12935-019-0760-y

Wang, T. T., Fan, C. G., Yao, A. R., Xu, X. W., Zheng, G. X., You, Y., Jiang, C. Y., Zhao, X. Q., Hou, Y. Y., Hung, M. C., & Lin, X. (2018). The Adaptor Protein CARD9 Protects against Colon Cancer by Restricting Mycobiota-Mediated Expansion of Myeloid-Derived Suppressor Cells. Immunity, 49 (3), 504-+ https://doi.org/10.1016/j.immuni.2018.08.018

Wang, X., Zhao, R., & Yuan, W. (2020). Composition and secondary structure of proteins isolated from six different quinoa varieties from china. Journal of Cereal Science, 103036. https://doi.org/10.1016/j.jcs.2020.103036

Wang, Y.-L., Yang, J.-J., Dai, S.-C., Tong, X.-H., Tian, T., Liang, C.-C., Li, L., Wang, H., & Jiang, L.-Z. (2022). Formation of soybean protein isolate-hawthorn flavonoids non-covalent complexes: Linking the physicochemical properties and emulsifying properties. Ultrasonics Sonochemistry, 84, 105961.https://doi.org/10.1016/j.ultsonch.2022.105961

Ward, N. L., Phillips, C. D., Nguyen, D. D., Shanmugam, N. K. N., Song, Y., Hodin, R., Shi, H. N., Cherayil, B. J., & Goldstein, A. M. (2016). Antibiotic Treatment Induces Long-lasting Changes in the Fecal Microbiota that Protect Against Colitis. Inflammatory Bowel Diseases, 22 (10), 2328-2340 https://doi.org/10.1097/Mib.0000000000000914

Weichert, W. (2009). HDAC expression and clinical prognosis in human malignancies. Cancer Letters, 280(2), 168-176. https://doi.org/10.1016/j.canlet.2008.10.047

West, A. C., & Johnstone, R. W. (2014). New and emerging HDAC inhibitors for cancer treatment. Journal of Clinical Investigation, 124(1), 30-39. https://doi.org/10.1172/Jci69738

Wilczak, J., Blaszczyk, K., Kamola, D., Gajewska, M., Harasym, J. P., Jalosinska, M., Gudej, S., Suchecka, D., Oczkowski, M., & Gromadzka-Ostrowska, J. (2015). The effect of low or high molecular weight oat beta-glucans on the inflammatory and oxidative stress status in the colon of rats with LPS-induced enteritis. Food & Function, 6(2), 590-603.http://doi.org/10.1039/c4fo00638k

Wu, E. Q., Song, J. Z., Pei, L. P., & Ling, Y. Q. (2021). Comparison of the Gut Microbiota Disturbance in Rat Models of Irritable Bowel Syndrome Induced by Maternal Separation and Multiple Early-Life Adversity. Frontiers in Cellular and Infection Microbiology, 10 https://doi.org/10.3389/fcimb.2020.581974

Wu, M. N., Wu, Y. Q., Li, J. M., Bao, Y. H., Guo, Y. C., & Yang, W. C. (2018). The Dynamic Changes of Gut Microbiota in Muc2 Deficient Mice. International Journal of Molecular Sciences, 19 (9) https://doi.org/10.3390/ijms19092809

Wu, X. L., Chen, X., Liu, H., He, Z. W., Wang, Z., Wei, L. J., Wang, W. Y., Zhong, S. H., He, Q., Zhang, Z. C., Ou, R. Y., Gao, J., Lei, Y. C., Yang, W. J., Song, G. B., Jin, Y., Zhou, L. L., Xu, Y. S., & Tang, K. F. (2020). Rescuing Dicer expression in inflamed colon tissues alleviates colitis and prevents colitis-associated tumorigenesis. Theranostics, 10 (13), 5749-5762 https://doi.org/10.7150/thno.41894

Wu, X., Song, M. Y., Cai, X. K., Neto, C., Tata, A., Han, Y. H., Wang, Q., Tang, Z. H., & Xiao, H. (2018). Chemopreventive Effects of Whole Cranberry (Vaccinium macrocarpon) on Colitis-Associated Colon Tumorigenesis. Molecular Nutrition & Food Research, 62 (24) https://doi.org/10.1002/mnfr.201800942

Wyatt, M., & Greathouse, K. L. (2021). Targeting Dietary and Microbial Tryptophan-Indole Metabolism as Therapeutic Approaches to Colon Cancer. Nutrients, 13(4). https://doi.org/10.3390/nu13041189

Xu, K., & Wang, J. (2019). Discovering the effect of alum on UV photo-degradation of gelatin binder via FTIR, XPS and DFT calculation. Microchemical Journal, 149, 103934.https://doi.org/10.1016/j.microc.2019.05.034

Yan, W., Sun, C. J., Yuan, J. W., & Yang, N. (2017). Gut metagenomic analysis reveals prominent roles of Lactobacillus and cecal microbiota in chicken feed efficiency. Scientific Reports, 7. https://doi.org/10.1038/srep45308

Yang, J., McDowell, A., Kim, E. K., Seo, H., Lee, W. H., Moon, C. M., Kym, S. M., Lee, D. H., Park, Y. S., Jee, Y. K., & Kim, Y. K. (2019). Development of a colorectal cancer diagnostic model and dietary risk assessment through gut microbiome analysis. Experimental and Molecular Medicine, 51.http://doi.org/10.1038/s12276-019-0313-4

Yang, T. W., Lee, W. H., Tu, S. J., Huang, W. C., Chen, H. M., Sun, T. H., Tsai, M. C., Wang, C. C., Chen, H. Y., Huang, C. C., Shiu, B. H., Yang, T. L., Huang, H. T., Chou, Y. P., Chou, C. H., Huang, Y. R., Sun, Y. R., Liang, C., Lin, F. M., Ho, S. Y., Chen, W. L., Yang, S. F., Ueng, K. C., Huang, H. D., Huang, C. N., Jong, Y. J., & Lin, C. C. (2019). Enterotype-based Analysis of Gut Microbiota along the Conventional Adenoma-Carcinoma Colorectal Cancer Pathway. Scientific Reports, 9 https://doi.org/10.1038/s41598-019-45588-z

Yang, W., Feng, Q. H., Li, M. J., Su, J. Q., Wang, P. Y., Wang, X., Yin, Y. C., Wang, X., & Zhao, M. D. (2021). Sinomenine Suppresses Development of Hepatocellular

Carcinoma Cells via Inhibiting MARCH1 and AMPK/STAT3 Signaling Pathway. Frontiers in Molecular Biosciences, 8 https://doi.org/10.3389/fmolb.2021.684262

Yang, Z., de Campo, L., Gilbert, E. P., Knott, R., Cheng, L., Storer, B., Lin, X., Luo, L., Patole, S., & Hemar, Y. (2022). Effect of NaCl and CaCl2 concentration on the rheological and structural characteristics of thermally-induced quinoa protein gels. Food Hydrocolloids, 124, 107350.https://doi.org/10.1016/j.foodhyd.2021.107350

Yao, Y., Zhu, Y., Gao, Y., Shi, Z., Hu, Y., & Ren, G. (2015). Suppressive effects of saponin-enriched extracts from quinoa on 3t3-l1 adipocyte differentiation. Food & Function, 6(10), 3282–3290. https://doi.org/10.1039/c5fo00716j

Yin, S.-W., Tang, C.-H., Wen, Q.-B., & Yang, X.-Q. (2010). Functional and conformational properties of phaseolin (Phaseolus vulgris L.) and kidney bean protein isolate: A comparative study. Journal of the Science of Food and Agriculture, 90(4), 599-607.https://doi.org/10.1002/jsfa.3856

Yoo, S. W., Oh, G., Safi, A. M., Hwang, S., Seo, Y. S., Lee, K. H., Kim, Y. L., & Chung, E. (2018). Endoscopic non-ablative fractional laser therapy in an orthotopic colon tumour model. Scientific Reports, 8 https://doi.org/10.1038/s41598-018-19792-2

Yousif, A. M., Snowball, R., D'Antuono, M. F., Dhammu, H. S., & Sharma, D. L. (2020). Water droplet surface tension method - an innovation in quantifying saponin content in quinoa seed. Food Chemistry, 128483. https://doi.org/10.1016/j.foodchem.2020.128483

Yu, M., Lin, S., Ge, R., Xiong, C., Xu, L., Zhao, M., & Fan, J. (2022). Buckwheat self-assembling peptide-based hydrogel: Preparation, characteristics and forming mechanism. Food Hydrocolloids, 125, 107378.https://doi.org/10.1016/j.foodhyd.2021.107378

Yuan, L., Sun, L. P., & Zhuang, Y. L. (2018). Preparation and identification of novel inhibitory angiotensin-I-converting enzyme peptides from tilapia skin gelatin hydrolysates: inhibition kinetics and molecular docking. Food & Function, 9(10), 5251-5259. https://doi.org/10.1039/c8fo00569a

Zeng, X. J., Jia, H., Zhang, X., Wang, X., Wang, Z. L., Gao, Z. P., Yuan, Y. H., & Yue, T. L. (2021). Supplementation of kefir ameliorates azoxymethane/dextran sulfate sodium induced colorectal cancer by modulating the gut microbiota. Food & Function, 12 (22), 11641-11655 https://doi.org/10.1039/d1fo01729b

Zhang, B. W., Xu, Y. C., Liu, S., Lv, H., Hu, Y. Z., Wang, Y. Y., Li, Z., Wang, J., Ji, X. M., Ma, H., Wang, X. W., & Wang, S. (2020). Dietary Supplementation of Foxtail Millet Ameliorates Colitis-Associated Colorectal Cancer in Mice via Activation of Gut Receptors and Suppression of the STAT3 Pathway. Nutrients, 12(8). http://doi.org/10.3390/nu12082367

Zhang, L. B., Bu, L., Hu, J., Xu, Z. Y., Ruan, L. B., Fang, Y., & Wang, P. (2018). HDAC1 knockdown inhibits invasion and induces apoptosis in non-small cell lung cancer cells. Biological Chemistry, 399(6), 603-610. https://doi.org/10.1515/hsz-2017-0306

Zhang, Q., Song, Y., Chen, W., Wang, X., Miao, Z., Cao, L., Li, F., & Wang, G.

(2015). By recruiting HDAC1, MORC2 suppresses p21 Waf1/Cip1 in gastric cancer. Oncotarget, 6(18), 16461-16470. https://doi.org/10.18632/oncotarget.3889

Zhang, X., Zuo, Z., Ma, W., Yu, P., & Wang, L. (2021). Assemble behavior of ultrasound-induced quinoa protein nanoparticles and their roles on rheological properties and stability of high internal phase emulsions. Food Hydrocolloids, 117, Article 106748. https://doi.org/10.1016/j.foodhyd.2021.106748

Zhang, Y., Fu, T. T., Ren, Y. X., Li, F. C., Zheng, G. X., Hong, J. J., Yao, X. J., Xue, W. W., & Zhu, F. (2020). Selective Inhibition of HDAC1 by Macrocyclic Polypeptide for the Treatment of Glioblastoma: A Binding Mechanistic Analysis Based on Molecular Dynamics. Frontiers in Molecular Biosciences, 7. https://doi.org/10.3389/fmolb.2020.00041

Zhang, Y., Liu, W., Zhang, D., Yang, Y., Wang, X., & Li, L. (2021). Fermented and Germinated Processing Improved the Protective Effects of Foxtail Millet Whole Grain Against Dextran Sulfate Sodium-Induced Acute Ulcerative Colitis and Gut Microbiota Dysbiosis in C57BL/6 Mice. Front Nutr, 8, 694936.http://doi.org/10.3389/fnut.2021.694936

Zhao, C., Chu, Z., Miao, Z., Liu, J., Liu, J., Xu, X., Wu, Y., Qi, B., & Yan, J. (2021). Ultrasound heat treatment effects on structure and acid-induced cold set gel properties of soybean protein isolate. Food Bioscience, 39, 100827.https://doi.org/10.1016/j.fbio.2020.100827

Zhao, G., Liu, Y., Zhao, M., Ren, J., & Yang, B. (2011). Enzymatic hydrolysis and their effects on conformational and functional properties of peanut protein isolate. Food Chemistry, 127(4), 1438-1443.https://doi.org/10.1016/j.foodchem.2011.01.046

Zhao, Y. L., Hu, X. Q., Zuo, X. Y., & Wang, M. F. (2018). Chemopreventive effects of some popular phytochemicals on human colon cancer: a review. Food & Function, 9 (9), 4548-4568 https://doi.org/10.1039/c8fo00850g

Zhou, W. L., Zhang, D., Li, Z. P., Jiang, H. Q., Li, J. N., Ren, R. R., Gao, X. F., Li, J. F., Wang, X., Wang, W. F., & Yang, Y. S. (2021). The fecal microbiota of patients with pancreatic ductal adenocarcinoma and autoimmune pancreatitis characterized by metagenomic sequencing. Journal of Translational Medicine, 19(1). https://doi.org/10.1186/s12967-021-02882-7

Zhou, Z., Mo, S. B., Gu, R. Q., Dai, W. X., Zou, X. H., Han, L. Y., Zhang, L., Wang, R. J., & Cai, G. X. (2020). Hematopoietic Gene Expression Regulation Through m(6)A Methylation Predicts Prognosis in Stage III Colorectal Cancer. Frontiers in Oncology, 10 https://doi.org/10.3389/fonc.2020.572708

Zhu, H. Q., Shan, L. M., Schiller, P. W., Mai, A., & Peng, T. Q. (2010). Histone Deacetylase-3 Activation Promotes Tumor Necrosis Factor-alpha (TNF-alpha) Expression in Cardiomyocytes during Lipopolysaccharide Stimulation. Journal of Biological Chemistry, 285(13), 9429-9436. https://doi.org/10.1074/jbc.M109.071274

Zuo, Z., Zhang, X., Li, T., Zhou, J., Yang, Y., Bian, X., & Wang, L. (2022). High internal phase emulsions stabilized solely by sonicated quinoa protein isolate at various pH values and concentrations. Food Chemistry, 378, 132011.https://doi.org/10.1016/j.foodchem.2021.132011

Appendix-Publications

1. **Fan, X.**, Guo, H., Richel, A., Zhang, L., Liu, C., Qin, P., Blecker, C., Ren, G. (2023). Preparation, physicochemical properties, and formation mechanism of quinoa self-assembled peptide-based hydrogel. Food hydrocolloids, 145, 109139. DOI: 10.1016/j.foodhyd.2023.109139.

2. **Fan, X.**, Guo, H., Teng, C., Yang, X., Qin, P., Richel, A., Zhang, L., Blecker, C., Ren, G. (2023). Supplementation of quinoa peptides alleviates colorectal cancer and restores gut microbiota in AOM/DSS-treated mice. Food Chemistry, 408, 135196. DOI: 10.1016/j.foodchem.2022.135196.

3. **Fan, X.**, Guo, H., Teng, C., Zhang, B., Blecker, C., Ren, G. (2022). Anti-Colon Cancer Activity of Novel Peptides Isolated from In Vitro Digestion of Quinoa Protein in Caco-2 Cells. Foods, 11 (2), 194. DOI: 10.3390/foods11020194.

4. **Fan, X.**, Qin, P., Hao, Y., Guo, H., Blecker, C., Everaert, N., Ren, G. (2020). Overexpression of soybean-derived lunasin in wheat and assessment of its anti-proliferative activity in colorectal cancer HT-29 cells. International Journal of Molecular Sciences, 21 (24), 9594. DOI: 10.3390/ijms21249594.

5. Ren, G., **Fan, X.** (co-first author), Teng, C., Li, Y., Everaert, N., Blecker, C. (2021). The beneficial effect of coarse cereals on chronic diseases through regulating gut microbiota. Foods, 10 (11), 2891. DOI: 10.3390/foods10112891.

6. Zhang, Z., **Fan, X.** (co-first author), Zou, L., Xing, B., Zhu, M., Yang, X., Ren, G., Yao, Y., Zhang, L., Qin, P. (2022). Phytochemical properties and health benefits of pregelatinized Tartary buckwheat flour under different extrusion conditions. Frontiers in Nutrition, 9, 1052730. DOI: 10.3389/fnut.2022.1052730.